2008

Modification of olanzapine to control the metabolic disorders associated with schizophrenia therapy

Somayeh Jafari
University of Wollongong

Modification of Olanzapine to Control the Metabolic Disorders Associated With Schizophrenia Therapy

A thesis submitted in partial fulfillment of the requirements for the award of the degree of

Masters by Research

From

The University of Wollongong

By

Somayeh Jafari

BACHELOR OF CHEMISTRY

Supervisors: Prof. Stephen G. Pyne

Prof. Xu-Feng Huang

Assoc. Prof. Renate Griffith

School of Chemistry

August, 2008

CERTIFICATION

I, Somayeh Jafari, declare that this thesis, submitted in partial fulfillment of the requirements for the award of Master by Research, in the School of Chemistry, Faculty of Science, University of Wollongong, is wholly my own work unless referenced or acknowledged. The document has not been submitted for qualifications at any other academic institution.

Somayeh Jafari

August, 2008

TABLE OF CONTENTS

LIST OF FIGURES

LIST OF SCHEMES

LIST OF TABLES

LIST OF ABBREVIATIONS

5-HT_2	5-hydroxytryptamine
A	Activity
ACTH	Adrenocorticotrophic hormone
ARC	Arcuate nucleus
BMI	Body mass index
bp	Boiling point
Calcd	Calculated
CeA	Central nucleus of the amygdala
CCK	Cholecystokinin
CHAPS	3-[(3-Cholamidopropyl)dimethylammonio]-1-propanesulfonate
CI	Chemical ionization
Ci	Curie
CNS	Central nervous system
Correl	Correlation
CPM	Count per minute
CRH	Corticotrophin releasing hormone
d	Doublet
D	Dopamine
DCC	Dicyclohexylcarbodiimide
DEPT	Distortionless enhancement by polarisation transfer
DIPEA	*N*,*N*-Diisopropylethylamine
DMAP	Dimethylaminopyridine
DMF	*N*,*N*-dimethylformamide
DMH	Dorsomedial nucleus of the hypothalamus
DMSO	Dimethylsulfoxide
DTT	Dithiothreitol

EA	Estimated activity
EC_{50}	Effective concentration (half maximal)
EDCI	1-[3-(dimethylamino)propyl]-3-ethylcarbodiimide
EDTA	Ethyl(carboxymethyl)amino]acetic acid
EI	Electron impact
EPS	Extrapyramidal symptoms
eq	Equivalents
ESI	Electrospray ionization
Est	Estimated
Exp	Experimental
Ev	Excluded volumes
FDA	Food and Drug Administration
g	gram
GC-MS	Gas chromatography – mass spectrometry
GCOSY	Gradient correlation spectroscopy
GHMBC	Gradient heteronuclear multiple bond correlation
GHSQC	Gradient heteronuclear single quantum correlation
h	Hours
H	Histamine receptor
H	Hydrogen/proton
HA	Histamine
Hal	Aliphatic hydrophobic
Har	Aromatic hydrophobic
HBA	Hydrogen bond acceptor
HBD	Hydrogen bond acceptor
HEPES	(4-(2-Hydroxyethyl)-1-piperazineethanesulfonic acid
HOBt	1-Hydroxybenzotriazole
HP	Histaprodifen
HPLC	High performance liquid chromatography
HRMS	High resolution mass spectrometry
Hz	Hertz

IC_{50}	Inhibitory concentration (half maximal)
J	Coupling constant
Kd	Dissociation constant
Ki	Inhibition constant
Kcal	Kilo calories
LRMS	Low resolution mass spectrometry
LHA	Lateral hypothalamic area
Lit.	Literature
m	Multiplet
M	Molar
M	Muscarinic receptor
MA	Most active
ME	Medial eminence
MEM	Minimum Essential Medium
MHz	Mega hertz
min	Minutes
mL	Milliliters
mmol	Millimole
m.p.	Melting point
MS	Mass spectrometry
MW	Molecular weight
m/z	Mass to charge ratio
n	Normal
nM	Nanomolar
NMP	*N*-methylpiperazine
NMR	Nuclear magnetic resonance
NPY	Neuropeptide Y
NRWG	Non-rapid Weight Gain Group
o	Ortho
OC	Optic chiasm
PBS	Phosphate buffered saline

PC	Positive charge
pH	Potential of hydrogen
PI	Positive ionizable
POHA	Preoptic anterior hypothalamus
PPM	Part per million
PVN	Paraventricular nucleus
RA	Ring aromatic
R_f	Retention factor
RMS	Root-mean-square
rp	Reverse phase
Rt	Retention time
RWG	Rapid Weight Gain Group
SAR	Structure activity relationship
t	Triplet
t	Tert
TD	Tardive dyskinesia
TFA	Trifluoroacetic acid
THF	Tetrahydofuran
TLC	Thin layer chromatogeraphy
TMS	Tetramethylsilane
TRIS	Tris(hydroxymethyl)aminomethane
Unc	Uncertainty
UOW	University of Wollongong
UV	Ultraviolet
VMH	Ventromedial nucleus of the hypothalamus
A	Adrenergic receptor
μ	Micro
δ	Chemical shift (in parts per million, downfield from TMS)

ACKNOWLEDGMENTS

I would like to take this opportunity to acknowledge all those people who helped me to successfully complete this project. I am most grateful to my supervisors **Professor Stephen Pyne, Professor Xu-Feng Huang** and **Assoc. Professor Renate Griffith** for all that they have contributed to my project. I am deeply appreciative for all their motivation, guidance, patience and support during this journey. I also would like to take this opportunity to thank **Prof. John Bremner** for his supervision during the first six months of my Master degree.

Furthermore, I would like to extend my appreciation particularly to **Dr. Michael Kelso** and **Dr. Joseph Ambrus** for teaching me many valuable laboratory skills in organic synthesis and also for being my mentors during my difficult times. I also owe many thanks to **Ms. Mei Han** who taught me many biological laboratory skills in the early stages of my pharmacological testing. I am deeply indebted to **Mr. Simon Bland** for all of his technical help during my computer modeling studies. I also would like to acknowledge all technical staff members in the School of Chemistry in particular, **Dr. Wilford Lie**, **Ms. Sandra Chapman**, **Dr. John Korth**, **Ms. Karin Maxwell** and **Mr. Roger Kanitz**.

To all other researchers in the **Pyne research group** and **Huang research group**, I would like to thank them for their support, help and friendship. Particularly, I would like to appreciate **Dr. Jasmine Jury** and **Dr. Kittiya Somphol** for their valuable guidance and friendship during my Master study. Especially, I would like to express my gratitude to **Mr. Marc E. Bouillon** for sharing his knowledge and his laboratory skills with me. I am not able to explain my appreciation in words to him, but I would like to deeply thank him for all of his encouragement and emotional support. I wish him all the best for his PhD study.

Finally, I would like to dedicate this thesis to my mother, **Ms. Zahra Sadeghi** and to my father **Professor Mohammad Reza Jafari**. I am extremely thankful for their emotional and financial support which made this research project possible for me. I hope they are proud of me and support my further career.

ABSTRACT

"Modification of Olanzapine to Control The Metabolic Disorders Associated with Schizophrenia Therapy"

Schizophrenia is a complex mental disorder which is accompanied with various positive and/or negative symptoms. Among the prescribed antipsychcotics for treatment of schizophrenia, atypical antipsychotics including olanzapine (zyprexa) have been used as the first line of therapeutic programs. The unique therapeutic feature of olanzapine associated with low incidence of EPS (Extrapyramidal Symptoms) has been recognized to be correlated with its broad neuronal receptor binding benefits including binding to the D-2, D-4, 5-HT_{2A} and 5-HT_{2C} as well as D-1, α-1, α-2 and M-1 receptors. However, the H-1 antagonist propensity of olanzapine, and that of other atypical antipsychotics, induces excessive weight gain, type II diabetes and obesity-related conditions such as cardiovascular disease.

This dissertation focused on structural modification of olanzapine to a new antipsychotic with H-1 agonist activity or to a new drug with lower affinity for the H-1 receptor. Computer-aided drug design techniques were utilized, centering on the development of a H-1 agonist pharmacophore based on the available published ligands. The resulting pharmacophore proposed three modifications to the structure of olanzapine including: 1) replacement of the methyl group with an ethyl group at position C-2; 2) substitution of a hydroxymethyl group at position C-3; and 3) removal of the distal nitrogen from position N-4′ (Table 3.1, page 41).

The diazepine compounds **99** and **101** were synthesised successfully representing a single modification at position C-2 and N-4′, respectively. Substitution of a

hydroxymethyl group at position C-3 of olanzapine was not successful; however, the formamide compound **145** with a formamide group at position N-10 was accidentally obtained (Scheme 3.21, page 69). The diazepine derivatives **99**, **101**, **145** and also **102** with two modifications at positions C-2 and N-4′ were subjected to pharmacological evaluation. In the scope of this project competitive binding assays were attempted. The obtained IC_{50} value from these experiments revealed that the diazepine compound **99** (IC_{50}: 9.78 x 10^{-7} M) had significant reduced binding affinity compared to that of olanzapine (IC_{50}: 2.08 x 10^{-9} M) for the H-1 receptor. This result was related to the effect of the ethyl group at position C-2. The formamide compound **145** (IC_{50}: 3.70 x 10^{-8} M) also had reduced binding affinity of olanzapine to the H-1 receptor; however, due to the poor dose-response behavior of the diazepine compound **101** (IC_{50}: 0.5 M) the effect of removing the distal nitrogen from position N-4′ is questionable and needs further investigations.

CHAPTER 1: INTRODUCTION

1.1 Background

Schizophrenia is a complex neuropsychiatric disorder characterized by abnormalities in the perception of reality.[1] The symptoms of schizophrenia appear in young adulthood[2] with approximately 1% of the worldwide adult population affected.[3, 4] Schizophrenic patients may experience various positive symptoms. Positive symptoms regarded as a manifestation of psychosis include auditory hallucinations, delusions, deterioration of thought and memory, distortion in communication (disorganized speech) and in behavior (grossly disorganized or catatonic behavior). They can also experience negative symptoms such as avolition (restriction in motivation), affective flattening (restriction in emotional expression), alogia (restriction in speech), anhedonia (lack of pleasure) and social withdrawal.[1, 5]

Pharmacological treatment by antipsychotic drugs is as essential as psychotherapy programs for most schizophrenic patients. The antipsychotic drugs are generally classified into two major groups including conventional (typical) and novel (atypical) neuroleptic drugs. Typical antipsychotics, the first generation of antipsychotics, were discovered in the 1950s. Such drugs are conventional neuroleptic agents that primarily block the dopamine receptor subtype 2 (D-2).[6]

The various antipsychotics have different antagonist activities at different receptors so that they differ in their side-effect profiles. It has been suggested that all typical antipsychotic medications are associated with extrapyramidal symptoms (EPS) such as tardive dyskinesia (TD), dystonia, akathesia and Parkinsonism[7] resulting from the dopamine antagonist property of the typical neuroleptics. Therefore, blockade of the D-2 receptor in the mesolimbic dopamine pathway leads to the therapeutic profiles, however, its blockade in the nigrostriatal pathway influences the exterapyramidal system and causes various movement disorders.[6]

In spite of typical antipsycotics which are only capable of controlling positive symptoms of schizophrenia, the second generation of antipsycotics, are believed to deliver additional therapeutic effects for the negative symptoms and cognitive abnormalities.[7] While both typical and atypical antipsychotics share similar features of blocking effects on D-2 receptors, the atypical antipsychotics primarily affect the mesolimic system. A proper balanced ratio of dopamine D-2 and serotonin 5-HT_2 receptor activities in the limbic system is the main therapeutic strategy of atypical antipsychotic drugs in treatment of schizophrenia. Thus, the second generation of antipsychotics has fewer EPS than typical antipsycotics.[6, 8, 9] Common typical and atypical antipsycotics along with their pharmacological classification are summarized in Table 1.1.

Table 1.1: Classification of typical and atypical antipsychotic drugs [10]

Typical	Phenothiazine	Chlorpromazine , Fluphenazine, Thioridazine
	Thioxantenes	Thiothixene
	Butyrophenones	Haloperidole, Trifluperidole
	Dibenzoxazepines	Loxapine
	Diphenylbutylpiperidines	Fluspirilene, Penfluridol, Pimozide
Atypical	Dibenzodiazepine	Clozapine
	Thienobenzodiazepine	Olanzapine
	Indoles	Sertindole, Ziprasidone
	Dihydroindolones	Molindone

As shown in Table 1.1, a number of structural classes of atypical antipsychotics have been synthesized. The dibenzepine type with the central seven-membered ring substituted with oxygen, sulfur, nitrogen or carbon has been found to exhibit the desired atypical profile with preference for the mesolimbic over the nigrostriatal dopamine receptors.[11, 12] Clozapine (Figure 1.1, page 3), one of the dibenzepine type antipsychotics, was the first antipsychotic to be approved by the Food and Drug Administration (FDA) due to the evidence of its superiority over other antipsychotics for the treatment of unresponsive patients.[13] The unique therapeutic feature of clozapine associated with low incidence of EPS has been recognized to be correlated with its broad neuronal receptor binding benefits including binding to the D-2, D-4, 5-HT_{2A} and 5-HT_{2C}, as well as, D-1, α-1, α-2, M-1 and H-1 receptors.[8, 10, 11, 14]

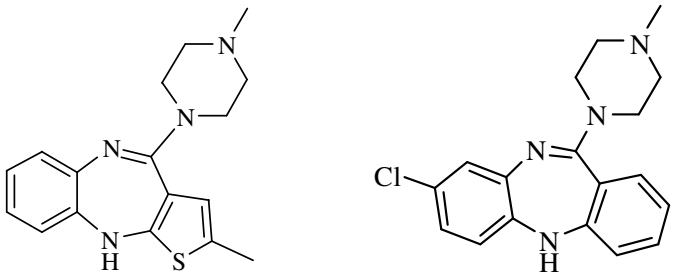

a **b**

Figure 1.1: Structure of (**a**) olanzapine; (**b**) clozapine.

Olanzapine (Figure 1.1), a recently developed "clozapine-like" antipsychotic, possesses structural similarity with clozapine and it is classified as a thienobenzodiazepine. Due to its property in alleviating negative schizophrenic symptoms and reducing EPS, olanzapine has been clinically administrated as the first line of therapy for medicating schizophrenia. Similar pharmacological activities of olanzapine to that of the prototype clozapine have been reported. [15] In their research Bymastre *et al*.[15] have explored the affinity of olanzapine at various neuronal receptors *in vitro*, in cell line transfected selectively with receptor subtypes and receptor-selective isolated tissue studies. Olanzapine antagonized 5-HT_{2A}, 5-HT_{2B}, 5-HT_{2C}, α-1 adrenergic, H-1 histamine and D-1, D-2 and M-1 – M-5 receptors, however, it did not show any agonist activity at any of the examined receptors. A summary of the activities of olanzapine at the examined receptors is illustrated in Table 1.2.[15]

Table 1.2: Pharmacology property of olanzapine. [a]Data from Calligaro *et al*. [16]

	Binding	Antagonism
Receptors	K_i (nM)	IC_{50}(nM)
5-HT_{2A}	2.5	36±12
5-HT_{2B}	12	42±8
5-HT_{2C}	29	16220±3790
5-HT_{2c}		105±36
Dopamine D-1	119	404±81
Dopamine D-2[a]	20±8	
Muscarinic M-1	2.5	680±295
Muscarinic M-2	18	8170±2350
Muscarinic M-3	13	970±470
Muscarinic M-4	10	600±294
Muscarinic M-5	6	995±300
α_1-Adrenergic	19	286±23
Histamine H-1	7	50±8

As shown in Table 1.2, olanzapine is a potent antagonist of 5-$HT_{2A, 2B, 2C}$, α-1, D-2 and H-1 receptors. It also has a weaker propensity to antagonize the D-1 and the five muscarinic receptors. Olanzapine also showed high affinity for the $5HT_6$ receptor subtype. [17]

Olanzapine showed *in vivo* antagonist activity at the 5-HT_2, muscarinic, dopamine and α-1 receptors. For instance, olanzapine blocked apomorphine-induced climbing in mice and also pergolide-induced increases in serum corticosterone in rats presenting its potency to antagonize the D-1 and D-2 receptors.[18, 19] In addition, the increased level of the striatal tissue concentrations of the dopamine metabolites, 3,4-dihydroxyphenylacetate acid, homovanillic acid and 3-methoxytyramine due to olanzapine treatment was a result of the blockade of the D-2 receptor.[20]

Despite their therapeutic benefits, olanzapine and most of the prescribed novel antipsychotics have been found to result in excessive weight gain, type II diabetes mellitus and metabolic disorders including dyslipidemia, cardiovascular disease, hypertension and osteoarthritis.[21-23] It has been well documented that obesity-related conditions induced by antipsychotics would increase the rate of

mortality.[3] In addition, weight gain is significantly associated with a noncompliance in taking medication, which drastically increases the relapse rate for patients.[24] Therefore, changing the face of schizophrenia treatment with novel antipsychotics has reduced the concern about EPS and tardive dyskinesia, but it has significantly increased the degree of risk imposed by obesity and its consequences. [3, 25]

The extent of antipsychotic-induced weight gains has been explored by various clinical trials.[26-28] It has been recognized that the amount of weight gained by atypical antipsychotics is greater than in those administrated typical antipsychotics. The weight gain after 10 weeks of novel antipsychotic treatment at a standard dose showed the mean increases as follows: 4.45 Kg, clozapine; 4.15 Kg, olanzapine; 2.92 Kg, sertindole; 2.10 Kg, risperidole and 0.04 Kg, ziprasidole. These can be compared to the weight gain of 1.1 Kg with the typical antipsychotic haloperidol.[22] Another study reported that the greatest amount of weight gain had been experienced by clozapine and olanzapine treated patients compared with risperidole-treated patients over 28 weeks. [23]

Olanzapine `s association with weight gain over a period 52 weeks has been investigated by Kinon *et al.*[29] In their study schizophrenic patients have been classified into two major groups including a rapid Weight Gain Group (RWG) and a Non-rapid Weight Gain Group (NRWG), based on the amount of increased weight during the first 6 weeks. RWG gained $\geq$ 7% of their original body weight while NRWG lost weight, gained no weight or gained < 7%. After 52 weeks of treatment it was concluded that approximately 15% of the patient population were in the RWG group while 85% of patients gained weight more slowly.[29] The other study showed that after 2 years, 66% of olanzapine-treated patients gained less than 10 Kg, 7% of patients gained more than 20 Kg whereas 1 in 4 patients lost weight or did not gain any weight.[23] An increased weight of 12 Kg after one year [30] and 6.26 Kg after 2.54 years[31] has been also observed. It has been reported that during long-term olanzapine treatment (up to 3 years) the increase in body weight reached a plateau at approximately 36-39 weeks when no noticeable weight change was observed on subsequent treatment.[23, 29, 31, 32] At the late stage of weight gain, patients developed metabolic disorders including Type II diabetes and cardiovascular diseases.

The reported results of double-blind clinical trails has suggested that baseline body mass index (BMI), increased appetite, age, race and clinical response are predictors of weight gain in olanzapine-treated patients.[23, 33] It has been found that during the first 13 weeks of olanzapine treatment the mean amount of weight gained in patients with high BMI values (>27.6) was significantly lower than those with medium BMI values (>23.6 to 27.6) or low BMI values (≤ 23.6). At the endpoint of treatment (3 years) the high-BMI patients had less than 4 Kg weight gain while the low-BMI group gained approximately 8 Kg.[23, 32] Increased appetite was the other predictor for weight gain during the treatment. Patients whose appetite increased gained more weight than those with a normal appetite. It has also been reported that younger age and nonwhite race patients are at a greater risk of gaining weight during olanzapine therapy.[23, 32] More noticeably, weight gain with olanzapine therapy has been reported to be accompanied with better clinical outcomes. Better clinical response, low baseline BMI and nonwhite race are similar factors among antipsychotics in predicting weight gain whilst the influence of increasing appetite and age differ between atypical (olanzapine) and typical (haloperidol) antipsychotic drugs.[23, 33]

Various studies have reported that weight gain associated with olanzapine and other antipsychotics are significantly attributed to the H-1 receptor antagonist property of these drugs.[34-38] It has also been investigated that the most important predictor of a drug tendency to induce weight gain is its affinity for the H-1 receptor. Newer antipsychotic drugs such as ziprasidone and aripiprazole having low affinity to the H-1 receptor showed low weight gain liabilities. However, clozapine and olanzapine accompanied with higher affinity to the H-1 receptor showed higher propensity to induce weight gain and subsequent hyperlipidemia, hypertension and hyperglycemia.[39, 40]

Histaminergic activity in the hypothalamus has been found to be involved in the regulation of food intake, including satiation, hyperphagia and anorexia.[35, 38, 40] In the central nervous system (CNS) histidine decarboxylase uses histidine as a CNS histamine source to synthesize histamine which is then transferred by histamine -*N*-methyltransferase in the brain.[41] A study of the rat brain reported that the

greatest amount of brain histamine, histidine decarboxylase and histamine -*N*-methyltransferase are concentrated in hypothalamus.[42, 43] Central histamine concentration is involved in several hypothalamic functions including feeding, drinking, neuroendoctrine secretion, sleep/wakefulness cycle, locomotor activities, catalepsy, thermoregulation, and free running rhythm.[36] The highest concentration of H-1, H-2 and H-3 receptors are also found in the hypothalamus. Different factors have been recognized that influence the activity of the central histaminergic system including concentration of hitamine and histamine receptors, diet composition and also bioperiodicity of histaminergic compounds.[35]

It has been documented that histaminergic activity in the hypothalamus affected by alteration in brain histamine levels and H-1 receptor concentration has a significant role in regulation of food intake-related pathophysiological states. An inverse relationship between brain histamine levels and food intake has been reported.[36] Increasing central histamine levels alleviates food intake while decreasing central histamine levels elevates food intake. Thus, dietary involvement which can modify food intake has the potential impact on the histaminergic system.[37] Mercer *et al*.[38] have investigated the correlation between CNS histamine, H-1 receptor concentrations and food intake regulation in rats. In their study, compared to rats fed a normal protein diet, rats fed a low protein diet showed higher H-1 receptor concentrations in the whole brain. Low protein diets resulted in increase serum and brain histidine and also histamine concentrations which led to a decrease in food intake and weight gain.

The mechanism of the regulation of the food intake through a cascading pathway has been reported in the literature.[38, 44] It has been documented that the binding of histamine to H-1 receptors stimulates the G-protein signal transduction leading to activation of a cascading pathway with corticotrophin releasing hormone (CRH) producing adrenocorticotrophic hormone (ACTH) which releases corticosteron. The subsequent increased levels of these neurotransmitters, neuromodulators and hormones result in a reduction of food intake.[44] Schematic pathways regulating food intake in the central hystaminergic system is depicted in Figure1.2.[38, 44]

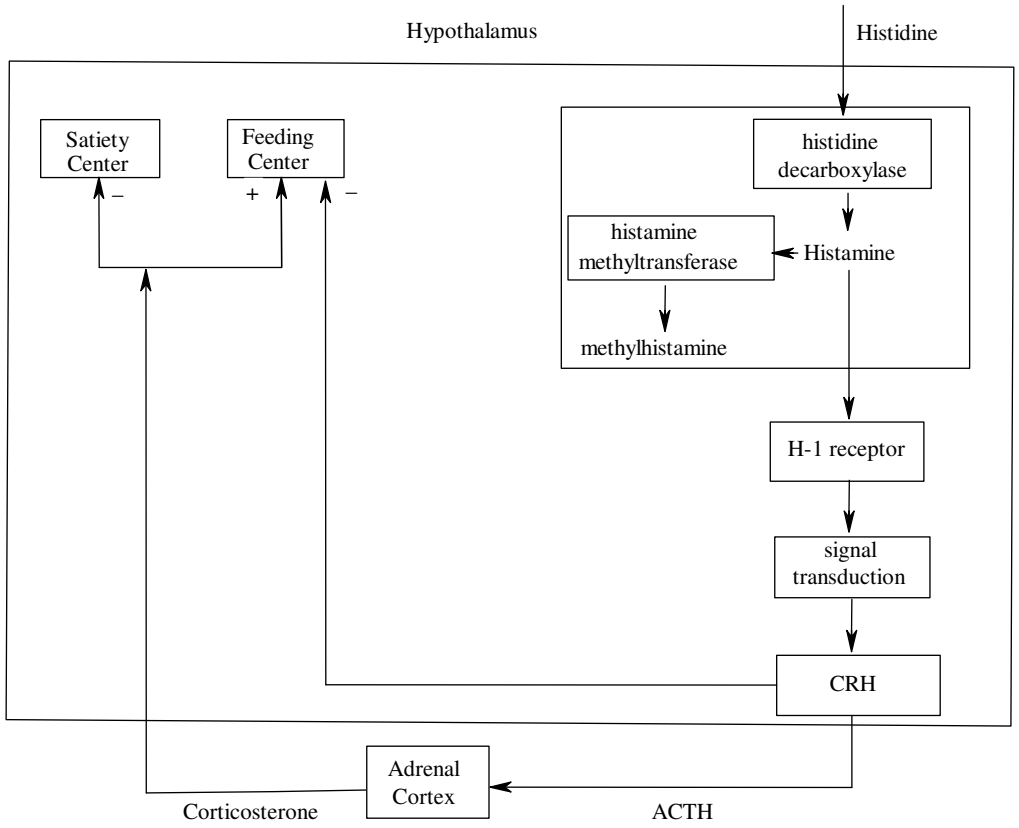

Figure 1.2: Proposed pathways regulating food intake through histaminergic system. CRH: Corticotrophic releasing hormone, ACTH: adrenocorticotrophic hormone.[38, 44]

The exact site of histaminergic modulation of food intake has been explored by various studies in the rat hypothalamus. The ventromedial nucleus of the hypothalamus (VMH) has been found as an important part of the brain for the regulation of energy metabolism and food intake.[45] It has been revealed that VMH lesions led to hyperphagia and obesity[46] while electrical stimulation of VMH reduced feeding and induce lipolysis.[47] In addition, glucose-sensing neurons and also essential receptors for energy metabolism including CCK, insulin, neuropeptide Y (NPY), corticotrophin-releasing hormone, melanocortine and orexine receptors have been found in the VMH.[45]

The imperative role of VMH in the regulation of energy metabolism and food intake has also been demonstrated through several anatomical studies. The VMH obtains input from other locations such as the hypothalamic arcuate nucleus (ARC), the lateral hypothalamic area (LHA), the amygdale and the lateral septum, which are

significantly involved in the regulation of energy metabolism. In addition, the VMH projects to the dorsomedial nucleus of the hypothalamus (DMH), the paraventricular nucleus (PVN), the nucleus accumbens, ARC, nucleus of the solitary tract, lateral hypothalamus and the ventral tegmental area.[45] The lateral view of hypothalamic nuclei in the brain is illustrated in Figure 1.3. The location of the VMH in the rat brain section is shown in Figure 1.4.

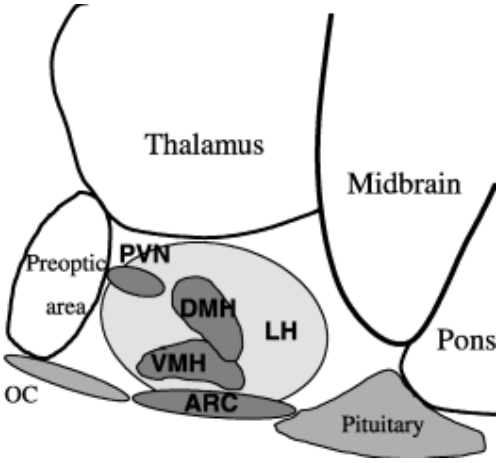

Figure 1.3: Lateral view of hypothalamic nuclei.[48] PVN: paraventricular nucleus, DMH: dorsomedial nucleus of the hypothalamus, VMH: ventromedial nucleus of the hypothalamus, ARC: arcuate nucleus, LH: lateral hypothalamus, OC: optic chiasm.

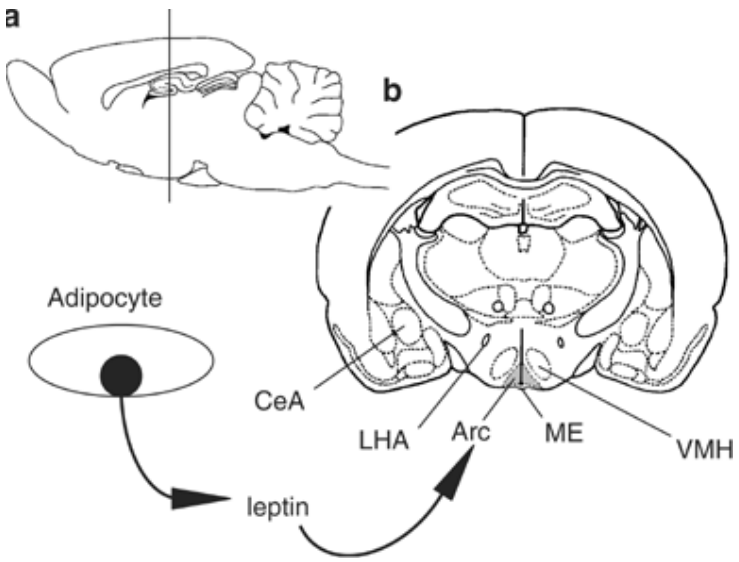

Figure 1.4: Schematic illustration of hypothalamic nuclei. (a) Lateral view of the rat brain. (b) Coronal section of the rat brain at a shown by a vertical line in (a). CeA: central nucleus of the amygdala, LHA: lateral hypothalamic area, Arc: arcuate nucleus, ME: medial eminence, VMH: ventromedial nucleus of the hypothalamus.[49]

Bilateral lesions of the VMH have lead to the development of obesity and these VMH-lesioned animals have been used to explore the mechanism of weight gain. It has been reported that bilateral VMH lesions in the rats resulted in an increase in their body weight; however, it led to a decrease in food intake in the unlesioned animals. VMH-lesioned rats overproduce a circulating satiety factor which can not be responded to by lesioned animals and subsequently resulted in food intake and obesity.[50] Cox *et al*. investigated the effect of the asymmetrical electrolytic lesions of the VMH and PVN on weight gain in rat. This study reported that damaging the VMH and PVN resulted in noticeable hyperphagia and weight gains with a mean value of 257.2 g during 56 postsurgical days, which was three times greater than those of the controls (89.8 g). The amount of weight gained in these rats was not remarkably different from that in rats with VMH lesions (277.2 g) or PVN lesions (188.2 g).[51]

In other study, a H-1 receptor antagonist was microinfused into the hypothalamus, the VMH, the LHA, the PVN, the DMH and the preoptic anterior hypothalamus (POAH). Bilateral microinfusion into the VMH at a dose of 26 nmol and into the PVN at a dose of 52 nmol affected food intake in all examined rats, however,

bilateral microinfusion into the LHA, the DMH or the POAH did not show any influence on ingestive behavior. Thus, it was concluded that H-1 receptors in the VMH and the PVN but not in the LHA, the DMH or the POAH, have a significant role in the regulation of food intake.[52]

In summary, the H-1 receptors antagonist activity of antipsychotics such as olanzapine has a significant role in weight gain and subsequent metabolic disorders. Manipulation of the central nervous system histamine and histaminergic receptor (H-1) in the VMH and the PVN of the hypothalamus has been found to have the greatest influence on food intake.[38] Moreover, as discussed above, the association between affinities for the blockade of the H-1 receptor and weight gain has been reported for antipsychotics. Therefore, it has been hypothesized that any antipsychotic drug with a similar therapeutic benefit as olanzapine but with a lower affinity for the H-1 receptor might result in less weight gain while maintaining the desired clinical profiles of olanzapine.[34]

In this project structural modification of olanzapine to a new antipsychotic drug with lower H-1 antagonist propensity was pursued. A survey of the literature revealed that coadministration of a histamine enhancer such as betahistine, a H-1 receptor agonist, has shown a putative weight attenuating influence on olanzapine.[53, 54] Thus, it was postulated that modification of olanzapine from a H-1 antagonist to a H-1 agonist or to a new antipsychotic drug with the lower affinity for the H-1 receptor may possibly reduce the weight gain effect of olanzapine. With the scope of this project, computer-aided drug design techniques were applied to generate a pharmacophore model for the H-1 receptor agonist represented through three-dimensional features. The pharmacophoric pattern was then used to drive the modification of olanzapine through several synthesis plans. The pharmacological evaluation of the new modified compounds was performed using brain tissue binding assays.

1.2 Aims of the project

The aims of this project were thus, to structurally modify olanzapine from a H-1 antagonist to a H-1 agonist or to a new drug with lower binding affinity to the H-1 receptor. This project has covered all aspects of a medicinal chemistry project commencing with a pharmacophoric modeling study for H-1 receptor agonists, followed by the synthesis of identified targets and then the pharmacological evaluation of target drugs.

In Chapter 2 of this thesis the design of the pharmacophore model for H-1 agonists will be discussed. Chapter 3 and 4 will cover the synthesis of several novel antipsychotic drugs based on a modified olanzapine structure. Chapter 5 will focus on the pharmacological evaluation of the new synthesized drugs. Chapter 6 will describe the conclusions and future directions of this project.

CHAPTER 2: COMPUTER MODELING

2.1 Introduction

For over twenty years computer aided molecular modeling has been widely used to provide knowledge of interactions between drugs and biological receptors. Pharmacophore generation is one of the most common approaches used to explain the structure-activity relationship (SAR) of a series of analogue compounds and also to design or modify ligands for particular biological targets. A pharmacophore is defined as a three-dimensional set of structural elements (chemical features) which form the necessary requirements for biological activity.[55]

To develop the correct pharmacophoric model, the steric and the interacting features of all the conformations of the drug molecules should be identified. The development of a pharmacophore model is initiated by selecting available known compounds with a variety of chemical structural features which have the same binding mechanism with the same receptor (a training set). This is followed by a conformational analysis and an electron density calculation of each compound in the set. After the conformational analysis step, a three–dimensional arrangement of the structural features is determined which is common to all active molecules.[56]

Feature-based pharmacophores can be created *via* several different programs including DISCO,[57] Catalyst,[58] GASP,[59] Phase,[60] and Galahad.[61] One of the most widely used programs for pharmacophore elucidation is Catalyst.[62] The Catalyst program can be used at the qualitative (HipHop) or quantitative (HypoGen) level. The HipHop algorithm utilizes information from training set compounds in order to construct common feature hypothesis models. The HypoGen algorithm aims to generate SAR hypothesis models from a set of compounds with measured activity values (IC_{50} or K_i) on the intended biological target. Catalyst/HipHop utilizes active compounds to generate a pharmacophore while Catalyst/HypoGen uses both active

and inactive compounds to identify the hypothesis which is common among the active compounds but not among the inactive ones.[55] HypoGen hypotheses consist of a net of three dimensional structural/electronic features and their locations in space. The feature locations are given as tolerance spheres, allowing for a feature to be found within the volume of the tolerance sphere. Features in a pharmacophore can also be assigned different weight according to their relative importance. HypoGen hypotheses fit to the training set compounds and are correlated to the active data.[63] The obtained pharmacophores can be used to direct syntheses and also as search queries to explore for potential leads from a three-dimensional database.[56]

The purpose of this chapter is to explain the general methodology of generating hypotheses using the Catalyst program, to give practical insight into the HypoGen algorithm strategy and finally to develop a pharmacophore model for H-1 receptor agonists. The pharmacophoric pattern was also used to drive the structural modifications of olanzapine through several attempted synthesis plans.

2.2 Pharmacophore Generation

2.2.1 General Method

Pharmacophore generation and analysis were conducted with the Catalyst program version 4.10 (Accelrys Inc., San Diego, CA, USA), on a Silicon Graphics O2 workstation.

2.2.2 Training Set Selection

The selection of the training set is an important part of pharmacophore generation. Due to its direct influence on the validity of the hypotheses, the training set should be informative and contain concise data. In order to generate a pharmacophore in Catalyst it is also imperative to select a training set with a series of compounds which include a variety of structural classes, but not so many that

they could cause redundancy within the training set. Inactive compounds due to steric hindrance should also be avoided since they will confuse HypoGen. In order to classify compounds as "active" or "inactive" Catalyst needs a wide range of activity data with an equal spread across the range. Moreover, one should avoid the use of two similar compounds with similar activities as this is a waste of computational time and it could bias the results. The bulkier compound should be eliminated from the training set in these cases.[63]

Training sets of human H-1 agonists were constructed from published data. EC_{50} and K_i values were obtained from the literature for each individual compound. The EC_{50} is used for agonists compounds and represents the concentration required to achieve half of the maximum effect .[64]

K_i values achieved from competition assays are used to determine affinity and selectivity of ligands. Compounds with the lowest K_i values have the greatest affinity for the receptor[64] thus, K_i values have to be used in Catalyst rather than pK_i values. IC_{50} is the functional strength of the inhibitor and it is not a direct indicator of affinity since this value is dependent on the conditions under which it is measured. However, K_i is an absolute inhibition constant which indicates binding affinity of the inhibitor. Therefore, it is preferable to use K_i values rather than IC_{50} or EC_{50}.

Tables 2.1 and 2.2 show the structures and activities of published human H-1 agonist ligands. As illustrated in these tables, K_i values for all compounds in the training set were not reported in the literature thus, the available EC_{50} values, representing the agonist activity of these compounds at H-1 receptor, were used in the pharmacophore generation. According to the structural differences, these compounds were divided into two groups: histamine and lisuride derivatives.

Table 2.1: H-1 agonist activity of Lisuride derivatives.[65]

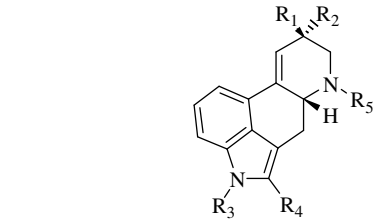

A

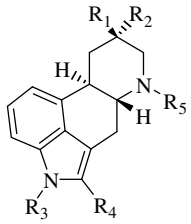

B

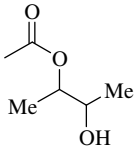

X_1

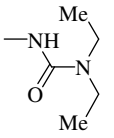

X_2

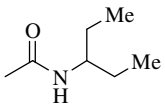

X_3

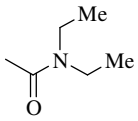

X_4

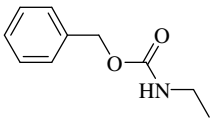

X_5

X_6

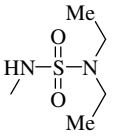

X_7

X_8

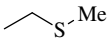

X_9

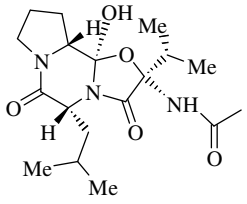

X_{10}

Compound	Structure	R_1	R_2	R_3	R_4	R_5	pK_i	pEC_{50}
8*R*-Lisuride	A	X_2	H	H	H	CH_3	7.9±0.1	7.9±0.1
8*S*-Lisuride	A	H	X_2	H	H	CH_3	6.3±0.1	6.3±0.1
8*R*-Terguride	B	X_2	H	H	H	CH_3	6.1±0.1	5.0
8*S*-Terguride	B	H	X_2	H	H	CH_3	6.1±0.1	5.0
Methysergide	A	X_3	H	CH_3	H	CH_3	N.D	5.6±0.3
Methergine	A	X_3	H	H	H	CH_3	N.D	5.7±0.1
LSD	A	X_4	H	H	H	CH_3	5.6±0.1	5.0
D-Lysergic acid	A	H	X_6	H	H	CH_3	5.7±0.1	4.0
Mesulergine	B	H	X_7	CH_3	H	CH_3	5.4±0.1	5.0±0.1
Bromocriptine	A	X_{10}	H	H	Br	CH_3	N.D	5.6±0.1
Metergoline	B	X_5	H	CH_3	H	CH_3	6.4±0.1	6.0±0.1
LY-53,857	B	X_1	H	X_8	H	CH_3	4.8±0.1	6.1±0.2
Pergolide	B	X_9	H	H	H	$(CH_2)_2CH_3$	N.D	5.8±0.2

Table 2.2: H-1 agonist activity of Histamine derivatives.[66, 67]

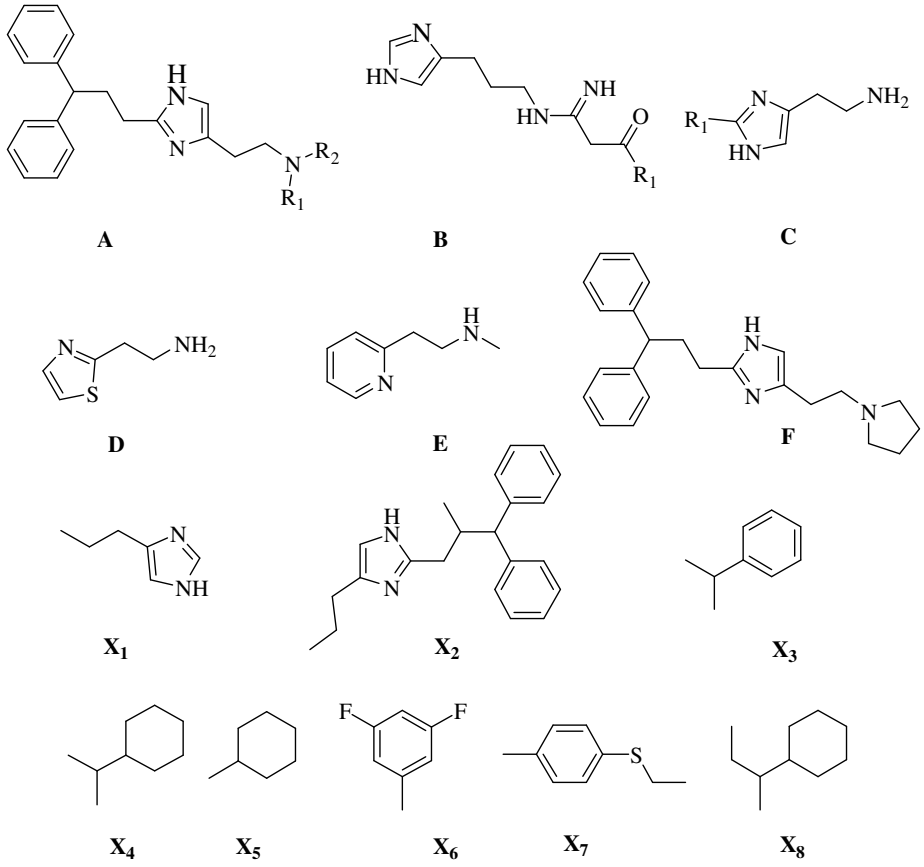

Table 2.2 (Cont`d): H-1 agonist activity of Histamine derivatives.[66, 67]

Compound	Structure	R_1	R_2	pK_i	pEC_{50}
Histamine (HA)	C	H		4.3±0.1	6.7±0.1
2-Methylhistamine	C	CH_3			6.1±0.1
Betahistine	E				5.8±0.1
Histaprodifen (HP)	A	H	H	5.6±0.1	5.9±0.1
MeHP	**A**	H	CH_3	6.0±0.1	6.3±0.1
Me_2HP	A	CH_3	CH_3		7.0±0.1
HP-HP	A	H	X_2	6.2±0.1	6.2±0.1
HP-HA	A	H	X_1	5.8±0.1	6.4±0.2
Pyrrolidinohistaprodifen	F				6.5±0.1
UR-AK46	B	X_5			4.9±0.1
UR-AK57	B	X_4			6.5±0.1
UR-AK68	B	X_3			5.4±0.1
UR-AK59	B	X_6			5.6±0.1
2-Benzylhistamine	C	$C_6H_5CH_2$			5.2±0.1
2-Phenylhistamine	C	C_6H_5			6.0±0.1
2-(2-Fluorophenyl)histamine	C	*o*-FC_6H_5			5.5±0.1
2-(3-Methylphenyl)histamine	C	*m*-$CH_3C_6H_5$			6.0±0.1
2-(3-Methoxyphenyl)histamine	C	*m*-$OCH_3C_6H_5$			6.6±0.1
2-(3-Fluorophenyl)histamine	C	*m*-FC_6H_5			6.2±0.1
2-(3-Trifluoromethylphenyl)histamine	C	*m*-$CF_3C_6H_5$			6.6±0.1
2-(3-Chlorophenyl)histamine	C	*m*-ClC_6H_5			6.4±0.1
2-(3-Bromophenyl)histamine	C	*m*-BrC_6H_5			6.7±0.1
2-(3-Iodophenyl)histamine	C	*m*-IC_6H_5			6.6±0.1
2-(4-Fluorophenyl)histamine	C	*p*-FC_6H_5			5.5±0.1
2-(4-Chlorophenyl)histamine	C	*p*-ClC_6H_5			4.8±0.1
2-(Methylphenylthiomethyl)histamine	C	X_7			5.6±0.1
2-(3,5-Difluoro-phenyl)histamine	C	X_8			6.1±0.1
2-(2-Thiazolyl)ethanamine	D				6.3±0.1

A conformational model for each compound was developed in Catalyst using the "Best" search option, 20 kcal/mol energy range and maximum number of 255 conformers. "Best" conformation generation is recommended to be used to construct a hypothesis automatically from a training set of molecules. Catalyst uses a specific algorithm for generating conformers, which emphases diversity. Since the hypothesis generator accepts only 255 conformers, the most efficient way of generating conformers is to select 255 as the maximum number of conformers.[68, 63]

2.2.3 Hypothesis Generation

Pharmacophore hypotheses are generated through the Catalyst program utilizing various chemical features in three–dimensional space. The commonly used features are H-bond acceptor (HBA); H-bond donor (HBD); general hydrophobic (HY); aromatic hydrophobic (Har); aliphatic hydrophobic (Hal); ring aromatic (RA), a vectored feature for the face-to-face interaction arrangement; positive charge (PC); positive ionisable (PI); negative charge and negative ionisable. The positive ionisable feature which is expected to interact with the conserved aspartate in the ligand binding pocket is a common feature in most of the agonist and antagonist ligands with a basic nitrogen. All features are represented by spheres which show the allowed volume for the group or atom corresponding to the feature to fit into. The vector features, HBD, HBA and RA, are represented *via* two spheres connected by a vector which displays the locations of interacting features on both ligand and receptor.[62]

In Catalyst training set data is used to generate ten hypothesis models using the HypoGen algorithm through three phases: "Constructive Phase", "Subtractive Phase" and "Optimization Phase". The Constructive Phase hypotheses are generated in three steps: 1) identifying the two most active compounds in the training set; 2) analyzing all the possible features and their pattern in three dimensions (maximum 5 different feature types) which fit the two most active compounds; and 3) identifying other active compounds according to the equation below:

$$MA \times Unc_{MA} - \frac{A}{Unc_A} > 0.0$$

Where *MA* is the activity of the most active compound, *Unc* is the user-specified uncertainty value, which is based on the experimental error value, and *A* is the activity of any questioned compounds. HypoGen keeps those hypotheses which fit the remaining active compounds.

In the subtractive phase, hypotheses generated in the constructive phase are analyzed in order to remove those hypotheses which fit most of the inactive compounds, as they are not able to distinguish between active and inactive compounds. In Catalyst an inactive compound is identified if its activity is 3.5 orders of magnitude greater than that of the most active compound:

$$log\ (A) - log\ (MA) > 3.5$$

In this equation *A* is the activity of the questioned compounds and *MA* is the activity of the most active compound.

The hypotheses created in the last two phases are optimized using a simulated annealing algorithm. In the optimization phase Catalyst aims to improve the hypothesis score (see below) by selection of a new hypothesis, addition or elimination of features or rotation of the vectored features. Lastly, the ten highest scoring pharmacophore hypotheses are reported.[63]

2.2.4 Assessment of Pharmacophore Hypotheses

Hypotheses are analyzed based on a number of statistical parameters which are calculated during the optimization step. These statistical criteria include: Correlation between actual and estimated activities (R^2), RMS (root-mean-square), Error cost, Fixed and Null cost. R^2 with the range value of 0.0-1.0 is the linear regression coefficient between measured activities (input) and estimated activities for the training set compounds using the hypothesis under investigation. The RMS value represents the differences between estimated and measured activities of the training set. The RMS value of the best hypothesis is close to 0.0. The error cost value increases with increasing RMS.[62]

Catalyst also measures two theoretical cost values including a “Fixed cost” with the minimum value and a “Null cost” with the highest score. These two theoretical cost values which are calculated in units of “bit” are used to predict the possibility of a successful experiment after 15 minutes from the start of a run. Each

hypothesis cost should be between these two values and should be closer to the fixed cost. The magnitude of the difference between the cost of an optimized hypothesis and the cost of the null hypothesis represents the chance of true correlation in the data. A difference higher than 60 bits indicates an outstanding chance for true correlation. A difference of 40-60 bits indicates that there is a 75-90% possibility of a true correlation in the data. When the difference drops below 40 bits, the chance of true correlation decreases to below 50%.

Apart from the cost, it is also recommended to take into consideration that the more active compounds should map all of the features. In contrast, the inactive compounds should not map most of the features. This is because they have poor interactions with the corresponding receptor features. Moreover, it is also imperative to check the configuration cost value is below 17.0. Configuration cost or entropy of the hypothesis space is a constant for all the generated hypotheses. For the training set if its value is less than 17.0 the entire space has been considered and all potential hypotheses have been inspected. If entropy is greater than 17.0, then the training set is too complex and should be modified.[63]

2.3 Developing H-1 Agonist Hypotheses

H-1 agonist hypotheses were developed through two major steps:

1) Initially, four hypotheses with different feature combination and uncertainty values, H-1 Agonist A, B, C and D, were runs where both histamine and lisuride derivatives were utilized in the selected training sets. This selection included 41 compounds (Table 2.1 and 2.2) with a range of activities between 1.2×10^{-8} M and 1.0×10^{-4} M. Attempted feature combinations were HBA, HBD, HY, PI and RA, and HBA, HBD, HY, PI and Har using uncertainty values of 3 or 4 (Table 2.3). As the molecules in the training sets were basic and protonated at physiological pH the Catalyst program was requested to find one positive ionizable feature for all molecules.

Table 2.3: H-1 Agonist Hypotheses, First Runs.

Hypothesis Generation Runs	Uncertainty	Allowed Features
H-1 Agonist A	3	HBA, HBD, HY, PI, RA
H-2 Agonist B	4	HBA, HBD, HY, PI, RA
H-3 Agonist C	3	HBA, HBD, HY, PI, Har
H-4 Agonist D	4	HBA, HBD, HY, PI, Har

Analysis of these runs showed that none of the generated hypotheses were acceptable in that the first output hypothesis in each run resulted in no correlation between data and no possibility of any feature. As an example, the statistical results of run A are summarized in Table 2.4.

Table 2.4: H-1 Agonist A.

Hypothesis	Total cost	RMS	Correl	Error Cost	Features
1	187.96	1.49	0	187.96	"empty"
2	189.55	1.27	0.53	174.94	2 RA HBD,
3	191.87	1.27	0.53	175.14	HBD, HY, RA
4	192.84	1.31	0.49	177.22	2 RA, HBD
5	193.05	1.31	0.48	177.37	2 RA, HBD
6	193.38	1.31	0.49	177.15	2 RA, HBD
7	194.11	1.28	0.52	175.75	HBD, HY, RA
8	194.36	1.36	0.41	180.03	2 RA, HBD
9	194.89	1.31	0.48	177.53	2 RA, HBD
10	194.32	1.32	0.48	177.74	2 RA, HBD
fixed cost	155.26	0	0	141.27	
null cost	187.96	1.49	0	187.96	

As illustrated in Table 2.4, the HY feature was not found often in the resultant hypotheses. Furthermore, the HBA and more importantly the PI feature did not appear in any of the output hypotheses. As was discussed before, PI is expected to be the most important feature of the pharmacophore since it could determine the basic nitrogen which is expected to make a salt bridge with the conserved aspartate in the ligand binding pocket.[69] Statistical analysis also confirmed that the resultant hypotheses were invalid because there were high predicted errors for the most active compound (8*R*-Lisuride) and low correlation between the training set data and the predicted activities. The value of total cost for each hypothesis was also greater than the cost of the null hypothesis. The same results were obtained from the H-1 Agonist B, C and D runs. Altering the uncertainty value and feature combination could not improve the output hypotheses.

2) At the second stage, hypotheses were independently generated for two training sets (Histamine and Lisuride derivatives). The major reason for reconsidering training sets was based on the different molecular structure of Histamine and Lisuride derivatives. It was assumed that simultaneously using Histamine derivatives with a flexible structure and Lisuride derivatives with a rigid structure could possibly cause the low correlation between data and the poor hypotheses outputs. The output hypotheses of Histamine derivatives (Table 2.2) using the feature composition of HBA, HBD, HY, PI and RA or HBA, HBD, HY, PI and Har with uncertainty values of either 3 or 4 did not show any improvement in the previous statistical results where the first hypothesis of some of the runs still showed no correlation between data. It was postulated that Histamine is much smaller than the other derivatives thus, possibly, by removing it from the training set that there would be a better correlation between the data and consequently a more acceptable resultant hypotheses, but this was not the case.

At the last stage of developing H-1 agonist pharmacophores, hypothesis generation was conducted with the HypoGen algorithm utilizing Lisuride derivatives (Table 2.1) as the training set. Feature composition and uncertainty values are displayed in Table 2.5.

Table 2.5: H-1 Agonist Hypotheses, Second Runs.

Hypothesis Generation Runs	Uncertainty	Allowed Features
H-1 Agonist-1	3	HBA, HBD, HY, PI, RA
H-1 Agonist-2	3	HBA, HBD, HY, PI, Har
H-1 Agonist-3	4	HBA, HBD, HY, PI, RA
H-1 Agonist-4	4	HBA, HBD, HY, PI, Har

Analysis of the resultant hypotheses suggested that H-1 Agonist-1 with the uncertainty value of 3 and the feature composition of HBA, HBD, HY, PI and RA was the best run because each of the ten hypotheses of this run contains 4-5 features which were either similar or different while other runs (H-1 Agonist-2, H-1 Agonist-3 and H-1 Agonist-4) only had 2 or 3 features per hypothesis. The statistical results for the ten H-1 Agonist-1 hypotheses are summarized in Table 2.6.

Table 2.6: H-1 Agonist-1 hypotheses.

Hypothesis	Total cost	RMS	Correl	Error Cost	Features
1	61.9	0.81	0.9	47.95	3 HY, HBA, PI
2	62.47	0.86	0.89	48.52	3 HY, RA
3	62.8	0.88	0.88	48.79	3 HY, RA
4	62.81	0.89	0.88	48.89	3 HY, RA
5	62.9	0.89	0.88	48.83	3 HY, HBD
6	62.92	0.9	0.88	48.99	3 HY, RA
7	62.97	0.9	0.88	48.96	3 HY, HBD
8	63	0.91	0.87	49.09	3 HY, RA
9	63.01	0.91	0.87	46.09	3 HY, HBD
10	63.098	0.91	0.87	49.17	3 HY, RA
fixed cost	57.64	0	0	43.73	
null cost	66.42	1.87	0	66.42	

As illustrated in Table 2.6, hypoythesis H-1 Agonist-1-1 included the highest number and the most variety of features and furthermore, it was the only hypothesis with the PI feature. Statistical analysis of hypothesis H-1 Agonist-1-1 showed very good correlation (0.90) and also a configuration cost below 17.0 (12.8). However, the cost difference between null and hypothesis cost was only 4.5. Statistical analysis of the other hypotheses in Table 2.6 also confirmed that they were not quantitatively valid to predict the biological activity of the target ligands in any absolute sense. However, since these hypotheses were the best ones available, it was still considered possible to utilize these pharmacophores as qualitative patterns to direct the synthetic pathways.

In the next step of pharmacophore development, hypothesis H-1 Agonist-1-1 was modified using excluded volume (ev) with the HypoRefine algorithm of Catalyst. Each exclusion sphere is placed as a solid sphere in which no mapping is possible so that the space accessible to the ligands is restricted. HypoRefine is used in order to attempt to optimize the correlation between actual activity values and the activity values estimated by Catalyst by placing exclusion spheres around the ligands.[70] Statistical results of the ten hypotheses H-1 Agonist-ev are summarized in Table 2.7.

Table 2.7: H-1 Agonist-ev hypotheses.

Hypothesis	Total cost	RMS	Correl	Error Cost	Features
1	62.26	0.73	0.92	47.22	3 HY, HBA, HBD
2	62.35	0.85	0.89	48.42	3 HY, RA
3	62.38	0.84	0.89	48.4	4 HY, HBA
4	62.59	0.87	0.88	48.68	3 HY, RA
5	62.59	0.86	0.89	48.59	2 HY, HBA, RA
6	62.8	0.88	0.88	48.79	3 HY, RA
7	63	0.91	0.87	49.09	3 HY, RA
8	63.03	0.9	0.88	48.98	2 HY, HBA, RA
9	63.14	0.92	0.87	49.22	3 HY, RA
10	63.23	0.89	0.88	48.89	2 HY, HBA, HBD, ev
fixed cost	57.64	0	0	43.73	
null cost	66.42	1.87	0	66.42	

As shown in Table 2.7, hypothesis 10 was the only one which contained a volume exclusion sphere (ev). Therefore, H-1 Agonist-10-ev with a correlation value of 0.89 and configuration cost of 12.8 was used qualitatively in order to distinguish any possible steric clashes between a region of the candidate ligands and the H-1 receptor. Ultimately, hypotheses H-1 Agonist-1-1 and H-1 Agonist-10-ev were merged to afford the new hypothesis “Merged 1” which was able to illustrate all feature combinations of the final optimized H-1 Agonist pharmacophore. (Figure 2.1)

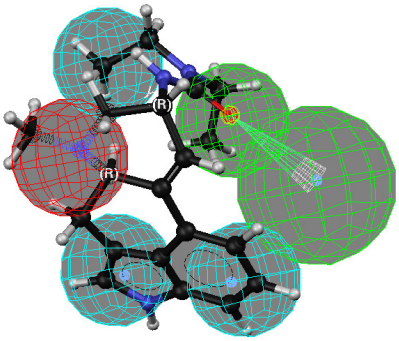

A; Est: 2.3 x 10^{-8}, Exp: 1.2 x 10^{-8}

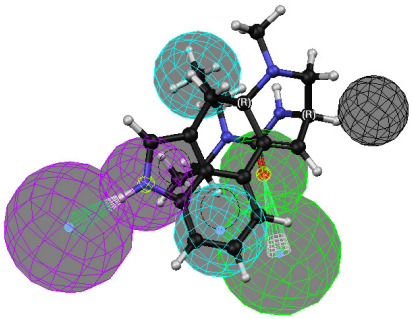

B; Est: 3.1 x 10^{-8}, Exp: 1.2 x 10^{-8}

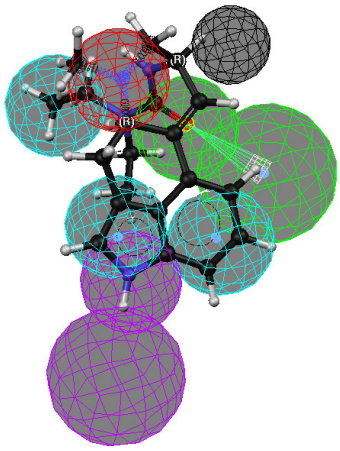

C

Figure 2.1: 8*R*-Lisuride Mapped into the H-1 Agonist-1-1 pharmacophore. (A), H-1 Agonist-10-ev pharmacophore (B), Merged 1(C). Est: estimated activity value in M (EC_{50}). Exp: actual activity value in M (EC_{50}). The colored spheres correspond to the pharmacophoric features with the following colors: blue, HY; green, HBA; red, PI; purple, HBD; black, ev.

2.4 Pharmacophore Use

One of the most useful applications of a pharmacophore model in medicinal chemistry is designing new therapeutic agents and modifying undesired side effects of drugs. A pharmacophore could be used quantitatively and qualitatively to predict and compare the activities of the different compounds and consequently to direct the synthesis route since compounds predicted to be more active are more likely to be worth synthesizing and testing. Hence, "olanzapine" was mapped into the three pharmacophores (H-1 Agonist-1-1 and H-1 Agonist-10-ev and Merged 1) in order to obtain some practical ideas regarding which types of modifications were required

to adjust the H-1 antagonist property of the drug to a H-1 agonist. H-1 Agonist-10 -ev and Merged 1 were used just to evaluate if any change to the structure of olanzapine proposed from pharmacophore H-1 Agonist-1-1 could possibly lead to steric clashes with the receptor.

2.4.1 Modification of Olanzapine (First Generation)

Modification of olanzapine was attempted through several steps. Initially, olanzapine was mapped to the pharmacophores H-1 Agonist-1-1 and H-1 Agonist-10-ev (Figure 2.2). The resultant E.A, "Estimated Activity", and "Fit" value were 4.5×10^{-5} M and 2.2×10^{-6} M and 5.9 and 5.0, respectively. The Catalyst program predicts the activity between ligand and the mapped pharmacophore and reports this value as the "Estimated Activity". "Fit" value shows the quality of interaction between ligand and different features of the pharmacophore. A ligand with higher fit value conforms better to the pharmacophore.[62]

The maximal possible fit value depends on the number of features in a pharmacophore and their weight values. Since the weight values of features did not change in generating pharmacophores the default of equal weight for all features was used. Every feature will then be given a weight of 2. The reason for this is that based on a very rough rule of thumb, the activity of a compound is expected to drop 100 fold for every feature that is missed when mapping a compound to a pharmacophore. The highest possible fit value is then the number of features in each pharmacophore multiplied by two. Therefore for the pharmacophore H-1 Agonist-1-1 with 4 features and the H-1 Agonist-10-ev with 5 features the highest possible fit value is 8.0 and 10.0, respectively.

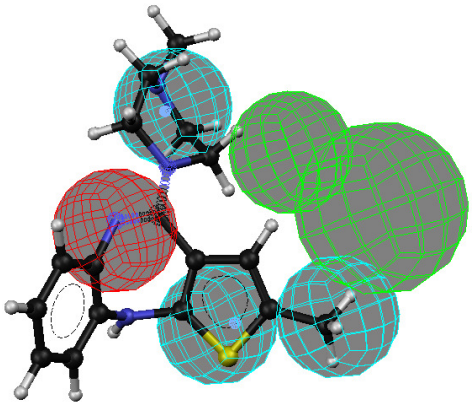

A; Est: 4.5 x 10^{-5}, Exp: 7.0 x 10^{-9}

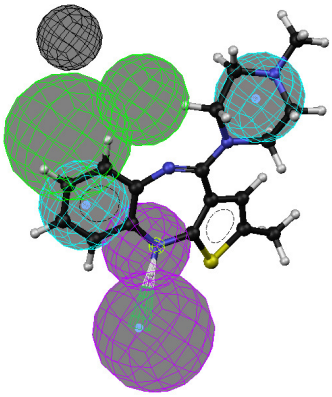

B; Est: 2.2 x 10^{-6}

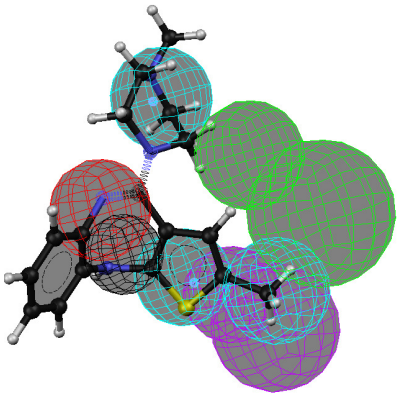

C

Figure 2.2: Olanzapine Mapped into the H-1 Agonist-1-1 pharmacophore. (A), H-1 Agonist-10-ev pharmacophore (B), Merged 1(C). Est: estimated activity value in M (EC_{50}), Exp: experimental activity value (K_i) of olanzapine with H-1 receptor in M.[16] The colored spheres correspond to the pharmacophoric features with the following colors: blue, HY; green, HBA; red, PI; purple, HBD; black, ev.

As discussed before, pharmacophores H-1 Agonist-1-1 and H-1 Agonist-10-ev were generated according to the training set (Table 2.1, page 16) containing agonist compounds with known activities (EC_{50}). The estimated activity of any new compounds mapped into these pharmacophore is then based on EC_{50} predicting agonist activity of these ligands. Experimental activity of olanzapine (K_i: 7.0 x 10^{-9} M, IC_{50}: 50 x 10^{-9} M)[15, 16] obtained from the literature indicates the antagonist activity of olanzapine at the H-1 receptor. Therefore, as shown in Figure 2.2, the activity of olanzapine, as an antagonist, was not well predicted in agonist pharmacophores (H-1 Agonist-1-1 and H-1 Agonist-10-ev).

To modify olanzapine from a H-1 antagonist to a H-1 agonist, various structural modifications were applied. As shown in Figure 2.2, no part of the molecule was mapped to the HBA feature (green). To improve the predicted H-1 agonist activity of olanzapine, a number of different chemical groups were accommodated in the thiophene ring at positions C-2 and C-3 (R_1 and R_2) and also in the *N*-methylpiperazine ring at position C-2′ , C-3′, C-5′ and C- 6' (R_3, R_4, R_5 and R_6). (Figure 2.3)

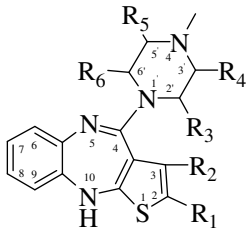

Figure 2.3: Structure of olanzapine derivatives showing atom numbering; R_1:CH_3; R_2, R_3, R_4, R_5 and R_6: H

At the outset of modifying olanzapine, HBA groups were placed on C-3′ (R_4), followed by the same modification on C-5′ (R_5), C-3 (R_2), C-6' (R_6), and also at positions C-3 and C-6′ simultaneously. Resultant estimated activity and fit values of the proposed ligands using pharmacophore H-1 Agonist-1-1 are summarized in Table 2.8.

Table 2.8: Proposed H-1 agonists. First Modification. (See Figure 2.3 for structure)

Compound	R_1	R_2	R_3	R_4	R_5	R_6	E.A (M)	Fit
1	CH_3	H	H	(*R*) OCH_3	H	H	6.3×10^{-5}	5.8
2	CH_3	H	H	(S) OH	H	H	3.8×10^{-5}	6.2
3	C_2H_5	H	H	(S) OH	H	H	3.9×10^{-6}	7.0
4	C_2H_5	H	H	H	(*S*) OH	H	2.2×10^{-6}	7.2
5	C_2H_5	H	H	H	(**S**) OH	H	2.2×10^{-6}	7.2
6	C_2H_5	H	H	H	(*R*)OCH_3	H	6.1×10^{-6}	6.8
7	C_2H_5	$COCH_3$	H	H	H	H	4.1×10^{-6}	6.9
8	C_2H_5	OCH_3	H	H	H	H	4.3×10^{-6}	6.9
9	C_2H_5	$NHCH_3$	H	H	H	H	8.1×10^{-6}	4.7
10	C_2H_5	CH_2NHCH_3	H	H	H	H	8.3×10^{-6}	6.6
11	C_2H_5	CH_2NH_2	H	H	H	H	7.7×10^{-6}	6.7
12	C_2H_5	NH_2	H	H	H	H	6.8×10^{-6}	6.7
13	C_2H_5	$COCH_3$	H	H	H	H	4.1×10^{-6}	6.9
14	H	C_2H_5	H	H	H	(*R*) $CH_2CH_2CH_3$	1.5×10^{-5}	6.4
15	H	C_2H_5	H	H	H	(*S*) $CH_2CH_2CH_3$	2.8×10^{-6}	7.1
16	C_2H_5	C_2H_5	H	H	H	(*S*) C_2H_5	3.2×10^{-6}	7.1
17	C_2H_5	C_2H_5	H	H	H	(*R*) C_2H_5	3.1×10^{-6}	7.1
18	**CH_3**	**$COCH_3$**	H	H	**(*R*) C_2H_5**	**H**	**6.6×10^{-7}**	**7.8**
19	CH_3	$COCH_3$	H	H	(*S*) C_2H_5	H	2.1×10^{-6}	7.2
20	CH_3	H	H	H	H	(*S*) $COCH_3$	1.8×10^{-6}	7.3
21	CH_3	H	H	H	H	(*R*) $COCH_3$	5.2×10^{-6}	6.9
22	CH_3	H	H	H	H	(*S*) CH_3,$COCH_3$	3.7×10^{-6}	7.0
23	CH_3	H	H	H	H	(*R*) CH_3,$COCH_3$	1.2×10^{-5}	6.5
24	CH_3	H	H	H	H	(*R*) C_2H_5,$COCH_3$	8.2×10^{-6}	6.7
25	CH_3	H	H	H	H	(S) C_2H_5,$COCH_3$	6.8×10^{-6}	6.7
26	CH_3	H	H	H	H	(*R*) C_3H_7, $COCH_3$	4.1×10^{-6}	7.0
27	**CH_3**	**CH_3**	**H**	**H**	**H**	**(*S*) C_2H_5, $COCH_3$**	**6.5×10^{-7}**	**7.8**
28	CH_3	CH_2NH_2	H	H	H	(*S*) C_2H_5, $COCH_3$	1.5×10^{-6}	7.4
29	CH_3	CH_2OH	H	H	H	(*S*) C_2H_5, $COCH_3$	1.2×10^{-6}	7.5
30	CH_3	$COCH_3$	H	H	(*R*) C_2H_5	(*S*) NH_2	7.2×10^{-6}	6.7
31	CH_3	$COCH_3$	H	H	(*R*) C_2H_5	(*R*) NH_2	9.0×10^{-6}	6.6
32	CH_3	$COCH_3$	H	H	(*R*) C_2H_5	(*R*) OCH_3	1.1×10^{-6}	7.5
33	CH_3	$COCH_3$	H	H	(*R*) C_2H_5	(*S*) OCH_3	2.0×10^{-6}	7.3
34	CH_3	CH_2NH_2	H	H	H	H	1.7×10^{-5}	6.4

Table 2.8 (Cont` d): Proposed H-1 agonists. First Modification. (See Figure 2.3 for structure)

Compound	R_1	R_2	R_3	R_4	R_5	R_6	E.A (M)	Fit
35	CH_3	NH_2	H	H	H	H	1.5×10^{-5}	6.4
36	CH_3	CH_2NH_2	H	H	H	(*S*) C_2H_5	3.0×10^{-6}	7.1
37	**CH_3**	**CH_2OH**	**H**	**H**	**H**	**(*R*) I, $COCH_3$**	**3.3×10^{-7}**	**8.1**
38	CH_3	CH_2OH	H	H	H	(*R*) Br, $COCH_3$	1.1×10^{-6}	7.5
39	CH_3	CH_2OH	H	H	H	(*S*) I, $COCH_3$	1.8×10^{-6}	7.8
40	CH_3	CH_2OH	H	H	(*R*) H, I	(*S*) $COCH_3$	1.4×10^{-6}	7.4
41	**CH_3**	**CH_2COCH_3**	**H**	**H**	**H**	**(*S*) C_2H_5, $COCH_3$**	**8.4×10^{-7}**	**7.6**
42	CH_3	CH_2NH_2	H	H	H	(*R*) C_2H_5, $COCH_3$	1.7×10^{-6}	7.3
43	CH_3	CH_2COCH_3	H	H	H	(*S*) C_2H_5, $COCH_3$	5.3×10^{-6}	6.8
44	CH_3	CH_2OH	H	H	H	(*R*) C_2H_5, $COCH_3$	1.2×10^{-6}	7.5
45	CH_3	CH_2OH	H	H	H	(*S*) $CHCH_2$, $COCH_3$	2.5×10^{-6}	7.2
46	**CH_3**	**CH_2OH**	**H**	**H**	**(*R*) C_2H_5**	**(*S*) C_2H_5, $COCH_3$**	**7.4×10^{-7}**	**7.7**
47	**CH_3**	**CH_2OH**	**H**	**H**	**(*S*) C_2H_5**	**(*S*) C_2H_5, $COCH_3$**	**5.5×10^{-7}**	**7.8**

As shown in Table 2.8, ligands **18**, **27**, **37**, **41**, **46** and **47** had the highest predicted activity (lowest EC_{50}) and fit values which were certainly greater than the original value of olanzapine. This progress was attributed to the locating of the functional groups $–CH_2OH$ and $–CH_2COCH_3$ at position C-3 and $– COCH_3$ at position C-6′. For instance, ligand **37** with E.A value of 3.3×10^{-7} M and fit value of 8.8 was completely mapped to all features of H-1 Agonist-1-1. Notably, there was also no possibility for this candidate to map to the volume exclusion feature. (Figure 2.4)

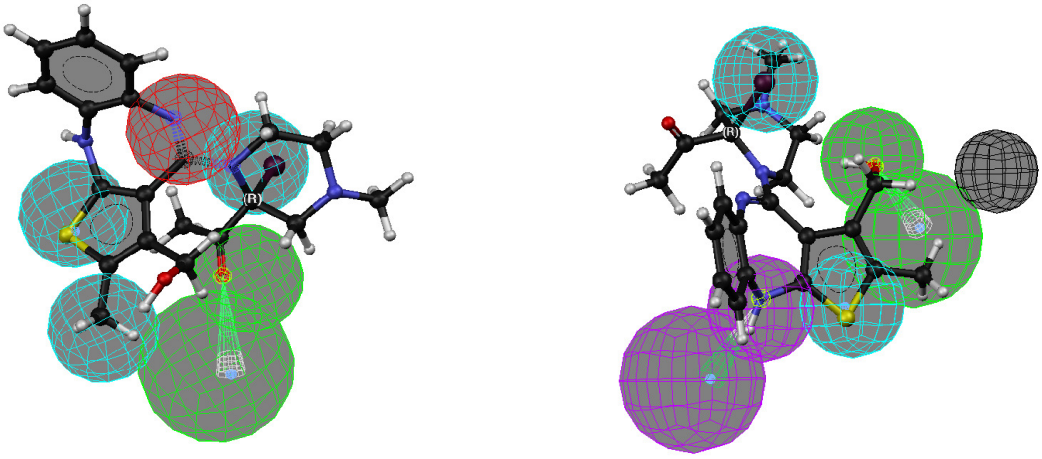

A; Est: 3.3 x 10^{-7} **B**; Est: 1.2 x 10^{-6}

Figure 2.4: Compound **37** Mapped into the H-1 Agonist-1-1 pharmacophore. (A), H-1 Agonist-10-ev pharmacophore (B). Est: estimated activity value in M. The colored spheres correspond to the pharmacophoric features with the following colors: blue, HY; green, HBA; red, PI; purple, HBD; black, ev

At the next stage of the modification of olanzapine, the *N*-methylpiperazine ring was replaced by more flexible amino groups. The resultant EA and Fit values (Table 2.9) suggested that ring-opened piperazine derivatives could potentially furnish highly active H-1 agonist ligands. These results were achieved where – CH_2OH, – $COCH_3$ or $–CH_2NH_2$ were substituted on C-3 as the optimized functional groups for H-1 agonist activity.

Table 2.9: Proposed H-1 agonists, Second Modification.

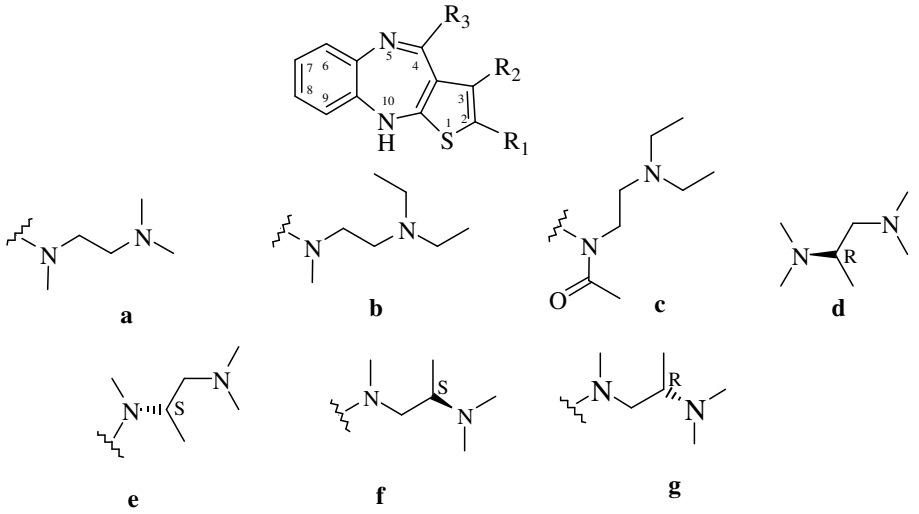

Table 2.9 (Cont` d): Proposed H-1 agonist. Second modification

Compound	R_1	R_2	R_3	E.A (M)	Fit
48	**CH_3**	**CH_2OH**	**a**	**1.7×10^{-7}**	**8.3**
49	CH_3	$COCH_3$	a	1.3×10^{-6}	7.4
50	CH_3	CH_2NH_2	a	4.7×10^{-6}	6.9
51	**CH_3**	**CH_2OH**	**b**	**1.7×10^{-7}**	**8.3**
52	CH_3	$COCH_3$	b	1.2×10^{-6}	7.5
53	CH_3	CH_2NH_2	b	2.8×10^{-6}	7.1
54	CH_3	CH_2OH	c	1.1×10^{-6}	7.5
55	CH_3	$COCH_3$	c	1.5×10^{-6}	7.4
56	CH_3	CH_2NH_2	c	2.6×10^{-6}	7.1
57	**CH_3**	**CH_2OH**	**d**	**8.1×10^{-7}**	**7.6**
58	**CH_3**	**$COCH_3$**	**d**	**7.1×10^{-7}**	**7.7**
59	CH_3	CH_2NH_2	d	2.8×10^{-6}	7.1
60	**CH_3**	**CH_2OH**	**e**	**3.9×10^{-7}**	**8.0**
61	CH_3	$COCH_3$	e	1.3×10^{-6}	7.5
62	CH_3	CH_2NH_2	e	2.4×10^{-6}	7.2
63	**CH_3**	**CH_2OH**	**f**	**2.8×10^{-7}**	**8.1**
64	CH_3	$COCH_3$	f	1.8×10^{-6}	7.3
65	CH_3	CH_2NH_2	f	1.9×10^{-6}	7.5
66	**CH_3**	**CH_2OH**	**g**	**5.0×10^{-7}**	**7.8**
67	CH_3	$COCH_3$	g	2.6×10^{-6}	7.1
68	CH_3	CH_2NH_2	g	4.1×10^{-6}	6.9

According to Table 2.9, compounds **48, 51**, **57**, **58**, **60**, **63**, **66** with the highest estimated activity and fit value in this group were the most worthy of synthesizing and testing.

All proposed candidates (**1**-**68**) like known atypical antipsychotics have more than one nitrogen atom in their molecular structures while pharmacophore Agonist-1-1 contains just one PI feature. Since the most basic nitrogen of antipsychotic drugs with H-1 antagonist activity is known to make a salt bridge with a conserved aspartate in the binding pocket, it is important to know or calculate which nitrogen is the most likely to be protonated in each molecule. For

that reason the pKa values of olanzapine were evaluated and they were found to be 4.69 and 7.37. [71] Based on the fact that the amidine nitrogen (N-5, Figure 2.5) has conjugated resonance with the fused aromatic ring, it is predicted that the free distal nitrogen of the piperazine ring (N-4′, Figure 2.5) is more basic. Thus, for olanzapine at physiological pH (7.40) a pKa value of 7.37 means approximately equal amounts of free and protonated amidine nitrogen are expected; however, since at this pH the ratio of protonated to free piperazine amine is about 10^3 (pKa 4.69), the distal nitrogen is more likely to be protonated. distal nitrogen of the piperazine ring was expected to be protonated at pH 7.40.

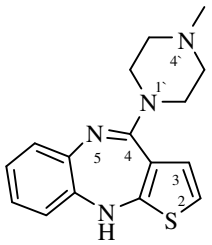

69

Figure 2.5: Structure of olanzapine showing atom numbering.

On the other hand, the conjugated nitrogen of the amidine moiety in all of the proposed ligands (**1**-**68**) was mapped to the PI feature of H-1 Agonist-1-1. Furthermore, one of the hydrophobic features of the pharmacophore was mapped to the piperazine ring. If the distal nitrogen is protonated as proposed, this would reduce the hydrophobicity of this ring. This might mean that the first generation of modified olanzapine derivatives will display lower activities than predicted.

These contradictions prompted us to remove the distal nitrogen of the *N*-methylpiperazine ring. Compounds **48** and **51** with the highest predicted activities were utilized for further modification. The estimated activity and fit value of truncated modifications of **51** (**70**-**85**) without the distal nitrogen were investigated where R_1 was a hydrophobic group such as CH_3, CH_2Br, CH_2Cl, C_2H_5, C_2H_4Br or C_2H_4Cl and R_2 was a hydrogen bond acceptor group such as CH_2OH or C_2H_4OH. The predictions are summarized in Table 2.10.

Table 2.10: Proposed H-1 agonists. Third Modification

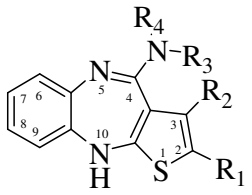

Compound	R_1	R_2	R_3	R_4	E.A (M)	Fit
70	CH_3	CH_2OH	C_2H_5	H	1.1×10^{-6}	7.5
71	C_2H_5	CH_2OH	C_2H_5	H	3.4×10^{-6}	8.1
72	CH_3	C_2H_5OH	C_2H_5	H	2.4×10^{-6}	7.2
73	C_2H_5	C_2H_5OH	C_2H_5	H	1.3×10^{-6}	7.5
74	CH_2Cl	CH_2OH	C_2H_5	H	4.3×10^{-7}	7.9
75	CH_2Br	CH_2OH	C_2H_5	H	3.3×10^{-7}	8.9
76	C_2H_4Cl	CH_2OH	C_2H_5	H	1.1×10^{-6}	7.5
77	**C_2H_4Br**	**CH_2OH**	**C_2H_5**	**H**	**5.4×10^{-7}**	**7.8**
78	**C_2H_5**	**CH_2OH**	**CH3**	**H**	**1.2×10^{-7}**	**8.5**
79	**CH_2Br**	**CH_2OH**	**C_2H_5**	**CH_3**	**1.5×10^{-7}**	**8.4**
80	C_2H_5	CH_2OH	$CH(CH_3)_2$	H	2.9×10^{-6}	7.1
81	CH_2Cl	CH_2OH	$CH(CH_3)_2$	H	1.7×10^{-6}	7.3
82	CH_2Br	CH_2OH	$CH(CH_3)_2$	H	2.5×10^{-6}	7.2
83	C_2H_5	CH_2OH	CH_3	CH_3	9.5×10^{-6}	6.6
84	**CH_2Cl**	**CH_2OH**	**C_2H_5**	**CH_3**	**1.3×10^{-7}**	**8.5**
85	**C_2H_5**	**CH_2OH**	**C_2H_5**	**C_2H_5**	**1.0×10^{-7}**	**8.0**
86	**C_2H_5**	**CH_2OH**	**C_2H_5**	**CH3**	**1.1×10^{-7}**	**7.1**

According to Table 2.10, compounds **75**, **78**, **79**, **84**, **85** and **86** showed significant estimated activities and fit values with the pharmacophore H-1 Agonist 1-1, where R_1 was modified to C_2H_5, CH_2Br and CH_2Cl, and CH_2OH was kept as the optimized functional group on C-3. Consequently, CH_2Br, CH_2Cl and particularly C_2H_5 were proposed as the best hydrophobic groups on C-2 to map one of the hydrophobic (HY) features.

In order to increase the flexibility in synthesis $-NR_3R_4$ (Table 2.10) was replaced by a series of cyclic bases including piperidine, 4-methylpiperidine, morpholine and pyrolidine using the optimized groups C_2H_5 and CH_2OH at position

C-2 and C-3, respectively. The resultant predicted activities and fit values are shown in Table 2.11.

Table 2.11: Proposed H-1 agonists- Fourth Modification.

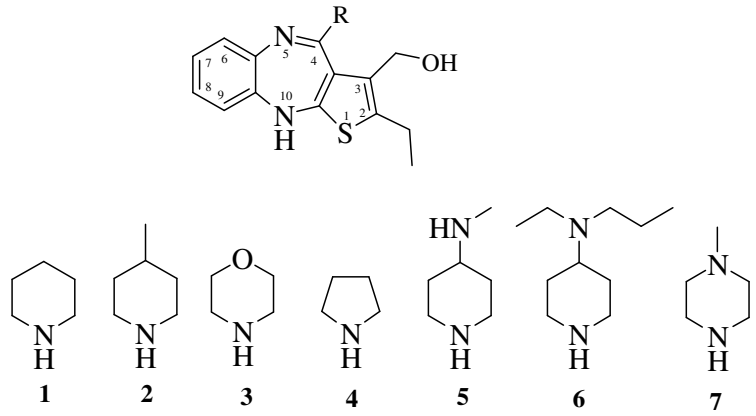

1 **2** **3** **4** **5** **6** **7**

Compound	R	E.A (M)	Fit
87	**1**	**6.0×10^{-7}**	**7.8**
88	2	1.0×10^{-6}	7.4
89	3	1.5×10^{-6}	7.4
90	**4**	**6.1×10^{-7}**	**7.8**
91	5	3.0×10^{-6}	7.1
92	**6**	**6.0×10^{-7}**	**7.8**
93	**7**	**4.9×10^{-7}**	**7.9**

As shown in the Table 2.11 compounds **87**, **90**, **92** and **93** with potential H-1 agonist activity were proposed as the most worthy synthetic alternatives.

2.4.2 Modification of Olanzapine (Second Generation)

The second generation of modified olanzapine derivatives was proposed based on the structure of typical antipsychotics including triprolidine (**94**), chlorpromazine (**95**) and prochlorperazine (**96**) (Figure 2.6)

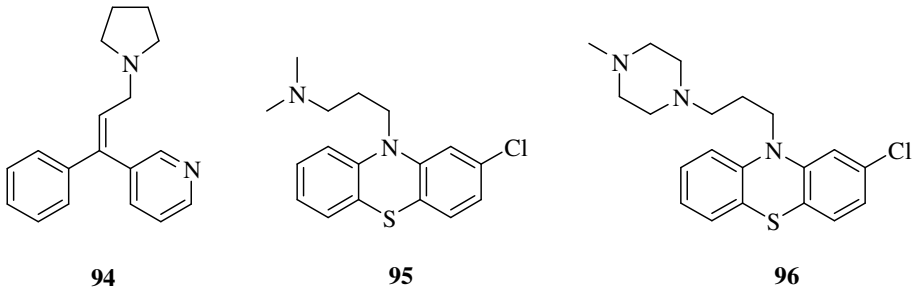

Figure 2.6: Chemical structure of Triprolidine (**94**), Chlorpromazine (**95**) and Prochlorperazine (**96**).

According to Figure 2.6, the distal amine of these typical antipsychotic drugs is linked to the centre of a tricyclic moiety *via* a $(CH_2)_n$ chain. To develop the second generation of modified olanzapine, a $(CH_2)_2$ link was inserted between the carbon and the basic nitrogen (N-1′) of the amidine group (**87** in Figure 2.7). The new candidate (**97**) (Figure 2.7) was mapped to the pharmacophore H-1 Agonist-1-1 (Figure 2.8). The resultant estimated activity and fit values, 4.1 x 10^{-6} M and 7.0, were slightly improved to 2.0 x 10^{-6} M and 7.3 when using a diethylamine group instead of a piperidine ring (**98**) (Figure 2.7). As discussed above, the pharmacophore mapping of the first generation of derivatives e.g. **93** and its analogues showed that the conjugated amidine nitrogen (N-5) rather than the N-4′ fitted to the PI feature of the pharmacophore H-1 Agonist-1-1. However, the distal nitrogen (N-1′) of **97** and **98** was now recognized by the pharmacophore as the ligand-receptor interaction site.

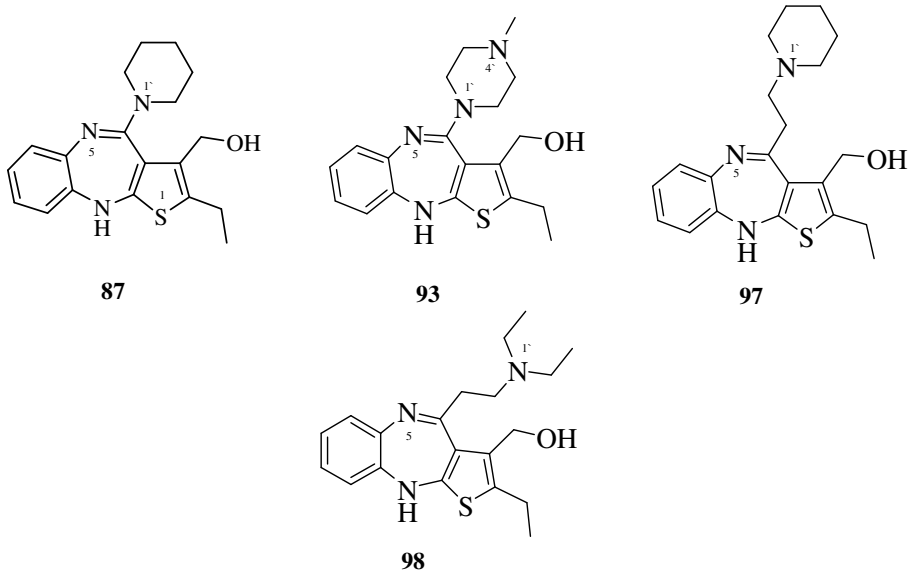

Figure 2.7: Chemical structure of **87**, **93**, **97** and **98** showing atom numbering.

The free distal nitrogen (N-1′) of **97** and **98** was expected to be more basic than the conjugated nitrogen (N-5), therefore, it was suggested that the second generation of modified olanzapine derivatives can be reasonable targets for synthetic direction and biological evaluation on H-1 receptor.

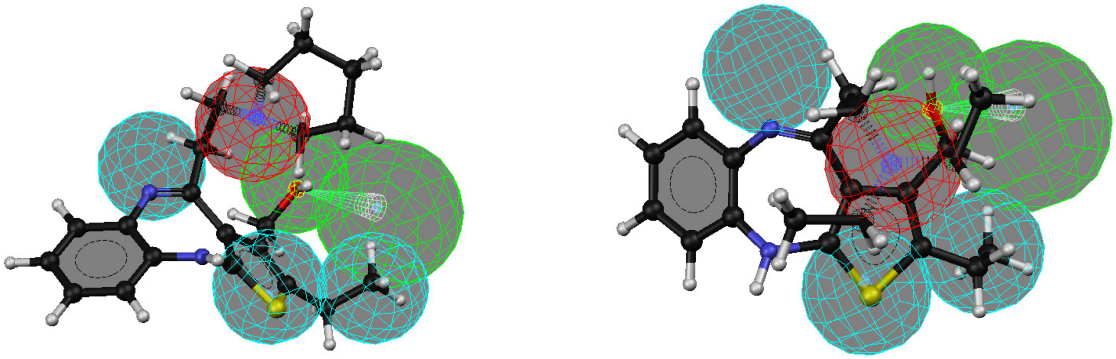

97; Est: 4.1 x 10^{-6} **98**; Est: 2.0 x 10^{-6}

Figure 2.8: Compounds **97** and **98** Mapped into the H-1 Agonist-1-1 pharmacophore. Est: estimated activity value in M. The colored spheres correspond to the pharmacophoric features with the following colors: blue, HY; green, HBA; red, PI; purple, HBD; black, ev

2.5 Conclusions

In conclusion, computer-aided drug design techniques were used to generate a pharmacophore model from published H-1 agonist ligands. The attempted hypothesis generation runs led to a number of hypotheses represented through three-dimensional pattern of features. Qualitative and quantitative analysis of these hypotheses proposed that hypothesis H-1 Agonist-1-1, with the most variety of features and also with the possibility for the PI feature, could be the best pharmacophoric pattern for modification of olanzapine. Subsequent to the four steps of modification, these three alterations to the structure of olanzapine were suggested: 1) replacing the methyl group at position C-2 with ethyl; 2) substituting hydroxymethyl (-CH_2OH) at position C-3; and 3) removing the distal nitrogen from position N-4′. The three modification sites are shown in Figure 2.9. Synthesis and pharmacological evaluation of these proposed modifications will be discussed in Chapters 3 and 5, respectively.

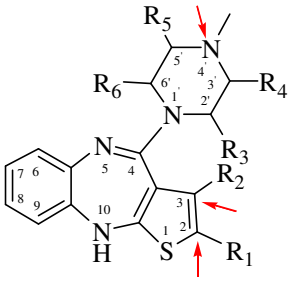

Figure 2.9: Structure of olanzapine derivatives showing atom numbering; R_1:CH_3; R_2, R_3, R_4, R_5 and R_6: H. Red arrows show three modification sites; C-2, C-3 and N-4′.

CHAPTER 3: SYNTHESIS

3.1 Introduction

As discussed in Chapter 2, three chemical structural modifications were proposed to the structure of olanzapine, including substituting the ethyl and the hydroxymethyl groups at positions C-2 and C-3 respectively, and also removing the nitrogen atom from position 4′ of the piperazine ring (Figure 2.9, page 40). In this chapter the attempted synthetic methodologies leading to these modified targets will be discussed. In Table 3.1, the molecular structure of the suggested candidates for synthesis and biological evaluation are illustrated. As shown, compounds **99**, **100** and **101** represent a single modification to the structure of olanzapine with the alteration of R_1 to C_2H_5 (**99**), substitution of a hydroxymethyl group at position C-3 (**100**) and replacement of the *N*-methylpiperazine ring with a piperidine ring (**101**). Compound **102** shows two modifications at positions C-2 and N-4′ while **87** contains all three afore-mentioned modifications. The synthetic possibilities of the proposed compounds will be evaluated in this chapter.

Table 3.1: Proposed modified compounds for synthesis.

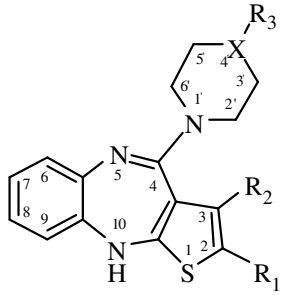

Compound	R_1	R_2	R_3	X
99	C_2H_5	H	CH_3	N
100	CH_3	CH_2OH	CH_3	N
101	CH_3	H	H	C
102	C_2H_5	H	H	C
87	C_2H_5	CH_2OH	H	C

Most available antipsychotic agents, including clozapine (Figure 1.1, page 3) and olanzapine (Figure 2.3, page 29) possess a tricyclic benzodiazepine system.[72] Over the last thirty years a number of synthetic methods for the preparation of olanzapine (2-methyl-4-(4-methyl-1-piperazinyl)-10*H*-thieno-[2,3,*b*][1,5]benzodiazepine) have been developed.[71-76] Two general synthetic routes are outlined in the Schemes 3.1 and 3. 2.

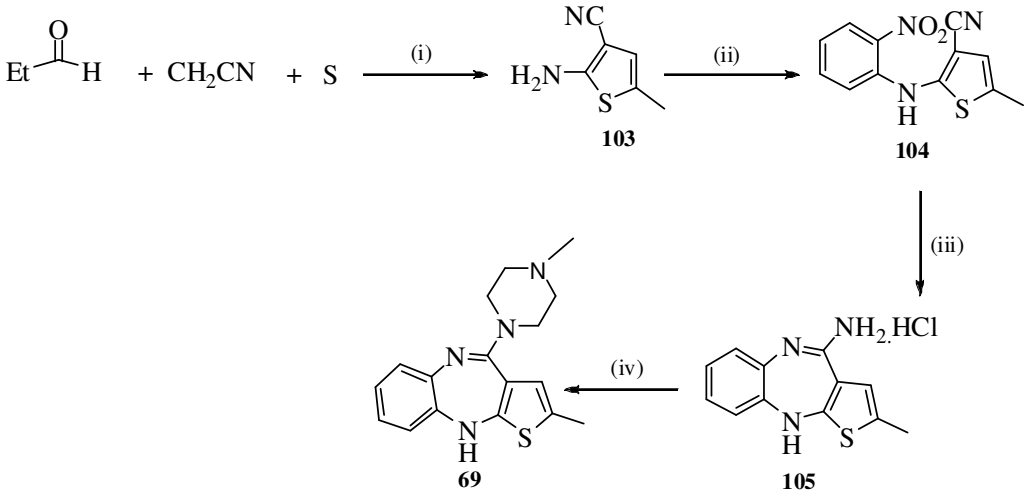

Scheme 3.1: Synthesis of olanzapine (route A). Reagents: (i) Et_3N, DMF; (ii) *o*-fluoronitrobenzene, K_2CO_3 or LiOH, DMSO or NaH, THF; (iii) $SnCl_2$, EtOH; (iv) *N*-methylpiperazine (NMP), toluene, DMSO.[16, 73, 74]

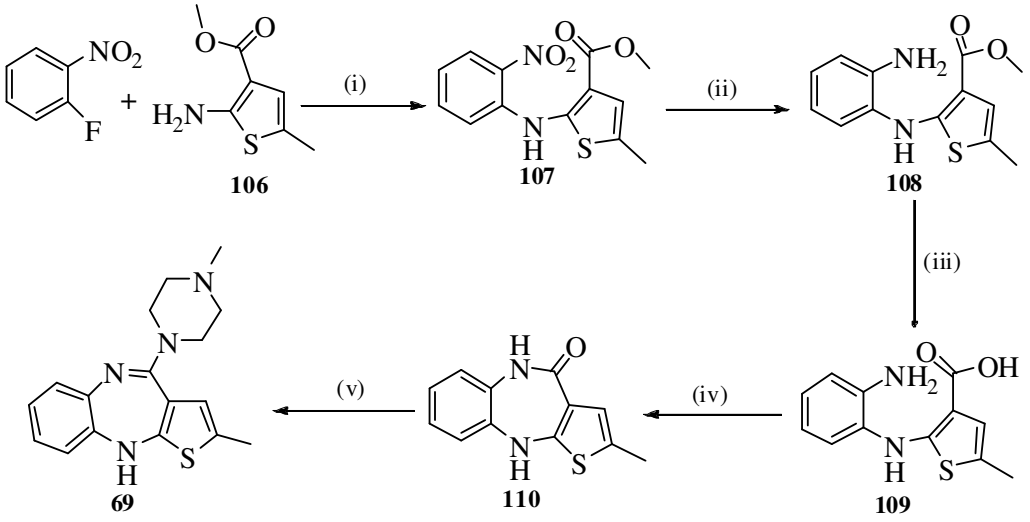

Scheme 3.2: Synthesis of olanzapine (route B). Reagents: (i) K_2CO_3 or LiOH, DMSO or NaH, THF; (ii) Pd/C, H_2, EtOH; (iii) NaOH, H_2O, EtOH; (iv) DCC, THF; (v) NMP, toluene, DMSO.[72]

Generally, route A[72-74] (Scheme 3.1) commenced with a Gewald reaction between malonitrile, propanal and sulfur to afford 2-amino-5-methyl-3-thiophenecarbonitrile (**103**). This was followed by a condensation reaction of **103** with *o*-fluoronitrobenzene, to give 2-(2-nitroanilino)-5-methylthiophen-3-carbonitrile (**104**). Reductive cyclization of **104** with stannous chloride in an aqueous-alcoholic solution of hydrogen chloride followed by condensation of the primary amidine hydrochloride product (**105**) with anhydrous *N*-methyl-piperidine gave olanzapine (Scheme 3.1).

The mechanism of the Gewald reaction has been proposed.[75] The first step is a Knoevenagel condensation between the ketone or aldehyde (**a**) and the α-cyanoester (**b**) (or malonitrile) to produce the stable intermediate **c**. The mechanism of the addition of the elemental sulfur is unknown. It is proposed to proceed through intermediate **d**. Cyclization and tautomerization will produce the thiophene product **f** (Scheme 3.3).

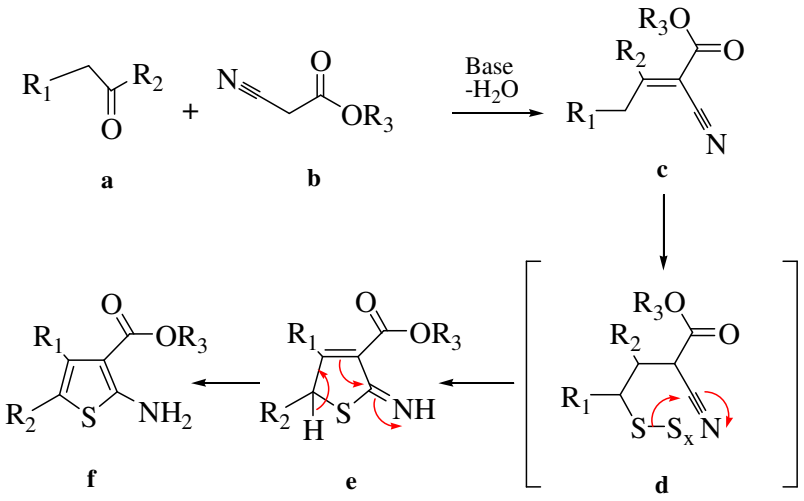

Scheme 3.3: The general mechanism of Gewald reaction.

The preparation of **104** has been reported by Chakrabarti and colleague,[72] utilizing *n*-butyl lithium as a base at -20 to -50 ºC to form an anion of **103** which was then added to a solution of *o*-fluoronitrobenzene in THF at room temperature to give the product **104** in yields of 35-50% (Scheme 3.1). Alteration of the reaction

conditions such as changing the reaction temperature and the nature of the base afforded **104** in similar yields. Calligaro *et al.*[16] also achieved a synthesis of the desired product **104**, but only in poor yield, using lithium hydroxide as the base in dimethylsulfoxide. In another paper, He *et al.*[76] reported a procedure using NaH as the base in dry THF which afforded **104** in 30% yield.

The synthesis of compound **105** was pursued through simultaneously reduction and cyclization of the starting nitrocarbonitrile **104** using anhydrous stannous chloride as a Lewis acid and reducing reagent in an aqueous-alcoholic solution of hydrogen chloride. $SnCl_2$ is widely used to selectively reduce aromatic nitro groups to anilines in usually excellent yields.[77] The reaction mechanism is depicted in Scheme 3.4.

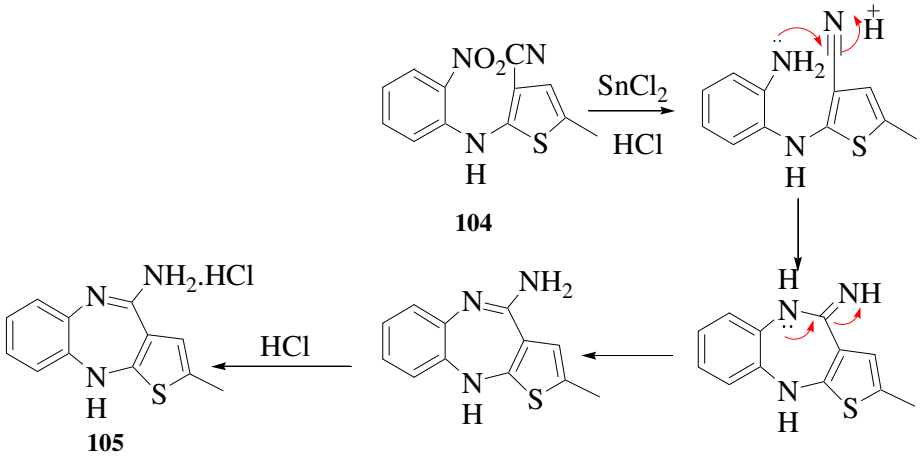

Scheme 3.4: Proposed mechanism for the reductive cyclization of **104** to **105**

To complete the preparation of olanzapine, compound **105** was treated with *N*-methylpiperazine in an organic solvent or solvent mixture at a temperature between 100 °C and 150 °C for approximately 20 hours. In a patent Shastri *et al.*[74] reported that the synthesis of olanzapine from **105** can proceed with or without solvent, as the solvent does not play any role in the reaction. However, the reaction can also be carried out in the presence of solvents such as toluene, *n*-butanol, methyl ethyl ketone, dimethylformamide or more preferably, dimethylsulfoxide. After workup, the crude olanzapine was crystallized from acetonitrile. The ultra-pure form

of olanzapine was achieved by Patel *et al.*[78] in 82% yield with a HPLC purity of 99.83%.

Alternatively, olanzapine can be prepared according to the synthetic route B (Scheme 3.2). This procedure involves 5 synthetic steps initiated by the reaction of methyl 2-(2-amino-4-fluoroanilino)-5-methylthiophen-3-carboxylate (**106**) with *o*-fluoronitrobenzene to form **107**. The newly synthesized nitro-ester (**107)** was first reduced to the amino-ester (**108**), which was then hydrolyzed to the amino acid (**109**). Finally, the synthesis of olanzapine was achieved by cyclization of the amino acid **109** to the diazepinone **110** using a coupling reagent such as DCC followed by the condensation reaction of **110** with *N*-methylpiperazine at 100 °C.

In this study we planned to utilize and also to optimize these two synthetic pathways in order to prepare the target molecules **99**, **100**, **101**, **102** and **87** for pharmacologic evaluation and *in vitro* binding assays.

3.2 Preparation of (*E*)-2-methyl-4-(piperidin-1-yl)-10*H*-benzo[*b*]thieno [2,3-*e*][1,4]diazepine (101)

Production of the target molecule **101** was achieved after 4 synthetic steps according to the reported procedure for the synthesis of olanzapine (route A).[72-74] The successful synthesis is illustrated in Scheme 3.5.

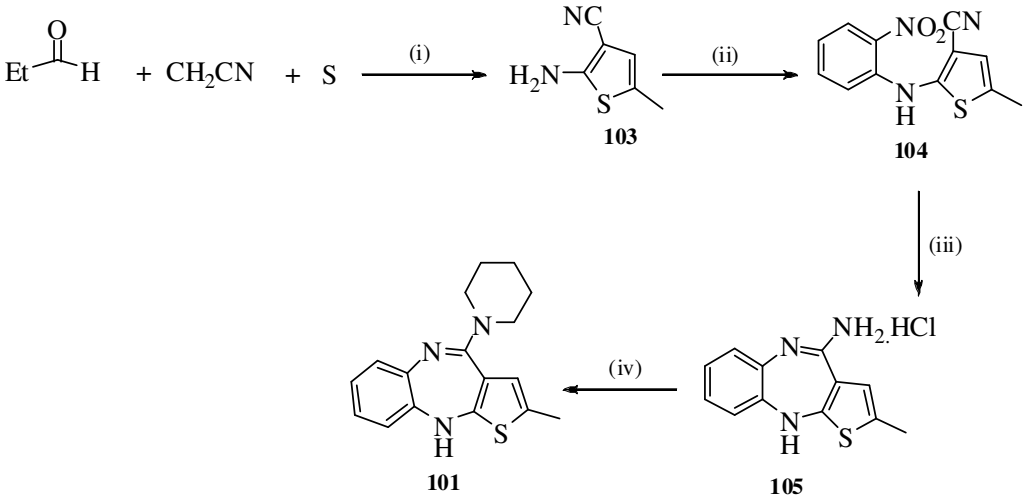

Scheme 3.5: Synthesis of **101**. Reagents: (i) Et_3N, DMF, 18 °C, 15 h, 60% yield; (ii) *o*-fluoronitrobenzene, NaH, THF, 18 °C, 24 h, 40% yield; (iii) $SnCl_2$, EtOH, 90 °C, 1 h, 65% yield; (iv) Piperidine, piperidine hydrochloride salt, DMSO, 100-110 °C, 20 h, 45% yield.

Based on the methodology outlined by He *et al.*[76], and Chakrabarti *et al.*[73] and Abd-El. Aziz *et al.*[79] the preparation of 2-amino-5-methyl-3-thiophenecarbonitrile (**103**) was carried out. Sulfur, propanal and malonitrile were stirred together in the presence of triethylamine in DMF solution for 15 hours at room temperature (Scheme 3.5). At the end of this time, the reaction mixture was quenched with ice to give an orange precipitate. The resultant solid was filtered, washed and dried to afford **103** in 60% yield. The structure of **103** was confirmed by NMR spectroscopic and mass spectrometric analysis. In the ^{1}H-NMR spectrum of **103**, three singlet proton signals at 2.23 (3H), 4.84 (2H) and 6.30 (1H) ppm were observed corresponding to the methyl group, the NH_2 group and the thiophene ring proton, respectively. In the ^{13}C-NMR spectrum the presence of the CN signal at 84.6 ppm and also the four thiophene ring signals between 117.3-165.3 ppm were consistent with the structure of **103**. HRMS (EI) of the product indicated a [M^+] ion at *m/z* 138.0259.

Having **103** in hand, the previously described methodology developed by He *et al.*[76] was applied to the synthesis of 2-(2-nitroanilino)-5-methylthiophne-3 -carbonitrile (**104**). A mixture of 2-amino-5-methyl-3-thiophenecarbonitrile and *o*-fluronitrobenzene in dry THF under a nitrogen atmosphere was added to a suspension of NaH in dry THF. The gradual addition of the reaction mixture to the

sodium hydride solution was associated with the formation of a persistent deep blue color. It is postulated that this color could be attributed to the deprotonation of the amino group and generation of the corresponding anion.[72] A similar color was also observed when base was added to the product. Therefore, potential deprotonation of the product could clarify the reason for the low to moderate yield of this reaction although this anion should have been quenched upon the aqueous workup. The reaction mixture was stirred for 24 hours and then quenched with ice, extracted into dichloromethane and then crystallized from ethanol to give the product **104** as a dark orange solid in 40% yield.

In the ^{1}H-NMR spectrum of the product **104**, the absence of a singlet at 4.84 ppm previously noted in the spectrum of **103** indicated the absence of the NH_2 protons. Extra ^{1}H-NMR signals in the aromatic proton region between 6.97 – 8.25 ppm and also a characteristic singlet at 9.63 ppm attributed to the N-H proton were observed. The ^{13}C-NMR spectrum of the product showed aromatic carbon signals between 113.9 – 149.2 ppm, indicating the successful coupling between thiophene carbonitrile (**103**) and *o*-fluoronitrobenzene. The molecular formula of the **104** was also substantiated by HRMS (EI).

The obtained nitro-carbonitrile **104** was then treated with anhydrous stannous chloride in 5 M hydrochloric acid/ethanol solution. The reaction mixture was heated at reflux for 1 hour and then crystallized from ethanol to give the hydrochloride salt of **105** as an orange solid in 65% yield. The ^{1}H-NMR spectrum of **105** showed a similar splitting pattern to that of the starting material **104** with the notable absence of a downfield singlet proton (9.61 ppm for **104**) in the spectrum of the product. Moreover, the hydrochloric salt **105** was not soluble in the same NMR solvent as the starting material **104** which provided further evidence for the desired structural transformation. Mass spectrometric analysis also confirmed the successful cyclization of **104**.

Before the synthesis of compound **101** was attempted, the reaction of **105** with diethylamine was investigated to give compound **85**. As shown in Table 2.10 (page 36) compound **85** with a predicted high activity and fit value in the pharmacophore

H-1 Agonist-1-1 model was one of the most worthy candidates for synthesis. Based on the general methodology for the synthesis of olanzapine (Scheme 3.1), this reaction was carried out in the presence of the excess amount of diethylamine in a 1:1 mixture of toluene and DMSO at reflux under a continuous flow of nitrogen to purge out the ammonia gas generated during the reaction. Monitoring of the reaction by analytical TLC showed no progress over 20 hours. It was assumed that the highly volatile diethylamine (bp: 55.5 °C) had evaporated at the reaction temperature during the first few hours. Carrying out the reaction in a sealed tube also did not give any of the desired product. Consequently, the synthesis of compound **101** ((*E*) -2-methyl-4-(piperidin-1-yl)-10*H*-benzo[*b*]thieno[2,3-*e*][1,4]diazepine) was proposed since piperidine has a high boiling point (bp: 106 °C) and the product was also a worthy candidate for biological evaluation.

The procedure above was applied to the synthesis of **101**. The reaction mixture was heated at reflux in DMSO in the presence of 10 equivalents of piperidine. After 20 hours, analytical TLC (CH_2Cl_2 : MeOH : NEt_3 / 100 : 1 : 0.1) showed that the starting material (R_f : 0) was completely consumed and a new spot had appeared with a R_f of 0.3. The reaction mixture was cooled to room temperature and then extracted with dichloromethane and washed with distilled water. After work up, the crude residue was purified *via* column chromatography to afford the desired product **101** in 27% yield. Structural conformation of **101** was provided by NMR spectroscopic and mass spectrometric analysis. In the ^{1}H-NMR spectrum of **101**, the characteristic signals for the piperidine CH_2 protons at 1.66 ppm (6H) and 3.50 (4H) ppm indicated the presence of this moiety in the product. The ^{13}C-NMR spectrum of **101** showed three additional carbon signals when compared to the spectrum of **105**, including the diagnostic CH_2 carbons (24.8, 26.2, 48.7 ppm) of the piperidine ring. The HRMS (ESI^+) confirmed the molecular formula of **101**.

With a low yield of **101** achieved using the method of Chakrabarti[73] and Patel,[78] it was decided to utilize another variation, that presented by Shastri *et al*. [74] This paper reported a method for the synthesis of olanzapine using *N*-methylpiperazine in conjugation with *N*-methylpiperazine hydrochloride. The reaction above was

repeated in the presence of 1:1 excess amount of piperidine and piperidine hydrochloride salt in DMSO to give the product **101** in 45% yield. According to the proposed mechanism (Scheme 3.6), compound **101** was formed from the nucleophilic attack of the piperidine base to the central carbon of the amidine moiety followed by elimination of ammonia. However, addition of piperidine base to the reaction mixture could deprotonate this ammonium cation so that the resulting free amino group would not be an active leaving group. Thus, by addition of piperidine hydrochloride salt this equilibrium would shift towards the formation of the protonated amino group (NH_3^+) which consequently, could improve the yield of the desired product.

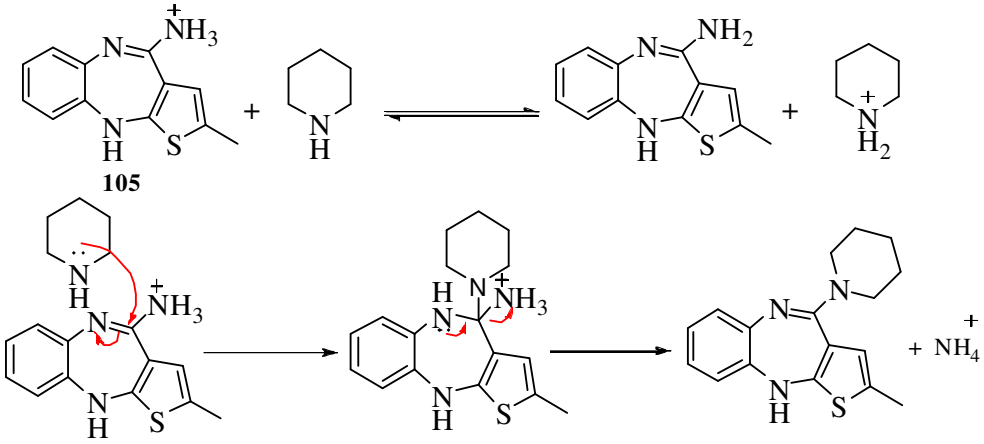

Scheme 3.6: Proposed mechanism of condensation of the amidine hydrochloride **105** with piperidine.

3.3 Preparation of (*E*)-2-ethyl-4-(piperidin-1-yl)-10*H*-benzo[*b*]thieno[2,3-*e*][1,4]diazepine (102) and (*E*)-2-ethyl-4-(4-methylpiperazin-1-yl)-10*H*-benzo[*b*]thieno[2,3-*e*][1,4]diazepine (99)

The synthesis of compounds **99** and **102** was based on the procedure previously developed for the preparation of **101**. Scheme 3.7 illustrates the four step synthesis of **99** and **102**, commencing with a Gewald reaction followed by aromatic ring condensation, cyclization and condensation of the primary amidine hydrochloride with *N*-methylpiperazine or piperidine, respectively.

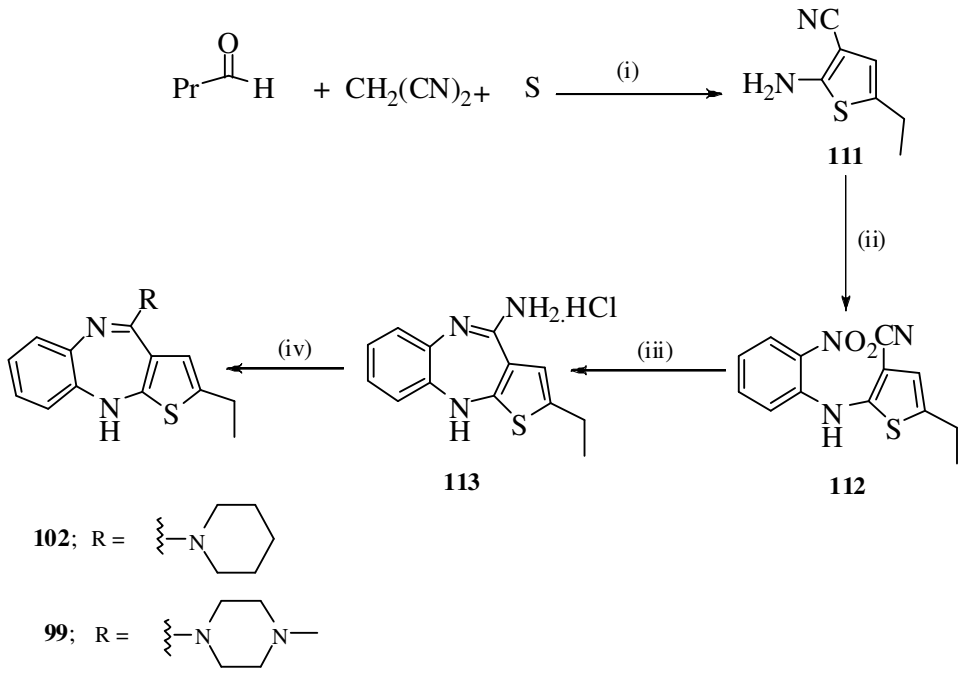

Scheme 3.7: Synthesis of **99** and **102**. Reagents: (i) Et_3N, DMF, 18 °C, 20 h; 20% yield (ii) *o*-fluoronitrobenzene, NaH, THF, 18 °C, 20 h, 51% yield; (iii) $SnCl_2$, EtOH, 1 h, 80 °C, 70% yield; (iv) (**101**) Piperidine, piperidine hydrochloride salt; (**99**) NMP and NMP hydrochloride salt, DMSO, 100-110 °C, 20 h, 40% yield (**99**), 48% yield (**102**).

Following the methodology for synthesis of **103**, 2-amino-5-ethylthiophene-3 -carbonitrile (**111**) was prepared by the reaction of sulfur, malonitrile and butanal in DMF in the presence of triethyamine at room temperature for 20 hours. After this time, analytical TLC analysis showed that all starting materials had been consumed and a new product had appeared. The reaction mixture was quenched with ice, and then extracted with dichloromethane. Purification of the crude product *via* column chromatography gave the desired product **111** as a dark brown oil with a low yield of 20%. The ^{1}H-NMR spectrum of **111** was consistence with the spectroscopic data discussed for that of **103** except that at 1.22 (t, 3H) and 2.62 (q, 2H) ppm the corresponding signals for the ethyl group of **111**, instead of the singlet signal of the methyl group of **103**, were observed. The ^{13} C-NMR spectrum also supported the ^{1}H-NMR with the presence of an additional signal for a CH_2 group at 23.2 ppm. The HRMS (CI) of the product indicated a [MH^+] ion at *m/z* 153.0895.

Preparation of 5-ethyl-2-(2-nitroanilino)thiophene-3-carbonitrile (**112**) was attempted through two different reaction conditions (Scheme 3.7). Initially, the same conditions for the synthesis of **104** were applied to the preparation of **112**. Reaction of **111** with *o*-fluoronitrobenzene and NaH in dry THF at room temperature for 20 hours furnished the desired product **112** in 51% yield. The formation of a deep blue color was also observed when the reaction mixture was added to the solution of NaH in THF. Alternatively, the thiophenecarbonitrile (**111**) was reacted with *o*-fluoronitrobenzene in DMF in the presence of anhydrous potassium carbonate as a base. The reaction was heated at reflux. Analytical TLC showed that after 90 minutes, the starting thiophenecarbonitrile (**111**) was fully consumed and four new spots had appeared. After work up and column chromatography the desired product **112** was separated in 26% yield. Although this reaction proceeded faster, yields were lower than those obtained using the conditions first trialed. The higher reaction temperatures seemed to give the desired product contaminated with byproducts which consequently decreased the yield of **112**.

In the ^{1}H-NMR spectrum of the product **112**, the absence of the 2H singlet at 4.65 ppm previously noted in the spectrum of **111** indicated the absence of the NH_2 protons. Extra signals in the aromatic proton region between 6.96 – 8.25 ppm and also a characteristic singlet at 9.63 ppm attributed to the N-H proton were observed. The ^{13}C-NMR spectrum of the product showed aromatic carbon signals between 116 - 136 ppm, indicating the successful coupling between the thiophenecarbonitrile (**111**) and *o*-fluoronitrobenzene. The molecular formula of the **112** was also substantiated by HRMS (CI).

Compound **113** was prepared according to the methodology utilized in the synthesis of the hydrochloric salt **105**. A mixture of **112** and anhydrous stannous chloride in 5M hydrochloric acid/ethanol was heated at reflux to give the desired product **113** in good yield (70%). The structure of the product **113** was assigned on the basis of its spectroscopic data. The ^{1}H-NMR spectrum of **113** showed a similar splitting pattern to that of the starting material **112** with the notable absence of a downfield singlet proton resonance (9.63 ppm) as seen in the spectrum of **112**. Moreover, the hydrochloric salt **113** was not soluble in the same NMR solvent as the

starting material **112** which provided further evidence for the desired structural transformation. Mass spectrometric analysis also confirmed the successful cyclizaition of **112**.

In order to synthesize **102** and **99**, the previous optimized reaction conditions for the preparation of **101** were employed. Compound **102** was synthesized in 41% yield based on the reaction of **113** with a 1:1 excess amount of piperidine and piperidine hydrochloride salt in DMSO. Structural confirmation of **102** was provided by NMR spectroscopic and mass spectrometric analysis. In the ^{1}H-NMR spectrum of **112** additional triplet and quartet signals (1.21 (3H) and 2.65 (2H) ppm) in place of a single signal for the methyl group, when compared to the spectrum of **101**, showed the presence of the ethyl moiety in the desired product. Analysis of the ^{13}C-NMR and DEPT spectra also supported the structure of **102** where the CH_3 and CH_2 signals corresponding to the ethyl group appeared at 15.7 and 24.1 ppm, respectively. HRMS (CI) of **102**, which showed a [MH^+] ion at *m/z* 326.1565, was consistent with the molecular formula.

Following the procedure above, the reaction of **113** with an excess amount of *N*-methylpiperazine and *N*-methylpiperazine hydrochloride (1:1) in DMSO afforded **99** in 40% yield. By comparison of the NMR spectra to that of olanzapine,[73] the presence of the ethyl signal, 1.22 (CH_3) and 2.65 (CH_2) ppm in the ^{1}H-NMR spectrum and at 15.8 (CH_3) and 46.2 (CH_2) ppm in the ^{13}C-NMR spectrum, confirmed the molecular structure of **99**.

3.4 Preparation of (*E*)-(2-methyl-4-(piperidin-1-yl)-5,10-dihydro-4*H*-benzo[*b*]thieno[2,3-e][1,4]diazepin-3-yl)methanol (100) and (*E*)-(2-ethyl-4-(piperidin-1-yl)-10*H*-benzo[*b*]thieno[2,3-*e*][1,4]diazepin-3-yl)methanol (87)

The preparation of **100** was first attempted by following the method for synthesis of **99**, **101** and **102**. As shown in Scheme 3.8, this synthetic pathway was based on the formation of the amino-diazepine (**117**) which was expected to simply be converted to the desired product (**100**) in two synthetic steps (Scheme 3.8).

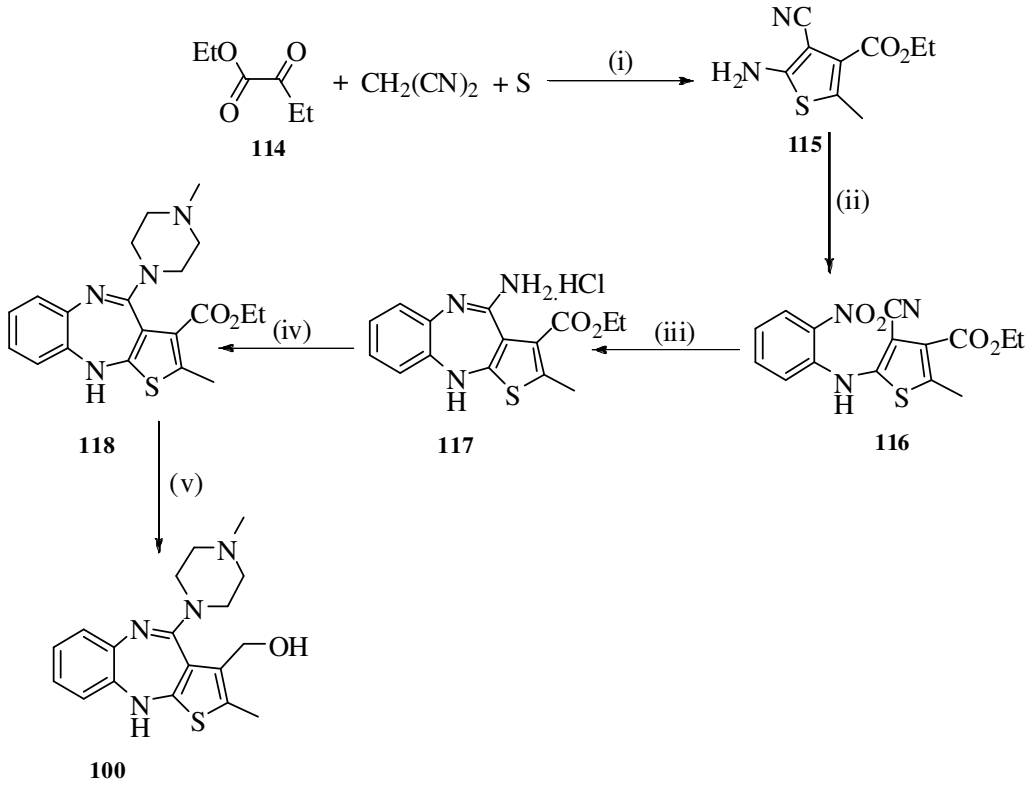

Scheme 3.8: Synthesis of **100** (route 1). Reagents: (i) Et_3N, EtOH, 100 °C 2 h, 20% yield (ii) NaH, *o*-fluoronitrobenzene, THF, 40 °C, 20 h, 70% yield; (iii) $SnCl_2$, EtOH, 90 °C, 60% yield; (iv) *N*-Methylpiperazine, Piperazine hydrochloride salt , DMSO, 110 °C, 22 h , (v) $LiBH_4$, EtOH.

In accordance with Scheme 3.8, the cyanothiophene (**115**) was synthesized by reacting ethyl 2-oxobutanoate (**114**) with malononitrile and sulfur in ethanol followed addition of triethylamine. The preparation of **114** is discussed on page 80 of Chapter 4. Workup and purification gave **115** in 20% yield. Structural confirmation of **115** was provided through ^{1}H-NMR and ^{13}C-NMR spectroscopic and mass spectrometric analysis, which were in agreement with that previously reported in the literature.[16, 73] Analysis of the ^{1}H-NMR spectrum of **115** revealed the absence of the signal corresponding to the H-4 proton of the thiophene ring which was observed in **103** and **111**. The appearance of a triplet (3H) and a quartet (2H) signal at 1.39 and 4.34 ppm respectively, was also noted and these were consistent with the signal for ethyl ester group. The ^{13}C-NMR spectrum also supported the ^{1}H-NMR spectrum with the presence of an additional signal at 161.8 ppm which was attributed to the ester carbonyl group. The signal ascribed to the CH_2 was observed

at 61.8 ppm in the ^{13}C-NMR spectrum of the product, which was consistent with the ethyl ester group. The LRMS (CI) of the product indicated a [MH^+] ion at *m/z* 211.0536.

Based on the procedure developed for the synthesis of **112**, **115** was converted to **116** in 70% yield. The structure of **116** was validated by ^{1}H-NMR and ^{13}C-NMR spectroscopic analysis and mass spectrometric analysis. In the ^{1}H-NMR spectrum of the product **112**, the absence of a 2H singlet at 4.74 ppm previously noted in the spectrum of **115** indicated the absence of the NH_2 proton. Extra ^{1}H-NMR signals in the aromatic proton region between 7.02 – 8.27 ppm and also a characteristic downfield singlet at 9.76 ppm attributed to the N-H proton were observed. The ^{13}C-NMR spectrum of the product showed aromatic carbon signals between 116.3 – 148.6 ppm, indicating the successful coupling between thiophenecarbonitrile (**115**) and *o*-fluoronitrobenzene. The NMR spectroscopic data was consistent with that of products **104** and **112**. HRMS (CI) of the product indicated a [MH^+] ion at *m/z* 273.3111.

Reduction and cyclization of **116** was attempted in the presence of 6 equivalents of anhydrous stannous chloride in an aqueous-alcoholic solution of hydrochloric acid. After 6 hours of heating at reflux the desired hydrochloride salt **117** was obtained as a yellow solid in 60% yield. The ^{1}H-NMR spectrum of **117** showed a similar splitting pattern to that of the starting material **116** with the notable absence of the singlet proton resonance (9.76 ppm) seen in the spectrum of **116**. Moreover, the hydrochloric salt **117** was not soluble in the same NMR solvent as the starting material **116** which provided further evidence for the desired structural transformation. Mass spectrometric analysis also confirmed the successful cyclization of **116**.

Production of **118** was attempted by reacting **117** with 1:1 mixture of piperidine and piperidine hydrochloride at 110 °C in DMSO. After 22 hours, the reaction mixture was stopped when analytical TLC showed that all the starting material had been consumed and one new spot with a R_f of 0.3 was observed. However, after workup, 5 new spots were found. Presumably, before workup the presence of salts

on the TLC plate did not allow all compounds to move off the baseline. It was also assumed that the desired product could undergo ester hydrolysis during workup. Therefore, the reaction was repeated with a modification in the workup procedure to avoid hydrolysis of the product. Unlike the work up procedure used for **99**, **101** and **102** (Chapter 4, page 78, 74, 79), the reaction mixture was basified under cold conditions (0-5 °C). However, the same result was acheived. Although a trace amount of the product **118** was detected by mass spectrometric analysis, separation of the product through chromatography was not successful.

With the failure of the first route, the preparation of **100** was attempted based on the methodology developed by Chakrabarti and co-workers[72, 80] and Shastri *et al.*[4] (Scheme 3.2, page 42). As outlined in Scheme 3.9, the general synthetic plan to **100** was a coupling reaction of the ethyl thiophenecarboxylate **119** with *o*-fluoronitrobenzene followed by a reduction of the thus formed nitro-ester **120** to the corresponding amino ester **121**. A cyclization reaction of **121** would then give the desired diazepinone **122.** Reduction of the ethyl ester group of **122** to the methyl alcohol, and lastly, a coupling reaction of **123** with *N*-methylpiperazine was expected to provide compound **100**.

The advantage of this synthetic route to the former one (Scheme 3.8) was that the reduction reaction of the ester group (**122**) to the alcohol would be less likely to involve the reduction of other functional groups. For instance, the reduction of compound **117** (Scheme 3.8) may be complicated by the reduction of both the ester and the primary amidine group (Scheme 3.8).

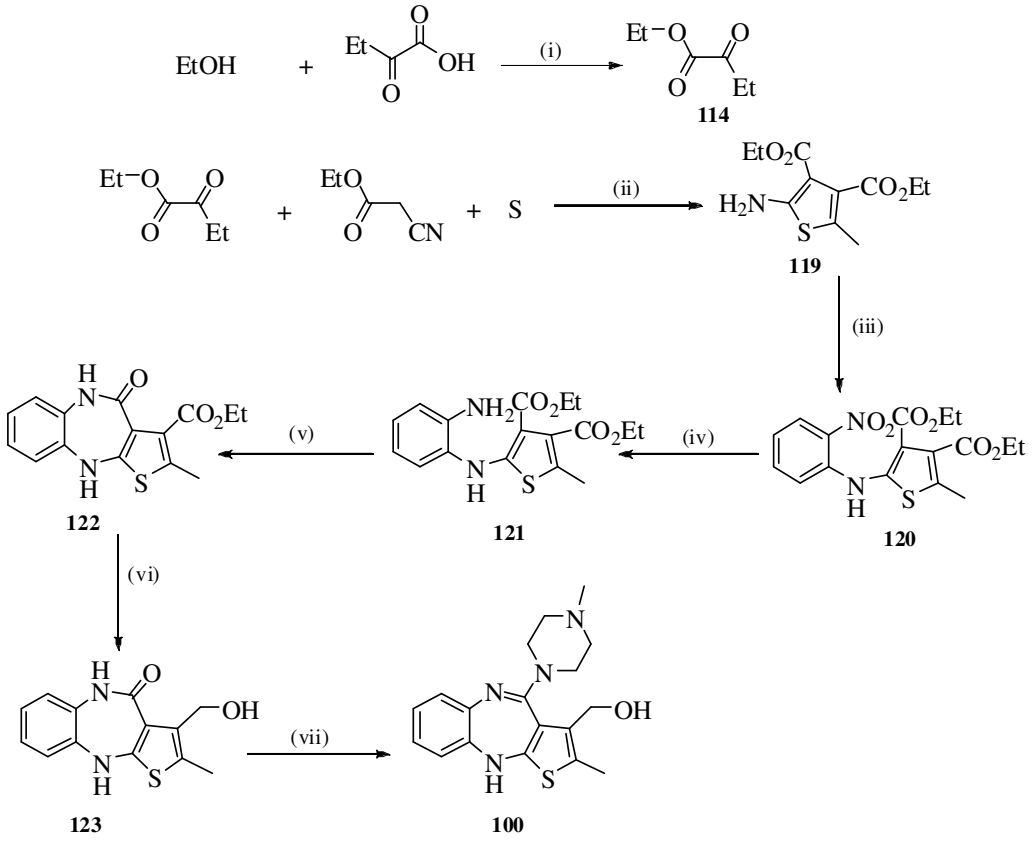

Scheme 3.9: Synthesis of **100** (route 2). Reagents: (i) *p*-$MeC_6H_4SO_3H$, benzene, 75 °C, 6 h; (ii) Et_2NH, EtOH, 70 °C, 1.5 h, 58% yield ; (iii) NaH, *o*-fluoronitrobenzene,THF, 40 °C, 20 h, 37% yield; (iv) $SnCl_2$, EtOH, 95 °C, 1 h, 66% yield; (v) $NaCH_2SOCH_3$, DMSO; (vi) $LiBH_4$, EtOH; (vii) *N*-Methylpiperazine, Piperazine hydrochloride salt, DMSO.

The preparation of diethyl 2-amino-5-methylthiophene-3,4-dicarboxylate (**119**) was based on the Gewald reaction between ethyl cyanoacetate and **114** in the presence of diethylamine in ethanol. The reaction mixture was stirred at 60 °C for 90 minutes. After workup and column chromatography the desired thiophene derivative **119** was obtained as a brown solid in 58% yield. The ^{1}H-NMR spectrum of **119** showed two characteristic triplet signals at ca. 1.34 ppm and two quartet signals at ca. 4.30 ppm, which were ascribed to the two ethyl ester groups. The ^{13}C-NMR spectrum of **119** also showed the presence of two carbonyl carbon signals at 164.9 and 166.1 ppm. LRMS (EI) analysis showed a molecular ion [M^+] at *m/z* 257.0719 which was consistent with the molecular formula of **119**.

The nucleophilic aromatic substitution reaction of **119** and *o*-fluoronitrobenzene using NaH as a base gave diethyl 2-methyl-5-(2-nitrophenylamino)thiophene-3,4-dicarboxylate **120** in moderate yield. In the first attempt, the previously optimized mild conditions to the synthesis of **112** were applied. The reaction mixture in dry THF was stirred at room temperature. Monitoring the reaction by TLC indicated that no substantial amount of product was formed during the first few hours. It was assumed that the electron withdrawing effect of the carboxylate group at position C-3 of the thiophene ring would deactivate the conjugated amine on C-2 to substitute fluoride on the *ortho* position of the benzene ring. Therefore, in comparison with the production of **112**, a lower yield and longer reaction time for the completion of the reaction were expected. In order to accelerate the progress, the reaction mixture was heated at 40 °C for 20 hours. After workup and column chromatography (hexane/ethyl acetate) the desired nitro-ester **120** was achieved as a red colored oil in 37% yield.

In the ^{1}H-NMR spectrum of **120**, the absence of a 2H singlet at 5.84 ppm which was previously observed in the spectrum of **119**, indicated the absence of signals for the NH_2 protons. Additional signals for the aromatic protons between 7.01 – 8.24 ppm and also a characteristic downfield singlet at 11.27 ppm attributed to the N-H proton were noted. The ^{13}C-NMR spectrum of the product showed aromatic carbon signals between 116 - 129 ppm, validating the structure of the desired product (**120**). The molecular formula of **120** was also substantiated by HRMS (CI) which showed a molecular ion [MH^+] at *m/z* of 379.0961.

The nitro-ester **120** was then reduced to the corresponding amino ester **121** with the previously described method utilizing 4 equivalents of anhydrous stannous chloride in an aqueous-ethanol solution of hydrochloric acid. After one hour of heating at reflux, the desired product **121** was produced as a yellow oil in 66% yield. The ^{1}H-NMR spectrum of **121** showed a similar splitting pattern to that of the starting material **120** with the upfield shift of a singlet N-H proton from 11.27 ppm in **120** to 8.80 ppm in the spectrum of the product. Remarkably, the presence of an extra singlet signal corresponding to the NH_2 proton

(2H at 3.85 ppm) indicated the successful reduction of the nitro group. Mass spectrometric analysis also confirmed the molecular structure of **121**.

In contrast to the described synthetic pathway for the preparation of olanzapine (Scheme 3.2), hydrolysis of the amino ester **121** to the amino acid was avoided because of the presence of the two ethyl ester groups in the molecule. It was presumed that hydrolysis of **121** to the corresponding amino bis-acid would make difficult the rest of the synthetic route as the amino bis-acid could be difficult to handle due to its polarity. Therefore, direct procedures for the cyclization of **121** without the hydrolysis step were pursued.

Intermolecular lactamization of diethyl 2-(2-aminophenylamino)-5 -methylthiophene-3,4-dicarboxylate (**121**) was attempted by various means. Initially, according to the procedure described by Carey and his co-worker[81] a solution of **121** in ethanol was heated at 200 °C in a microwave reactor at 200 watt and 20 bar for 2 hours. TLC analysis of the reaction did not show any progress. After this time, a catalytic amount of DMAP was added to the solution and the reaction mixture was heated again under the same conditions. It was postulated that the inclusion of DMAP as a nucleophilic catalyst could possibly increase the electrophilicity of the carbonyl group and subsequently cyclization rates. However, over the period of 12 hours no satisfactory result was achieved. The proposed mechanism is depicted in Scheme 3.10.

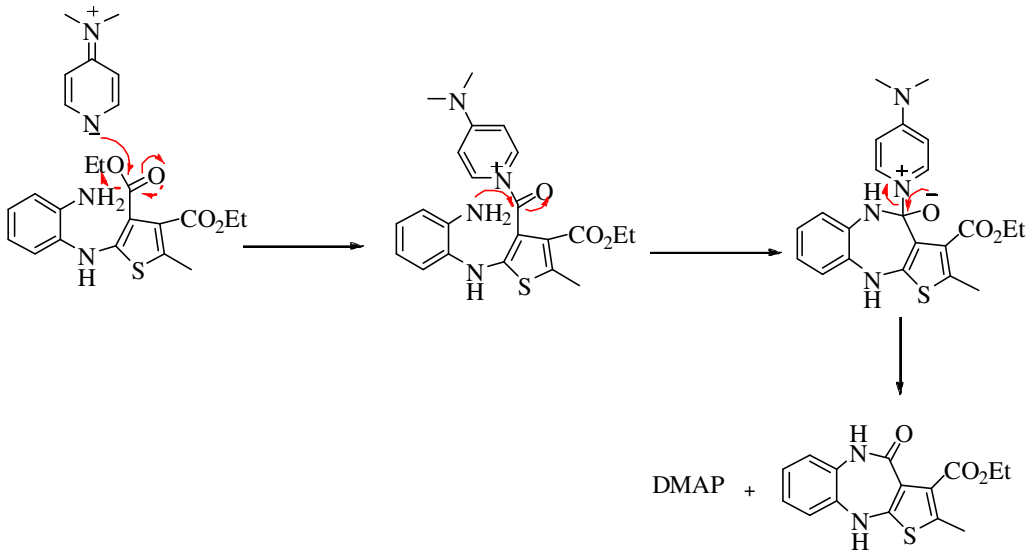

Scheme 3.10: Proposed mechanism for cyclization of **121** using DMAP.

A survey of the literature for other attempted methods for cyclisation of amino esters revealed the paper by Chakrabarti *et al.*[72, 80] and Pitt *et al.*[82] that utilized sodium methylsulfinylmethanide as a base (Scheme 3.11). According to the shown mechanism (Scheme 3.12) this regent could deprotonate the amine group hence providing a more reactive nucleophile to attack the carbonyl moiety and consequently produce a lactam.

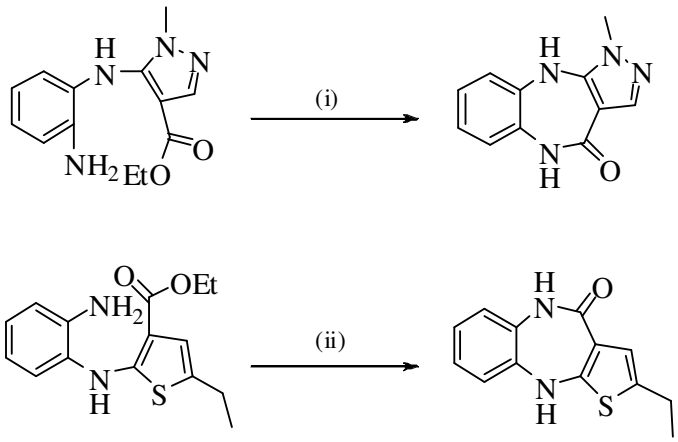

Scheme 3.11: Examples of attempted cyclization *via* $NaCH_2SOCH_3$. (i) 40%, [80, 82] (ii) 75%, [72]

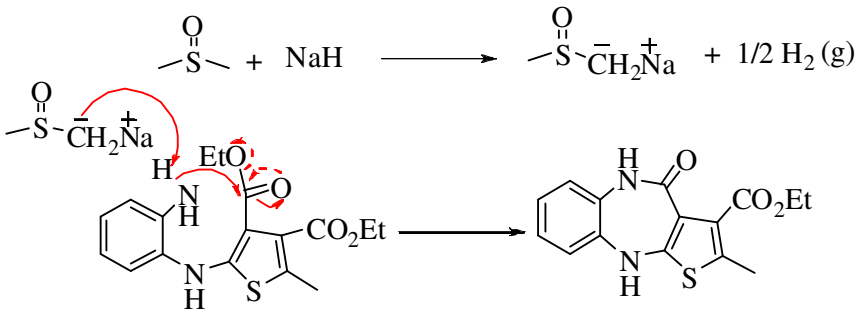

Scheme 3.12: Proposed mechanism for cyclization of **121** using $NaCH_2SOCH_3$.

Sodium methylsulfinylmethanide was generated *in situ* by treating sodium hydride with anhydrous dimethyl sulfoxide at 70 °C under nitrogen. At the next step, the amino ester **121** was added slowly to the 3 equivalents of the formed base. The reaction mixture was then stirred while the temperature was kept below 80 °C. Based on the literature, the reaction should be complete after 15 minutes, however, after a period of three hours only starting material was present from TLC analysis. Increasing the base to 5 equivalents also did not result in any product.

Since the cyclization reaction of the amino-ester **121** was not successful, it was concluded that the desired lactam **122** would possibly be obtained by the hydrolysis of **121** to the corresponding amino acid. However, as discussed before, in order to avoid of the formation of an amino bis-acid, it was decided to modify the last synthetic plan (Scheme 3.9) using a *t*-butyl ester instead of the ethyl ester which was expected to react with the aniline moiety. Thus, the hydrolysis of the *t*-butyl ester (**128**) using TFA would be selective over that of the ethyl ester group which should give the mono-acid **129** and ultimately the lactam **122** (Scheme 3.13).

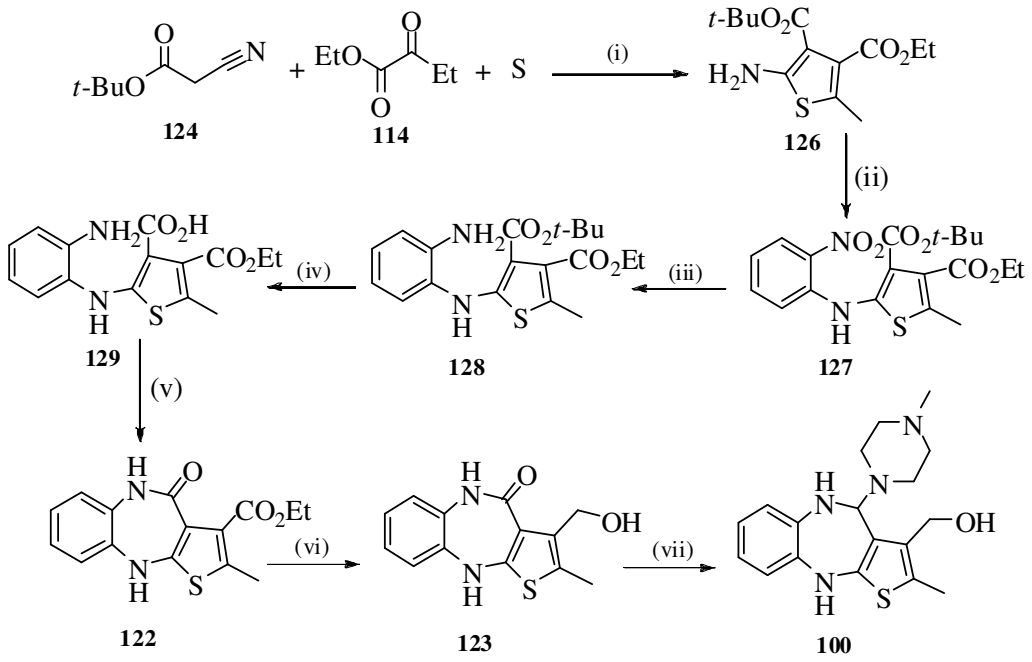

Scheme 3.13: Synthesis of **100** (route 3). Reagents: (i) Et_3N, DMF; (ii) NaH, *o*-fluoronitrobenzene, THF; (iii) Pd/C, EtOH; (iv) TFA, CH_2Cl_2, 18 °C, 6 h; (v) DCC, THF, or EDCI, HOBt, DIPEA, DMF; (vi) $LiBH_4$, EtOH (vii) *N*-Methylpiperazine, Piperazin hydrochloride salt, DMSO.

On the other hand, lack of time for the completion of the project prompted us to give up the synthesis of **100** and focus on the production of **87** as this compound was the ultimate target of the project. Due to the structural similarity of **100** and **87**, all discussion above was relevant to the synthesis of **87**. The general procedure to the synthesis of **87** is shown in Scheme 3.14.

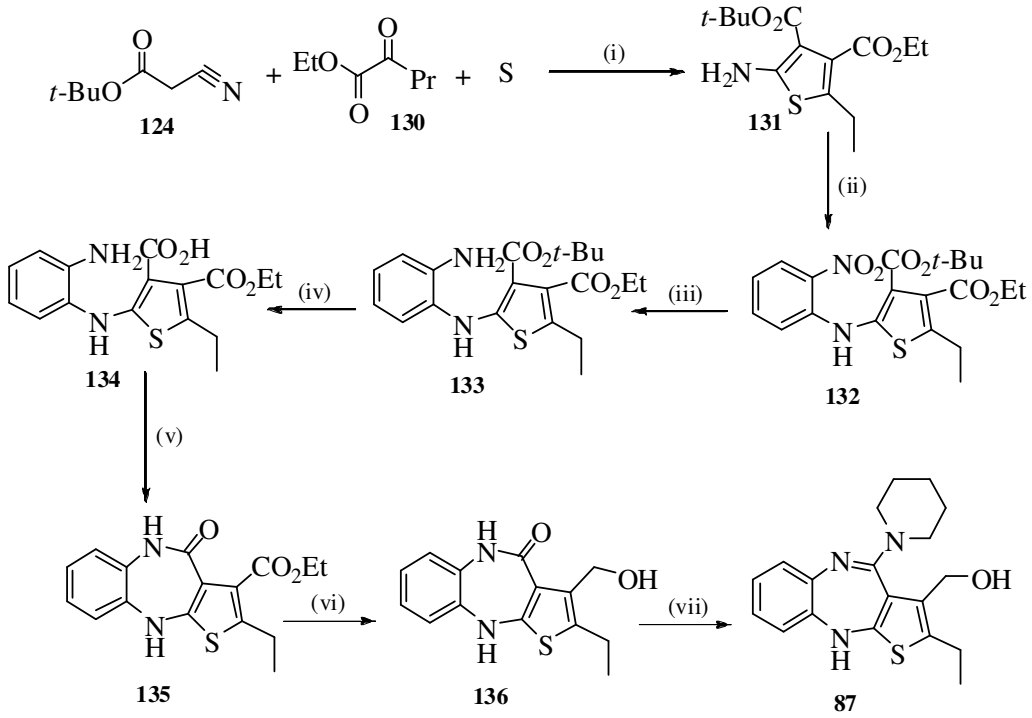

Scheme 3.14: Synthesis of **87**, Reagents: (i) Et_3N, DMF, 18 °C, 20 h; 55% yield (ii) NaH, *o*-fluoronitrobenzene, THF, 18 °C, 20 h; 56% yield (iii) Pd/C, EtOH, 45° C, 2 h, 81% yield; (iv) TFA, CH_2Cl_2, 18 °C, 6 h; (v) DCC, THF, 20 h, 18 °C or EDCI, HOBt, DIPEA, DMF, 18 °C; (vi) $LiBH_4$, EtOH (vii) Piperidine, Piperidine. hydrochloric salt, DMSO.

As shown in Scheme 3.14, the synthesis of **87** was initiated by the formation of the 2-aminothiophene derivative **131** using the previous explained conditions of the Gewald reaction.[79] Sulfur, *t*-butyl cyanoacetate (**124**) and ethyl 2-oxopentanoate (**130**) in DMF in the presence of triethylamine were stirred at room temperature for a period of 20 hours. The synthesis of **124** and **130** were discussed in Chapter 4. After workup and column chromatography (hexane : ethyl acetate), the thiophene **131** was obtained as an orange liquid in a good yield (55%). The product was fully characterized by ^{1}H-NMR and ^{13}C-NMR spectroscopic analysis. A comparison of the ^{1}H-NMR spectrum of **131** and **119** revealed a new signal at 1.44 ppm (s, 9H) which was ascribed to the *t*-butyl ester group. A resonance at 28.0 ppm in the ^{13}CNMR spectrum also confirmed the presence of the *t*-butyl ester group in the product. In the ^{1}H-NMR spectrum of **131**, the presence of the new signals corresponding to the ethyl group, a triplet signal at 1.12 (3H) and quartet signal at

2.56 (2H) ppm, and also the ethyl ester group, a triplet signal at 1.29 (2H) and quartet signal at 4.24 (2H) ppm, supported the structure of **131**. LRMS (CI) analysis showed a molecular ion [MH^+] at *m/z* of 300.1264 which was consistent with the molecular formula of **131**.

A solution of *tert*-butyl 4-ethyl-2-amino-5-ethylthiophene-3,4-dicarboxylate (**131**) and *o*-fluoronitrobenzene was added to a suspension of NaH (1.5 equivalents) in THF at room temperature. After stirring for 20 hours and then workup and purification of the crude product by column chromatography, the desired nitro-ester **132** was obtained as a red solid in a yield of 56%. In the ^{1}H-NMR spectrum of **132**, the absence of a 2H singlet at 5.94 ppm previously observed in the spectrum of **131**, indicated the absence of the NH_2 protons. Additional signals for the aromatic protons between 6.99 – 8.22 ppm and also a characteristic singlet at 11.00 ppm, attributed to the N-H proton, were noted. The ^{13}C-NMR spectrum of the product showed aromatic carbon signals between 117.3 – 135.7 ppm, confirming the structure of the desired product (**132**). The molecular formula of **132** was also substantiated by HRMS (EI) which showed a molecular ion [M^+] at *m/z* of 420.1366.

In the next step, the amino ester **133**, the key intermediate, was obtained by the hydrogenation of **132** in ethanol solution. The hydrogenation reaction was carried out over 10% palladium on activated carbon at 40 °-50 °C.[72, 74] After 2 hours, analytical TLC analysis showed that all of the starting nitro-ester had been consumed and a new spot below that of the starting material was observed. The catalyst was filtered off and the crude product was purified by column chromatography to furnish the product **133** in 81% yield. The ^{1}H-NMR spectrum of **133** showed a similar splitting pattern to that of the starting material **132** with the upfield shift of a singlet N-H proton from 11.00 ppm in **120** to 8.82 ppm in the spectrum of the product. Furthermore, the presence of an additional singlet signal corresponding to the NH_2 protons (2H at 3.84 ppm) indicated the successful reduction of the nitro group. The molecular structure of **133** was also proved by mass spectrometric analyses (CI) which showed a molecular ion [MH^+] at *m/z* of 391.1282.

The hydrolysis of the *t*-butyl ester group of **133** was attempted using 1 : 1 solution of TFA and CH_2Cl_2 at room temperature.[83] TLC analysis (1 : 4 ethyl acetate : petroleum spirit) showed that by the addition of TFA the starting material had disappeared. It was assumed that the addition of TFA led to the formation of TFA salt of the starting material at the beginning of reaction. Thus, the reaction was left and monitored by TLC for a few hours. Increasing the polarity of the solvent system (2 : 1 ethyl acetate : petroleum spirit) showed a complex mixture of products with no discrete spot but a streak of compounds over the plate. The ^{1}H-NMR spectrum of the reaction mixture was also not informative. Therefore, the reaction was stopped and the TFA was evaporated. Any further attempts to characterize the crude product were not successful. For instance, the crude product was treated three times with a 2 M solution of ether-hydrochloric acid in order to convert the obtained TFA salt to the hydrochloric salt. The NMR spectrum of the precipitated hydrochloric salt was difficult to analyze. Ultimately, it was presumed that the crude product contained the desired amino acid **134**. Therefore, based on the assumption that the amino acid compound was obtained, the crude product was directly utilized for the next reaction step.

Following the procedure developed by Chakrabarti *et al.*[72] the intermolecular cyclization of the amino acid **134** was first attempted using DCC as a coupling reagent. A mixture of **134** and one equivalent of DCC in THF solution under a nitrogen atmosphere was stirred for 20 hours. TLC analysis (1 : 4 ethyl acetate : petroleum spirit) showed that 6 new spots had appeared where two of them with a R_f of 3 and 3.5 were major. The solid was filtered off and the filtrate evaporated. Purification of the reaction mixture by column chromatography resulted in the two major isolated products; however, neither of these contained the expected molecular ion peak in the LRMS (EI^+) for the structure of the desired lactam **135**.

With the failure of the cyclization of **134** with DCC, it was assumed that due to the presence of both carboxylic acid and amine in the molecule of **134**, the amino moiety could be protonated. Thus, in order to cyclize **134**, the ammonium form should be converted to the free amine (Scheme 3.15). The deprotonation reaction of

134 was carried out in the presence of 1.5 equivalents of the DIPEA as a base following by the addition of the well established peptide coupling reagent EDCI[84, 85] as an alternative carbodiimide and HOBt. The reaction mixture in anhydrous DMF was stirred at room temperature under a nitrogen atmosphere. The progress of the reaction was monitored by analytical TLC for a period of 6 hours at which stage there was no apparent change in **134** and as a result the reaction was heated to 40 °C. After one more hour the reaction was stopped when no further progress of the reaction was observed.

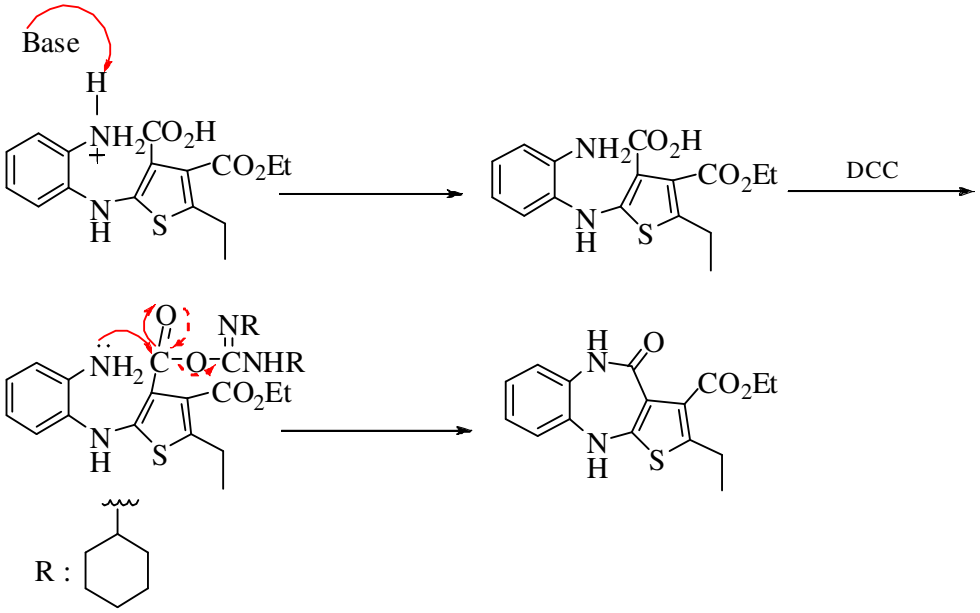

Scheme 3.15: Proposed mechanism for the cyclization of **134** using DCC.

At this stage of the project, due to the inadequate time for the completion of this synthetic plan (Scheme 3.14) other possible alternatives for the achievement of the target product **87** were explored. A subsequent review of the literature revealed that Calligaro *et al.*[16] had developed a synthetic method for the C-2 formylation reaction of a amino-diazepine derivative using Vilsmeier-Haack reaction conditions followed by the reduction of the crude product to the primary amidine alcohol. The synthetic route is outlined in Scheme 3.16.

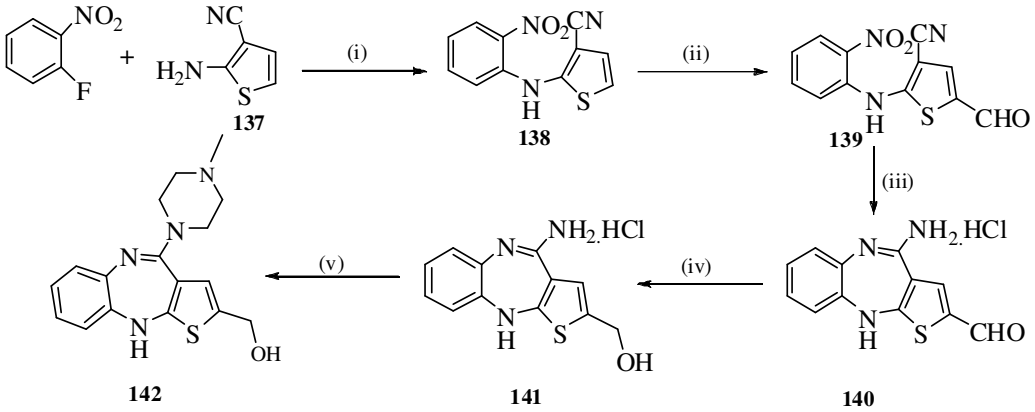

Scheme 3.16: Synthesis of **142**. Reagents: (i) LiOH, DMSO; (ii) $POCl_3$, DMF; (iii) $SnCl_2$, EtOH, HCl; (iv) $NaBH_4$, EtOH; (v) NMP, toluene, DMSO.[16]

According to the mechanism of the Vilsmeier-Haack reaction, *N*,*N*-dimethylformamide reacted with phosphorous oxychloride to afford a chloroiminium ion as a reactive electrophile. The electrophilic attack of this reactive species to the thiophene ring resulted in C-2 substitution of the iminium moiety which subsequently converted to the aldehyde during the aqueous workup. The mechanism of the reaction is depicted in Scheme 3.17.[86]

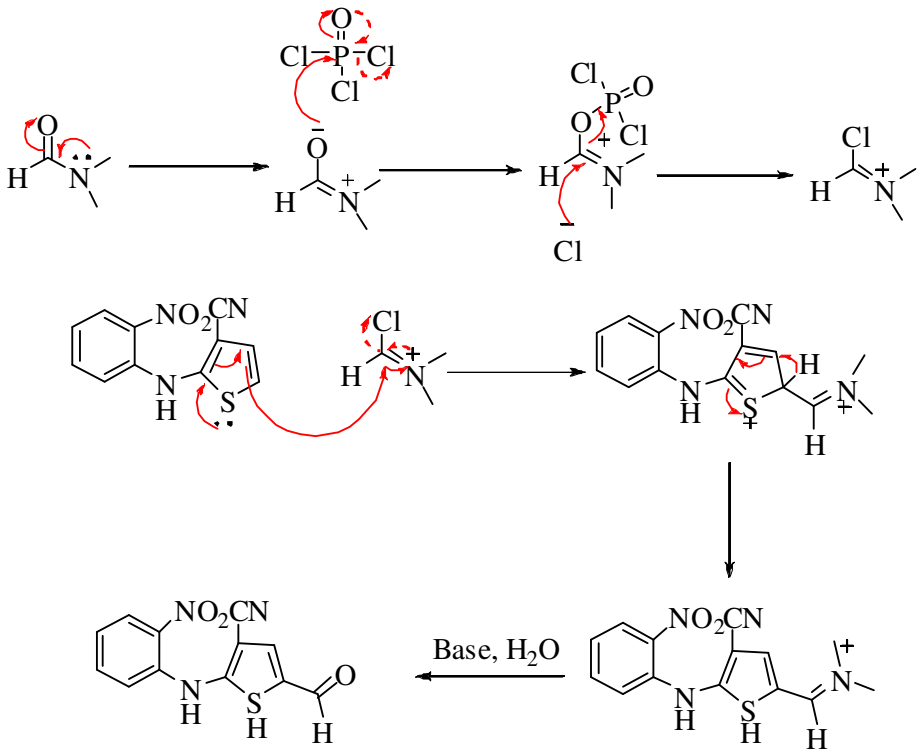

Scheme 3.17: The mechanism of the Vilsmeier-Haack reaction.

Further investigation of the literature indicated that the Vilsmeier-Haack reaction of 2,5-dimethylthiophene resulted in C-3 formylation with moderate yield (43%) (Scheme 3.18). [87]

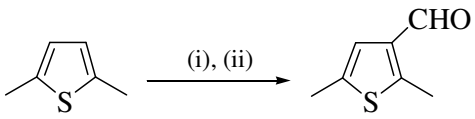

Scheme 3.18: Literature example of Vilsmeier-Haack reaction. Reagents (i) $POCl_3$, DMF (18 °C, 30 min; 80 °C, 3 h), (ii) NaOH, H_2O (10 °C, 43% yield). [87]

Therefore, based on the reasoning above and structure similarity of **87** and **142**, it was hypothesized that the formylation reaction of the synthesized thiophene **102** using the Vilsmeier-Haack reaction conditions followed by the reduction of the formed aldehyde could possibly furnish our desired product **87** (Scheme 3.19).

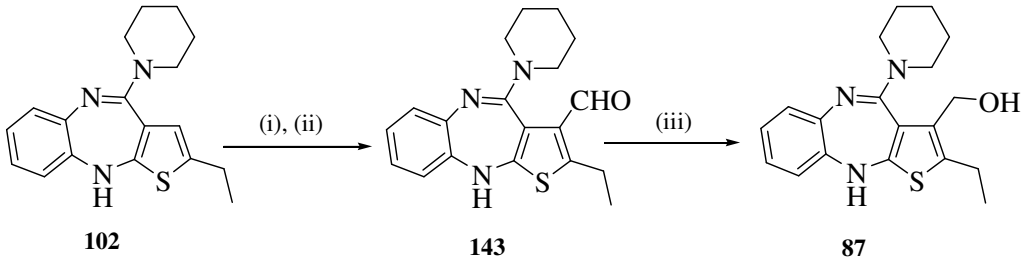

Scheme 3.19: Preparation of **87**. Reagents: (i) $POCl_3$, DMF (ii) NaOH, H_2O, (iii) $NaBH_4$, EtOH

However, due to the insufficient amount of **102** to explore our assumption, it was decided to investigate the Vilsmeier-Haack reaction of the commercially available olanzapine (Scheme 3.20).

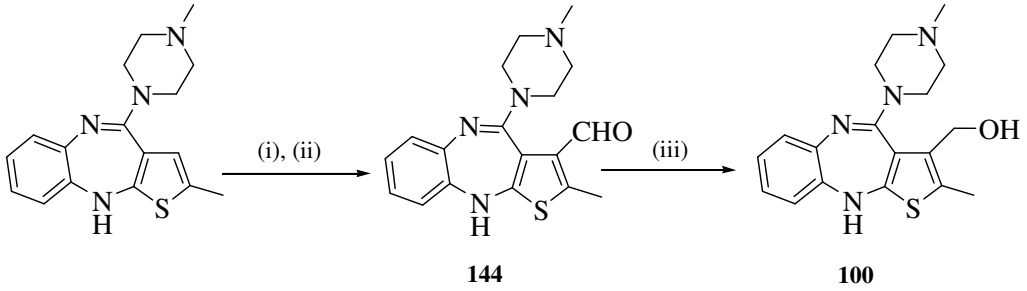

Scheme 3.20: Preparation of **100**. Reagents: (i) $POCl_3$, DMF (ii) NaOH, H_2O, (iii) $NaBH_4$, EtOH

The formylation reaction of olanzapine was attempted in the presence of a Vilsmeier`s complex prepared *in situ* from DMF and $POCl_3$. The reaction mixture was heated to 80 °C for a period of 3 hours. Monitoring the reaction by analytical TLC showed that by the completion of this time all of the starting material was consumed and a new product had been obtained. Mass spectrometric analysis of the crude product indicated the molecular ion peak in the LRMS (EI^+) which was matched with the structure of the desired product **144**. In accordance with the literature compound **140** was not stable to be chromatographed or crystallized.[16] Therefore, based on the assumption that the newly formed aldehyde could also be unstable, without any purification the crude product was directly treated with sodium borohydride. In contrast to our expectation that the reactive aldehyde should be quickly reduced to the corresponding alcohol, analytical TLC indicated that no reduction product was obtained after 5 hours. Presumably, the crude starting

material was not the desired aldehyde **144**. Therefore, the starting material of the reduction reaction was recovered and purified by column chromatography. Characterization of the isolated product indicated that the Vilsmeier-Haack reaction of olanzapine did not afford the expected aldehyde **144** but led to the formation of the formamide **145** (Scheme 3.21). When this reaction was repeated but without treatment with $NaBH_4$, the formamide **145** was obtained in 65% yield after purification by column chromatography.

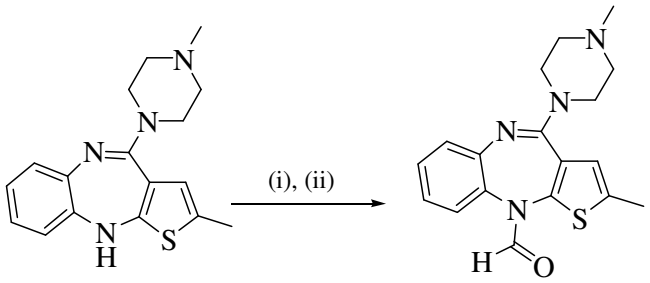

145

Scheme 3.21: Vilsmeier-Haack reaction of olanzapine. Reagents: (i) $POCl_3$, DMF (ii) NaOH, H_2O

The structural conformation of **145** was provided on the basis of the NMR spectral evidence. Analysis of the ^{1}H-NMR of **145** revealed the absence of a peak at around 4.9 ppm which was ascribed to the olanzapine N-H proton.[73] Furthermore, a characteristic singlet at 8.4 ppm was observed which was attributed to the formamide proton. The ^{13}C-NMR spectrum of **145** also contained a signal for the amide carbonyl at 162.3 ppm. The HRMS (EI^+) of **145** showed a [M^+] ion at *m/z* 340.1360, which was consistent with its molecular weight and was also the same as the molecular weight of **144**.

3.5 Conclusions

In summary, compounds **99** and **101** representing a single modification to the structure of olanzapine with the alteration of R_1 to C_2H_5 (**99**) and the replacement of the *N*-methylpiperazine ring with a piperidine ring (**101**) (Table 3.1, page 41) were successfully synthesized. Compound **102** was also achieved successfully indicating two modifications at positions C-2 and N-4′. However, all of the attempted synthetic

routes to achieve the synthesis of **100** and the ultimate target, **87**, failed since the substitution of the hydroxymethyl group at position C-3 was not successful (Table 3.1, page 41).

Finally, following the methodology developed in the literature,[16, 87] it was assumed that the Vilsmeier-Haack reaction of **102** and also olanzapine followed by a reduction reaction would possibly lead to the substitution of a hydroxymethyl group at position C-3 and ultimately the formation of **87** and **100**. Therefore, in order to investigation our assumption, the Vilsmeier-Haack reaction of the commercially available olanzapine was attempted. However, instead of the production of the desired aldehyde **144**, the formamide **145** was obtained.

Consequently, due to the lack of time for further exploration, the synthesized compounds **99**, **101** and **102** and also the accidentally achieved formamide **145** were subjected to pharmacological evaluation and also *in vitro* binding assays (Chapter 5).

3.6 Future Directions

The future direction for this Chapter could involve further exploration of the Vilsmeier-Haack reaction of **102** and olanzapine. This would involve finding a suitable amino (N-10) protecting group for olanzapine and compound **102**.

CHAPTER 4: EXPERIMENTAL

4.1. General Procedures

4.1.1 Experimental Procedures, Reagents and Solvents

All reactions were carried out utilizing standard laboratory equipment and standard laboratory glassware. All solvents and reagents used were purchased from Sigma-Aldrich Chemical Co. Inc., Lancaster International, Ochem. Inc., or Merck and were used as received. Petroleum spirit of boiling point range 40-60 °C was used. Anhydrous solvents were purified and dried according to Perrin and Armarego[88] and distilled immediately before use. Anhydrous THF and anhydrous Et_2O were distilled over sodium wire, in the presence of benzophenone as an indicator. Anhydrous DMF was purchased from Sigma-Aldrich Chemical Co. Inc., in a Sure-seal® bottle and was stored under an inert atmosphere.

Organic solvent extracts were dried using anhydrous magnesium sulfate. Solvents were removed under reduced pressure at 45 °C with a Büchi rotary evaporator. All solvents were AR grade and were used as received.

4.1.2 Analytical Thin Layer Chromatograpy (TLC), Column Chromatography and HPLC

Thin-layer chromatography (TLC) was used to monitor the progress of reaction using aluminium-backed sheets of Merck Silica Gel 60 F_{254} containing a fluorescent indicator and a UV lamp (254 nm), or *via* staining of the plate with a ninhydrine or anisaldehyde stain. Column chromatography was performed using Merck Kiesel Gel 60 F254 (230-400 mesh) silica gel under medium pressure. Solvent proportions are quoted as volume ratios.

Preparative rp-HPLC purification was performed using a Waters Delta Prep 4000 chromatography system fitted with a Waters 486 tunable absorbance detector with detection typically at 254 nm. These purifications were performed using gradient elution with solvent A (100% H_2O, 0.1% HCl) and B (90%, CH_3CN, 10% H_2O, 0.1% HCl). The column used was a (40 mm x 100 mm) column (run at 40 mL/min). Analytical HPLC analysis was performed using a Waters 600 controller and a Waters 486 tunable absorbance detector. The separations were performed using gradient elution A and B on a Phenomenex luna 5μ C18 (4.6 mm x 250 mm) column at a flow rate of 1.0 mL/min. A detection wavelength of 254 nm was used for each analysis. Microwave reactions were conducted in a CEM focused Microwave ™ synthesis system running on Synergy software.

4.1.3 Characterization and Instrumentation

4.1.3 ^{1}H- and ^{13}C-Nuclear Magnetic Resonance (NMR) spectra

Nuclear magnetic resonance (NMR) spectroscopy was performed on a Varian Inova 500 MHz spectrometer, where proton NMR (^{1}H-NMR) spectra and carbon NMR (^{13}C-NMR) spectra were acquired at 500 and 125 MHz, respectively or a Varian Unity 300 MHz spectrometer, where proton NMR (^{1}H-NMR) spectra and carbon NMR (^{13}C-NMR) spectra were acquired at 300 and 75 MHz, respectively. All spectra were recorded in deuterochloroform ($CDCl_3$) or deuteromethanol (CD_3OD) with 0.5% tetramethylsilane (TMS), obtained from Cambridge Isotope Laboratories Inc., unless otherwise stated. TMS (0.00 ppm) was used as the internal standard. Chemical shifts (δ) were measured in parts per million (ppm) and referenced against (TMS) and coupling constants (*J*) were measured in Hertz (Hz).

NMR assignments were made using standard gradient correlation spectroscopy (gCOSY), gradient heteronuclear single quantum correlation (gHSQC), gradient heteronuclear multiple bond correlation (gHMBC) and distortionless enhancement by polarisation transfer (DEPT) spectroscopy. Superscript letters indicate interchangeable assignments. Multiplicities are denoted as singlet (s), doublet (d), triplet (t), multiplet (m). The arrangement of ^{1}H-NMR spectral data is listed as

chemical shift, followed in brackets by multiplicity, integration, coupling constant(s) and ascribed assignment.

4.1.3.2 Mass spectrometry (MS)

Chemical Ionisation (CI^+) low-resolution mass spectrometry was performed on a Shimadzu QP-5000 MAT-44 quadrupole spectrometer using the direct insertion technique. The mass to charge (*m/z*) values of the principal ion peaks are stated with their relative intensities in parentheses. High-resolution mass spectrometry (HRMS EI and CI^+) was performed on a Fisons/VG Autospec-TOF mass spectrometer. GC-FID analysis was performed on a Varian 3700 gas chromatograph coupled with a Shimadzu C-R3A integrator. The accuracy of the measured HRMS relative to the required molecular weight is given in ppm. GC-MS analysis was performed by electron impact (EI, 70eV) mode with a Shimadzu QP-5000 system.

4.1.3.3 Melting points

Melting points were determined on a Reichert melting point apparatus. Temperatures are expressed in degrees Celsius (°C) and are uncorrected.

4.2 Toward the synthesis of 101

2-Amino-5-methyl-3-thiophenecarbonitrile (103) [73, 74, 76]

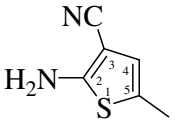

A solution of sulfur (1.60 g, 50 mmol), propanal (4.25 mL, 50 mol) and malononitrile (3.15 mL, 50 mmol) in DMF (4.25 mL) was cooled to about 0 °C and then triethylamine (4.25 mL) was added in a dropwise manner over 30 minutes. The resulting mixture was warmed to room temprature and stirred for one hour. A solution of malononitrile (3.14 mL) was slowely added to the reaction mixture and the solution was stirred for 15 hours. The reaction mixture was quenched by the addition of ice and water (200 mL) and a precipitate formed. The solid was filtered off to afford **103** (4.140 g, 60%) as a brown solid; m.p. 100-102 °C (lit.[76] m.p. 99-101 °C)

The spectroscopic data for **103** was not reported in the literature.

^{1}H-NMR (500 MHz, CD_3OD): δ 2.23 (s, 3H, C<u>H</u>$_3$), 4.84 (s, 2H, N<u>H</u>$_2$), 6.30 (s, 1H, H-4).

^{13}C-NMR (125 MHz, $CDCl_3$) δ 14.6 (CH_3), 84.6 (<u>C</u>N), 117.3 (C), 122.8 (C), 123.9 (CH), 165.3 (C)

HRMS (EI): *m/z* calcd for $C_6H_6N_2S$ [M^+], 138.0252; found, 138.0259

R$_f$: 0.3 (25% EtOAc in petroleum spirit)

2-(2-Nitroanilino)-5-methylthiophen-3-carbonitrile (104) [73, 74, 76]

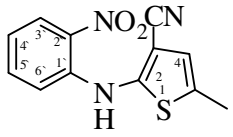

To a solution of **103** (276 mg, 2.0 mmol) and *o*-fluoronitrobenzene (0.30 mL, 2.79 mmol) in dry THF (2 mL) was added in a dropwise manner to a suspension of NaH (28.8 mg, 0.3 mmol) in dry THF (5 mL). The reaction mixture was stirred under a N_2 atmosphere for 24 hours and then poured onto cracked ice and extracted into CH_2Cl_2 (3 x, 15 mL). The combined extracts was washed with 2 N aqueous solution of hydrochloric acid (2 x, 10 mL) and then dried and the solvent was evaporated under reduced pressure. The crude product was crystallized from ethanol to give **104** (207.2 mg, 40%) as a dark orange solid; m.p. 125-127 °C (lit.[76] m.p. 127 °C). The spectroscopic data for **104** was not reported in the literature.[73, 74, 76]

^{1}H-NMR (500 MHz, $CDCl_3$): δ 2.48 (s, 3H, CH_3), 6.78 (s, 1H, H-4), 6.97 (t, 1H, *J* 7.5 Hz, H-4′) [a], 7.19 (d, *J* 8.5 Hz, H-6′) , 7.52 (t, 1H, *J* 7.5 Hz, H-5′) [a], 8.25 (d, *J* 8.5 Hz, H-3′) , 9.61 (s, 1H, N<u>H</u>).

^{13}C-NMR (125 MHz, $CDCl_3$) δ 15.8 (CH_3), 104.9 (C), 113.9 (CH), 116.3 (CH), 120.1 (CH), 122.3 (C), 124.2 (CH), 126.9 (CH), 136.4 (C), 136.4 (C), 141.5 (C), 149.2 (C).

HRMS (EI): *m/z* calcd for $C_{12}H_9N_3O_2S$ [M^+], 259.0415; found, 259.0420

R_f: 0.5 (25% EtOAc in petroleum spirit)

4-Amino-2-methyl-10*H*-thieno[2,3-*b*][1,5]benzodiazepine.hydrochloride (105) [73, 74]

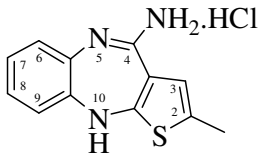

To a stirred slurry of **104** (75 mg, 0.29 mmol) in ethanol (5 mL) 50 °C was added slowly a solution of anhydrous stannous chloride (173 mg, 0.037 mol) in hydrochloric acid (0.6 mL, 5 M). The reaction mixture was stirred and heated at reflux for one hour. The solution was then concentrated under reduced pressure and then crystallized from ethanol to afford **105** (50 mg, 65%) as a yellow solid; m.p. 268-270 °C (decomposed). The m.p. and spectroscopic data for **105** was not reported in the literature.[73, 74]

^{1}H-NMR (500 MHz, CD_3OD): δ 1.02 (s, 3H, C<u>H</u>$_3$), 6.67 (s, 1H, H-3), 6.81 (d, 1H, *J* 8.0 Hz, H-6) [a], 6.93 (d, 1H, *J* 8.0 Hz, H-9) [a], 7.06 (t, 1H, *J* 7.5 Hz, H-8) [b], 7.14 (t, 1H, *J* 7.0 Hz, H-7) [b].

^{13}C-NMR (125 MHz, CD_3CD) δ 14.9 (CH_3), 109.0 (C-3a), 121.1 (C-5a), 122.3 (CH), 122.4 (C), 124.5 (CH), 126.1 (CH), 129.0 (CH) 130.0 (CH), 130.1 (C-9a), 142.5 (C-10a), 162.4 (C-4),

HRMS (EI): *m/z* calcd for $C_{12}H_9N_3O_2S$ [M^+], 229.0677; found, 229.0675.

2-Methyl-4-(piperidin-1-yl)-10*H*-benzo[*b*]thieno[2,3-*e*][1,4]diazepine (101)

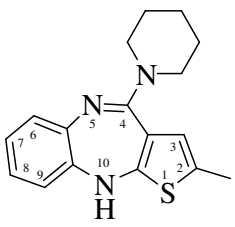

A solution of **105** (102 mg, 0.37 mmol), piperidine (638 mg, 7.5 mmol) and piperidine hydrochloride (914 mg, 7.5 mmol) in DMSO (5 mL) was heated at reflux for 20 hours, and then the organic layer was extracted with CH_2Cl_2. The dichloromethane phase was then extracted twice with 1 M aqueous HCl solution. The dark brown colored hydrochloride was separated and basified to pH 7.5 – 8.5, using 1 M aqueous NaOH solution. The attained solution was extracted

with dichloromethane. All the dichloromethane phases then were combined and washed with brine solution (2 x). The solvent was evaporated under reduced pressure to provide an oil. The oil was subjected to column chromatography using 1% : 0.1% methanol : triethyamine in CH_2Cl_2 to afford the desired product (**101**) (50 mg, 45%) as a brown solid.

Further purification for biological testing was obtained by preparative reverse-phase HPLC using a linear gradient of 10-90% acetonitrile and water and 0.1% HCl over 54 min. Analytical reverse-phase HPLC (10-90% CH_3CN/H_2O/0.1% HCl over 40 min., R_t = 30.1 min) confirmed the purity of **101** (96%); m.p. of HCl salt after HPLC 238-240 °C (decomposed).

^{1}H-NMR (500 MHz, $CDCl_3$): δ 1.66 (s, 6H, CH_2), 2.30 (s, 1H, CH_3), 3.50 (s, 4H, CH_2), 6.28 (s, 1H, H-3), 6.68 (d, 1H, *J* 8.0 Hz, H-6) [a], 6.86 (t, 1H, *J* 7.5 Hz, H-8) [b], 6.93 (t, 1H, *J* 7.5 Hz, H-7) [b], 7.08 (d, 1H, *J* 8.0 Hz, H-9) [a].

^{13}C-NMR (125 MHz, $CDCl_3$) δ 15.6 (CH_3), 24.8 (CH_2), 26.2 (CH_2), 48.7 (CH_2), 119.3 (CH), 122.9 (CH), 124.5 (CH), 124.6 (CH), 127.9 (CH), 129.3(C-3a), 138.4 (C-2), 139.7 (C-5a), 144.1 (C-9a), 158.5 (C-10a), 161.1 (C-4).

HRMS (CI): *m/z* calcd for $C_{17}H_{20}N_3S$ [MH^+], 298.1378; found, 298.1505.

R_f: 0.3 (1% : 0.1% / MeOH : NEt_3 in CH_2Cl_2)

4.2 Toward the synthesis of 99 and 102

2-Amino-5-ethylthiophene-3-carbonitrile (111)

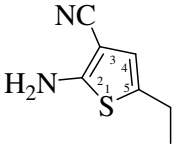

To a solution of sulfur (1.60 g, 50 mmol), butanal (4.6 mL, 50 mol) and malononitrile (3.15 mL, 50 mmol) in DMF (6 mL) was added dropwise triethylamine (4.25 mL). The reaction mixture was stirred at room temperature for 20 hours and then water was added and the mixture was extracted with CH_2Cl_2. The obtained crude product was purified by column

chromatography using 12.5% ethyl acetate in hexane to afford the title compound (**111**; 1.52 g, 20%) as a dark brown oil.

^{1}H-NMR (500 MHz, $CDCl_3$): δ 1.22 (t, 3H, *J* 7.5 Hz, $CH_2C\underline{H}_3$), 2.62 (q, 2H, *J* 7.5 Hz, $C\underline{H}_2CH_3$), 4.65 (s, 2H, $N\underline{H}_2$), 6.37 (s, 1H, H-4).

^{13}C-NMR (125 MHz, $CDCl_3$) δ 15.4 (CH_3), 23.2 (CH_2), 87.6 (C), 115.8 (C), 120.5 (C), 120.5 (CH), 160.7 (C)

HRMS (CI): *m/z* calcd for $C_7H_8N_2S$ [MH^+], 153.0908; found, 153.0895.

R_f: 0.3 (25% EtOAc in petroleum spirit)

5-Ethyl-2-(2-nitroanilino)thiophene-3-carbonitrile (112)

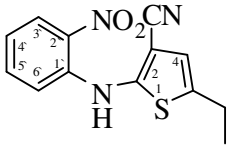

Method 1: A solution of **111** (425 mg, 2.79 mmol) and *o*-fluoronitrobenzene (0.30 mL, 2.79 mmol) in dry THF (5 mL) was added in a dropwise manner to a suspension of NaH (200 mg, 4.18 mmol) in dry THF (8 mL). The reaction mixture was stirred under a N_2 atmosphere for a period of 20 hours and then the solvent was evaporated under reduced pressure. The crude product was extracted into CH_2Cl_2 and then subjected to column chromatography using a gradient elution of 25-50% hexane in CH_2Cl_2 to give **112** (390.1 mg, 51%) as a red oil.

Method 2: A solution of **111** (326 mg, 2.14 mmol), *o*-flouronitrobenzene (0.23 mL, 2.14 mmol) and K_2CO_3 (887 mg, 6.42 mmol) in dry DMF (8 mL) was stirred under a N_2 atmosphere at 140 °C for 90 minutes. After this time, water was added and the mixture was extracted into CH_2Cl_2 and then purified by column chromatography using a gradient elution of 25-50% hexane in CH_2Cl_2 to give **112** (147 mg, 26%) as a red oil.

^{1}H-NMR (500 MHz, $CDCl_3$): δ 1.33 (t, 3H, *J* 7 Hz, $CH_2C\underline{H}_3$), 2.81 (q, 2H, *J* 7.5 Hz, $C\underline{H}_2CH_3$), 6.80 (s, 1H, H-4), 6.96 (t, 1H, *J* 7.7 Hz, H-4′) [a], 7.20 (d, *J* 8.5 Hz, H-3′) [b], 7.52 (t, 1H, *J* 7.5 Hz, H-5′) [a], 8.25 (d, *J* 8.5 Hz, H-6′) [b], 9.63 (s, 1H, N<u>H</u>).

^{13}C-NMR (125 MHz, $CDCl_3$) δ 15.4 (CH_3), 23.8 (CH_2), 116.3 (CH), 120.0 (CH), 122.4 (CH), 126.8 (CH), 136.3 (CH).

HRMS (CI): *m/z* calcd for $C_{13}H_{11}N_3O_2S$ [MH^+], 274.3213; found, 274.3215.

R_f: 0.5 (25% EtOAc in petroleum spirit)

4-Amino-2-ethyl-10*H*-thieno[2,3-*b*][1,5]benzodiazepine.hydrochloride (113)

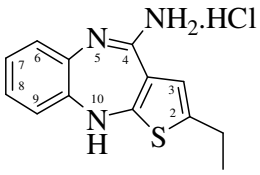

To a stirred slurry of **112** (150 mg, 0.55 mmol) in ethanol (6 mL) at 50 °C was added slowly a solution of anhydrous stannous chloride (625 mg, 3.3 mol) in hydrochloric acid (0.1 mL, 10 M). The reaction mixture was stirred and heated at reflux for 7 hours. The solution was then concentrated under reduced pressure and then crystallized from ethanol to afford **113** (195 mg, 70%) as a yellow solid; m.p. 265-267 °C (decomposed).

^{1}H-NMR (500 MHz, CD_3OD): δ 1.26 (t, 3H, *J* 6.7 Hz, $CH_2C\underline{H}_3$), 2.68 (q, 2H, *J* 7.5 Hz, $C\underline{H}_2CH_3$), 6.73 (s, 1H, H-3), 6.81 (d, 1H, *J* 8.0 Hz, H-9) [a], 6.94 (d, 1H, *J* 8.0 Hz, H-6) [a], 7.06 (t, 1H, *J* 7.5 Hz, H-8) [b], 7.14 (t, 1H, *J* 7.0 Hz, H-7) [b].

^{13}C-NMR (125 MHz, CD_3CD) δ 15.4 (CH_3), 23.9 (CH_2), 108.8 (C), 120.7 (CH), 121.1 (CH), 124.6 (CH), 126.2 (CH), 129.1 (CH), 130.1 (C-3a), 137.3 (C-5a), 142.7 (C-9a), 162.5 (C-10a), 164.4 (C-4).

HRMS (CI): *m/z* calcd for $C_{13}H_{14}N_3S$ [MH^+], 280.0895; found, 280.0904.

2-Ethyl-4-(4-methylpiperazin-1-yl)-10*H*-benzo[b]thieno[2,3-*e*][1,4]diazepine (99) [16, 72-74]

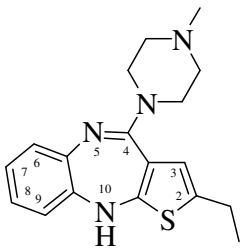

A solution of **113** (455 mg, 1.62 mmol), methyl piperazine (3.3 g, 16.2 mmol) and methyl piperazine hydrochloride (3.4 g, 16.2 mmol) in DMSO (15 mL) was heated to 110 °C for 20 hours, and then the organic layer was extracted with CH_2Cl_2. The dichloromethane phase was then extracted twice with 1 M aqueous HCl solution. The dark brown colored hydrochloride was separated and basified, to pH 7.5 – 8.5, using 1 M aqueous NaOH solution. The attained solution was extracted with dichloromethane. The dichloromethane phases then were combined and washed with brine solution (2 x). The solvent was evaporated under reduced pressure to provide an oil. The oil was subjected to column chromatography using 6% : 0.1% methanol : triethylamine in CH_2Cl_2 to afford the desired product (**99**) (211 mg, 40%) as a yellow powder; m.p. 190-193 °C.

Analytical reverse-phase HPLC (0-100% CH_3CN/H_2O/0.1% HCl over 45 min., Rt = 17.2 min) confirmed the purity of **99** (95%).

^{1}H-NMR (500 MHz, $CDCl_3$): δ 1.22 (t, 3H, *J* 8.0 Hz, $CH_2C\underline{H}_3$), 2.35 (s, 3H, CH_3), 2.51 (s, 4H, CH_2), 2.65 (q, 2H, *J* 7.5 Hz, $C\underline{H}_2CH_3$), 3.54 (s, 4H, CH_2), 5.04 (s, 1H, N<u>H</u>), 6.31 (s, 1H, H-3), 6.60 (d, 1H, *J* 8.0 Hz, H-6) [a], 6.87 (t, 1H, *J* 8.0 Hz, H-7) [b], 6.96 (t, 1H, *J* 8.0 Hz, H-8)[b], 7.02 (d, 1H, *J* 8.0 Hz, H-9) [a].

^{13}C NMR (125 MHz, $CDCl_3$) δ 15.8 (CH_3), 23.7 (CH_2), 46.2 (CH_2), 46.9 (CH_3), 55.2 (CH_2), 119.1 (CH), 119.4 (C), 121.3 (CH), 123.9 (CH), 124.8 (CH), 128.3 (CH), 136.8 (C-3a), 141.0 (C-5a), 142.7 (C-9a), 151.8 (C-10a), 157.9 (C-4).

HRMS (EI): *m/z* calcd for $C_{18}H_{22}N_4S$ [M^+], 326.1565; found, 326.1565.

R_f: 0.1 (6% : 0.1% / MeOH : NEt_3 in CH_2Cl_2)

2-Ethyl-4-(piperidin-1-yl)-10*H*-benzo[*b*]thieno[2, 3-*e*][1,4]diazepine (102)

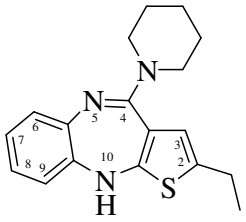

A solution of **113** (80.5 mg, 0.28 mmol), piperidine (638.6 mg, 7.5 mmol) and piperidine hydrochloride (915 mg, 7.5 mmol) in DMSO (5 mL) was heated at 110 °C for 20 hours. The mixture was cooled and then water was added. The solution was extracted with CH_2Cl_2. The combined dichloromethane phase was then extracted twice with 1 M aqueous HCl solution. The dark brown colored hydrochloride was separated and basified to pH 7.5 – 8.5, using 1 M aqueous NaOH solution. The obtained solution was extracted with dichloromethane. The dichloromethane phases then were combined and washed with brine (2 x). The solvent was evaporated under reduced pressure to provide an oil. The oil was purified by column chromatography using a gradient elution of 1% - 2% : 0.1% methanol : triethylamine in CH_2Cl_2 to give the desired product (**102**) (35 mg, 41%) as a yellow solid.

Further purification for biological testing was obtained by preparative reverse-phase HPLC using a linear gradient of 0-100% acetonitrile and water and 0.1% HCl over 60 min. Analytical reverse-phase HPLC (0-100% CH_3CN/H_2O/0.1% HCl over 60 min., R_t = 46.7 min) confirmed the purity of **102** (96%); m.p. of HCl salt after HPLC 236-237 °C (decomposed)

^{1}H-NMR (500 MHz, $CDCl_3$): δ 1.21 (t, 3H, *J* 7.5 Hz, $CH_2C\underline{H}_3$), 1.64 (s, 8H, CH_2), 2.65 (q, 2H, *J* 7.5 Hz, $\underline{C}H_2CH_3$), 3.44 (s, 2H, CH_2), 4.98 (s, 1H, N$\underline{H}$), 6.32 (s,1H, H-3), 6.60 (d, 1H, *J* 8.0 Hz, H-6) [a], 6.84 (t, 1H, *J* 8.0 Hz, H-7) [b], 6.95 (t, 1H, *J* 8.0 Hz, H-8) [b], 7.02 (d, 1H, *J* 8.0 Hz, H-9) [a].

^{13}C NMR (125 MHz, $CDCl_3$) δ 15.7 (CH_3), 24.1 (CH_2), 24.6 (CH_2), 26.9 (CH_2), 48.5 (CH_2), 120.9 (CH), 122.1 (CH), 125.8 (CH), 127.1 (CH), 129.3 (CH)[a], 129.9 (C-3a)[a], 138.8 (C-5a), 139.9 (C-9a), 149.2 (C-10a), 160.8 (C-4).

HRMS (CI): *m/z* calcd for $C_{18}H_{22}N_3S$ [MH^+], 312.1534; found, 312.1544.

R_f: 0.3 (1% : 0.1% / MeOH : NEt_3 in CH_2Cl_2)

4.3 Toward the synthesis of 100

Synthesis of ethyl 2-oxobutanoate (114)[89,90]

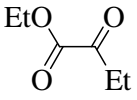

Method 1[89]: To a stirring solution of diethyl oxalate (6.0 g, 0.041 mmol) in dry diethyl ether (50 mL, 0.8 M) at -78 °C under a N_2 atmosphere was added dropwise a 3 M solution of ethyl magnesium bromide (5.4 mL, 0.041 mmol). The reaction mixture was stirred vigorously for the period of 2 hours. A mixture of ice (20 mL) diethyl ether (25 mL) and concentrated hydrochloric acid (3 mL) was then added to the reaction mixture. The mixture was extracted with diethyl ether (3 x, 100 mL) and washed with water (25 mL). The solvent was removed under reduced pressure to give a green oil (3 mL). The crude product was distilled at 57 °C, at 3 mm Hg, using a kugolrohr apparatus to afford the title product (**114**) as a colorless liquid (400 mg, 10%).

Method 2[90]: A solution of 2-oxobutanoic acid (3.0 g, 29 mmol), anhydrous *p*-toluenesulfonic acid (0.06 g), ethanol (25 mL) and benzene (12 mL) was heated at reflux for 6 hours. After the addition of triethanolamine (0.06 mL), the reaction mixture was concentrated under reduced pressure. The crude product was then distilled at 57 °C at 3 mm Hg, using a kugolrohr apparatus to afford the title product (**114**) as a colorless liquid (3.0 g, 80%). Spectroscopic data matched that reported in the literature.[89, 90]

Ethyl 5-amino-4-cyano-2-methylthiophene-3-carboxylate (115)

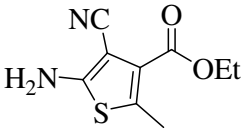

To a solusion of sulfur (483 mg, 15.06 mmol), ethyl 2-oxobutanoate (1.54 g, 15.06 mmol) and malononitrile (994 mg, 15.06 mmol) in ethanol (15 mL) was added dropwise triethylamine (1.0 mL). The reaction mixture was stirred and heated at reflux for 2 hours and then the crude product was dissolved in CH_2Cl_2 and the solution was

washed with water. The mixture was purified by column chromatography using a gradient elusion of 14.5 – 25% ethyl acetate in hexane to afford the title compound (**115**; 472 mg, 20%) as a brown solid; m.p. 105-108 °C.

^{1}H-NMR (500 MHz, $CDCl_3$): δ 1.39 (t, 3H, *J* 6.7 Hz, $OCH_2C\underline{H}_3$), 2.56 (s, 3H, $C\underline{H}_3$), 4.34 (q, 2H, *J* 6.7 Hz, $OC\underline{H}_2CH_3$), 4.74 (s, 2H, $N\underline{H}_2$).

^{13}C NMR (125 MHz, $CDCl_3$) δ 14.2 (CH_3), 15.1 (CH_3), 61.2 ($O\underline{C}H_2$), 88.7 (C), 115.1 (C), 124.6 (C), 135.1 (C), 159.0 (C), 161.8 (C=O).

HRMS (CI): *m/z* calcd for $C_9H_{11}N_2O_2S$ [MH^+], 211.0541; found, 211.0536.

R_f: 0.2 (25% EtOAc in petroleum spirit)

Ethyl 4-cyano-2-methyl-5-(2-nitrophenylamino)thiophene-3-carboxylate (116)

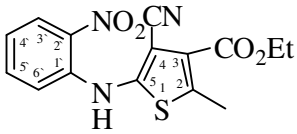

A solution of **115** (172 mg, 0.82 mmol) and *o*-fluoronitrobenzene (0.09 mL, 0.83 mmol) in dry THF (2 mL) was added in a dropwise manner to a suspension of NaH (60 mg, 1.22 mmol) in dry THF (9 mL). The reaction mixture was stirred under a N_2 atmosphere for 20 hours and then the solvent was evaporated under reduced pressure. The crude product was dissolved in CH_2Cl_2 and the solution was washed with water and then subjected to column chromatography using a gradient elution of 10-50% ethyl acetate in hexane to give **112** (390 mg, 70%) as an orange solid; m.p. 143-145 °C.

^{1}H-NMR (300 MHz, $CDCl_3$): δ 1.43 (t, 3H, *J* 7.5 Hz, $CH_2C\underline{H}_3$), 2.73 (s, 3H, $C\underline{H}_3$), 4.41 (q, 2H, *J* 7.2 Hz, $C\underline{H}_2CH_3$), 7.02 (t, 1H, *J* 8.7 Hz, H-4′) [a], 7.27 (d, *J* 8.5 HZ, H-3′) [b], 7.55 (t, 1H, *J* 7.5 Hz, H-5′) [a], 8.27 (d, *J* 7.2 Hz, H-6′) [b], 9.76 (s, 1H, N$\underline{H}$).

^{13}C-NMR (125 MHz, $CDCl_3$) δ 14.2 (CH_3), 15.9 (CH_3), 61.8 ($O\underline{C}H_2$), 116.3 (CH), 116.8 (C-5), 120.7 (CH), 127.0 (CH), 136.3 (CH), 143.9 (C-2′), 148.6 (C-4), 161.3 (C=O).

HRMS (CI): *m/z* calcd for $C_{13}H_{12}N_3O_2S$ [MH^+], 273.3101; found, 273.3111.

R_f: 0.3 (25% EtOAc in petroleum spirit)

Ethyl 4-amino-2-methyl-10*H*-benzo[*b*]thieno[2,3-*e*][1,4]diazepine-3-carboxylate (117)

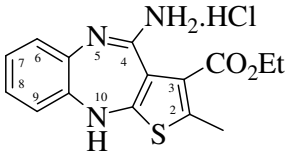

A stirred slurry of **116** (190 mg, 0.57 mmol) in ethanol (10 mL) at 50 °C was added slowly to a solution of anhydrous stannous chloride (660 mg, 3.42 mol) in hydrochloric acid (0.1 mL, 10 M). The reaction mixture was stirred and heated at reflux for 6 hours. The solution was then concentrated under reduced pressure and then crystallized from ethanol to afford **113** (200 mg, 60%) as a yellow solid; m.p. 278 °C (decomposed).

^{1}H-NMR (500 MHz, CD_3OD): δ 1.36 (t, 3H, *J* 7.0 Hz, $OCH_2C\underline{H}_3$), 2.56 (s, 3H, CH_3), 4.31(q, 2H, *J* 7.5 HZ, $OC\underline{H}_2CH_3$), 6.94 (d, 1H, *J* 7.5 Hz, H-6) [a], 7.14 (m, *J* 8.0 HZ, H-9 [a], H-7 [b]) , 7.23 (t, *J* 7.5 HZ, H-8) [b].

^{13}C-NMR (125 MHz, CD_3OD) δ 14.4 (CH_3), 15.1 (CH_3), 62.4 ($O\underline{C}H_2$), 121.3 (CH), 125.4 (CH), 126.3 (CH) , 126.4 (C), 129.3 (CH), 129.9 (C-10a), 141.0 (C-3)[a], 145.9 (C-4)[a], 163.6 (C=O).

HRMS (CI): *m/z* calcd for $C_{15}H_{16}N_3O_2S$ [MH^+], 302.0963; found, 302.0966.

Diethyl 2-amino-5-methylthiophene-3, 4-dicarboxylate (119)

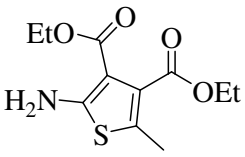

To a solusion of sulfur (80 mg, 2.5 mmol), ethyl 2-oxobutanoate (330 mg, 2.5 mmol) and ethyl cyanoacetate (283 mg, 2.5 mmol) in ethanol (5 mL) was added dropwise diethylamine (0.2 mL). The reaction mixture was stirred and heated at reflux for 1.5 hours. The excess sulfur was filtered off and then the solvent was evaporated under reduced pressure. The obtained crude product was purified by

column chromatography using 12.5% ethyl acetate in hexane to afford the title compound (**119**; 372 g, 58%) as a dark brown oil.

^{1}H-NMR (500 MHz, $CDCl_3$): δ 1.30 (t, 6H, *J* 7.5 Hz, $COOCH_2C\underline{H}_3$), 1.35 (t, 6H, *J* 7.0 Hz, $COOCH_2C\underline{H}_3$), 2.26 (s, 3H, $C\underline{H}_3$), 4.24 (q, 4H, *J* 7.0 Hz, $COOC\underline{H}_2CH_3$), 4.31 (q, 4H, *J* 7.0 Hz, $COOC\underline{H}_2CH_3$), 5.84 (s, 2H, $N\underline{H}_2$).

^{13}C-NMR (125 MHz, $CDCl_3$) δ 13.1 (CH_3), 14.2 (CH_3), 14.3 (CH_3), 60.0 ($O\underline{C}H_2$), 61.2 ($O\underline{C}H_2$), 104.7(C), 122.4 (C), 128.6 (C), 160.9 (C), 164.5 ($\underline{C}$=O), 166.1 ($\underline{C}$=O).

HRMS (EI): *m/z* calcd for $C_{11}H_{15}NO_4S$ [M^+], 257.0722; found, 257.0719.

R_f: 0.3 (25% EtOAc in petroleum spirit)

Diethyl 2-methyl-5-(2-nitrophenylamino)thiophene-3,4-dicarboxylate (120)

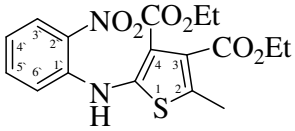

A solution of **119** (120 mg, 0.46 mmol) and *o*-fluoronitrobenzene (65 mg, 0.46 mmol) in dry THF (2 mL) was added in a dropwise manner to a suspension of NaH (33 mg, 0.69 mmol) in dry THF (8.5 mL). The reaction mixture was stirred at 40 °C under a N_2 atmosphere for the period of 20 hours and then the solvent was evaporated under reduced pressure. Water was added and the crude product was extracted in CH_2Cl_2 and then subjected to the column chromatography using 17% ethyl acetate in hexane to give **120** (140 mg, 37%) as a red oil.

^{1}H-NMR (500 MHz, $CDCl_3$): δ 1.33 (t, 3H, *J* 7.0 Hz, $COOCH_2C\underline{H}_3$), 1.37 (t, 3H, *J* 7.5 Hz, $COOCH_2C\underline{H}_3$), 2.44 (s, 3H, $C\underline{H}_3$), 4.35 (q, 4H, *J* 7.0 Hz, $COOC\underline{H}_2CH_3$), 7.01 (t, 1H, *J* 8.0 Hz H-4′), 7.56 (t, *J* 8.0 Hz, H-5′), 7.73 (d, 1H, *J* 8.5 Hz, H-3′) [a], 8.24 (d, 1H, *J* 8.5 Hz, H-6′) [a], 11.27 (s, 1H, $N\underline{H}$).

^{13}C-NMR (125 MHz, $CDCl_3$) δ 13.6 (CH_3), 14.3 (CH_3), 61.3 (O<u>C</u>H_2), 61.5 (O<u>C</u>H_2), 116.3 (C-2), 117.0 (CH), 120.7 (CH), 127.0 (CH), 129.2 (CH), 135.8 (C-1′), 135.8 (C-5), 138.8 (C), 147.7 (C-2′), 163.4 (<u>C</u>=O), 165.1 (<u>C</u>=O).

HRMS (CI): *m/z* calcd for $C_{17}H_{19}N_2O_6S$ [MH^+], 379.0964; found, 379.0961.

R_f: 0.4 (25% EtOAc in petroleum spirit)

Diethyl 2-(2-aminophenyl amino)-5-methylthiophene-3,4-dicarboxylate (121)

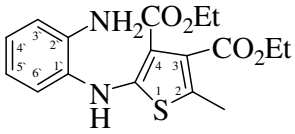

To a stirred solution of **120** (104 mg, 0.27 mmol) in ethanol (7 mL) at 50 °C was added slowly a solution of anhydrous stannous chloride (208 mg, 1.90 mol) in hydrochloric acid (0.75 mL, 10 M). The reaction mixture was stirred and heated at reflux for one hour. The reaction mixture was concentrated under reduced pressure, dissolved in an aqueous solution of $NaHCO_3$, washed with water and then extracted into CH_2Cl_2. The crude product was subjected to column chromatography using a gradient elution of 17 - 25% ethyl acetate in hexane to afford **121** (230 mg, 66%) as a yellow oil.

^{1}H-NMR (500 MHz, $CDCl_3$): δ 1.31 (t, 3H, *J* 6.5 Hz, $COOCH_2C\underline{H}_3$), 1.37 (t, 3H, *J* 7.0 Hz, $COOCH_2C\underline{H}_3$), 2.33 (s, 3H, $C\underline{H}_3$), 3.85 (s, 2H, $N\underline{H}_2$), 4.27 (q, 2H, *J* 6.0 Hz, $COOC\underline{H}_2CH_3$), 4.33 (q, 2H, *J* 6.0 Hz, $COOC\underline{H}_2CH_3$), 6.76 (t, 1H, *J* 7.5 Hz, H-4′) [a], 6.80 (d, *J* 8.0 HZ, H-3′) [b], 7.06 (t, 1H, *J* 7.5 Hz, H-5′) [a], 7.23 (d, 1H, *J* 8.0 Hz, H-6′) [b], 8.80 (s, 1H, N<u>H</u>).

^{13}C NMR (125 MHz, $CDCl_3$) δ 13.1 (CH_3), 14.3 (CH_3), 14.4 (CH_3), 60.2 (O<u>C</u>H_2), 61.3 (O<u>C</u>H_2), 103.9 (C), 116.6 (CH), 119.1 (CH), 122.3 (CH), 125.2 (CH), 127.3 (C), 127.7 (C), 128.7 (C), 141.7 (C), 161.9 (C), 164.9 (<u>C</u>=O), 166.1 (<u>C</u>=O).

HRMS (CI): *m/z* calcd for $C_{17}H_{21}N_2O_4S$ [MH^+], 349.1222; found, 349.1219.

R_f: 0.5 (25% EtOAc in petroleum spirit)

4.4 Toward the synthesis of 87

t-Butylcyanoacetate (124) [90]

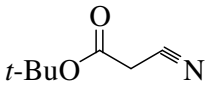

To a stirred solution of cyanoacetic acid (858 mg, 10 mmol) and *tert*-butanol (1.2 mL, 12.5 mmol) in acetonitrile (10 mL) was added a solution of DCC (2.253 g, 11 mmol) in acetonitrile (10 mL). The reaction mixture was stirred for 15 minutes and then the solid was filtered off. The crude product was then purified by column chromatography using 10% ethyl acetate in hexane to give **124** as yellow liquid in 75% yield. All spectroscopic data matched that reported in the literature.[90]

Synthesis of ethyl 2-oxopentanoate (130)[91]

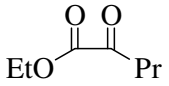

To a stirred solution of diethyl oxalate (6.78 mL, 50 mmol) in dry diethyl ether (25 mL) at -78 °C under a N_2 atmosphere was added dropwise a 2 M solution of propylmagnesium chloride (25 mL, 50 mmol). The reaction mixture was stirred vigorously for the period of 30 minutes. The reaction mixture then was poured without warming into a mixture of ice (20 mL), diethyl ether (25 mL) and concentrated hydrochloric acid (4.5 mL). The organic layer was extracted with diethyl ether (100 mL) and washed with water (3 x, 25 mL). The solvent was removed under reduced pressure to give a colorless oil (6.2 g, 92%). The TLC analysis showed one major spot. Thus, the obtained product was used without furthur purification in the next reaction. All spectroscopic data matched that reported in the literature.[91]

3-*tert*-Butyl 4-ethyl 2-amino-5-ethylthiophene-3,4-dicarboxylate (131)

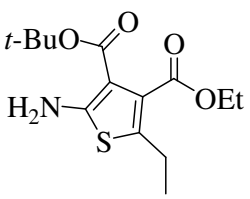

To a solution of sulfur (454 mg, 14.17 mmol), **130** (2.04 g, 14.17 mmol mol) and **124** (2.00 g, 14.17 mmol) in DMF

(8 mL) was added dropwise triethylamine (1.2 mL). The reaction mixture was stirred at room temperature for 20 hours. Water was added and then the mixture was extracted into CH_2Cl_2. The crude product was purified by column chromatography using a gradient elution of 11 – 14% ethyl acetate in hexane to afford the title compound (**131**; 2.33 g, 55%) as an orange liquid.

^{1}H-NMR (500 MHz, $CDCl_3$): δ 1.12 (t, 3H, *J* 7.5 Hz, $CH_2C\underline{H}_3$) [a], 1.29 (t, 3H, *J* 7.5 Hz, $OCH_2C\underline{H}_3$) [a], 1.44 (s, 9H, $C\underline{H}_3$), 2.56 (q, 2H, *J* 11.0 Hz, $C\underline{H}_2CH_3$), 4.24 (q, 2H, *J* 10.0 Hz, $OC\underline{H}_2CH_3$), 5.94 (s, 2H, $N\underline{H}_2$).

^{13}C NMR (125 MHz, $CDCl_3$) δ 14.1 (CH_3), 15.8 (CH_3), 21.3 (CH_2), 28.0 (CH_3), 61.0 (OCH_2), 80.5 (C), 105.6 (C), 113.5 (C), 127.8 (C), 128.9 (C), 164.0 (C=O), 166.0 (C=O).

HRMS (CI): *m/z* calcd for $C_{14}H_{22}NO_4S$ [MH^+], 300.1270; found, 300.1264.

R_f: 0.4 (25% EtOAc in petroleum spirit)

3-*tert*-Butyl 4-ethyl 5-ethyl-2-(2-nitrophenylamino)thiophene-3,4-dicarboxylate (132)

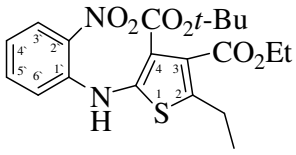

A solution of **131** (2.20 g, 7.3 mmol) and *o*-flouronitrobenzene (1.03 g, 7.3 mmol) in dry THF (10 mL) was added in dropwise manner to a suspension of NaH (530 mg, 11.2 mmol) in dry THF (10 mL). The reaction mixture was stirred at room temperature under a N_2 atmosphere for 20 hours and then the solvent was evaporated under reduced pressure. Water was added and the mixture was extracted into CH_2Cl_2 and then subjected to the column chromatography using 9% ethyl acetate in hexane to give **132** (1.71 g, 56%) as a red solid; m.p. 92 °C.

^{1}H-NMR (500 MHz, $CDCl_3$): δ 1.28 (t, 3H, *J* 7.5 Hz, $CH_2C\underline{H}_3$) [a], 1.37 (t, 3H, *J* 7.5 Hz, $OCH_2C\underline{H}_3$) [a], 1.50 (s, 9H, $C\underline{H}_3$), 2.84 (q, 2H, *J* 7.5 Hz, $C\underline{H}_2CH_3$), 4.35 (q, 2H, *J*

7.0 Hz, OC<u>H</u>$_2$CH$_3$), 6.99 (t, 1H, *J* 7.7 Hz, H-4′) [b], 7.55 (t, 1H, *J* 8.0 Hz, H-5′) [b], 7.68 (d, 1H, *J* 8.5 Hz, H-3′) [c], 8.22 (d, 1H, *J* 8.5 Hz, H-6′) [c], 11.0 (s, 1H, N<u>H</u>).

^{13}C NMR (125 MHz, $CDCl_3$) δ 14.3 (CH_3), 16.0 (CH_3), 22.0 (CH_2), 28.2 (CH_3), 61.4 (OCH_2), 82.5 (C), 117.3 (CH), 118.8 (C), 120.4 (CH), 126.8 (CH), 128.3 (C), 135.6 (CH), 135.7 (CH), 137.6 (C), 139.5 (C), 146.4 (C), 162.8 (C=O), 165.0 (C=O).

HRMS (EI): *m/z* calcd for $C_{20}H_{25}N_2S_6O$ [M^+], 420.1366; found, 420.1366.

R_f: 0.5 (25% EtOAc in petroleum spirit)

3-*tert*-Butyl 4-ethyl 2-(2-aminophenylamino)-5-ethylthiophene-3,4-dicarboxylate (133)

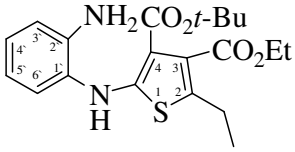

A solution of **132** (1.0 g, 2.3 mmol) in ethanol (100 mL) was hydrogenated over 10% Pd-C (100 mg). The reaction mixture was stirred at 40 – 50 °C for 2 hours. The catalyst was then filtered off and the solvent removed under vacuum. The crude product was subjected to column chromatography using 8% ethyl acetate in petroleum spirit to give **133** (726 mg, 81%) as a yellow oil.

^{1}H-NMR (500 MHz, $CDCl_3$): δ 1.16 (t, 3H, *J* 7.5 Hz, $CH_2C\underline{H}_3$) [a], 1.37 (t, 3H, *J* 7.0 Hz, $OCH_2C\underline{H}_3$) [a], 1.53 (s, 9H, $C\underline{H}_3$), 2.61 (q, 2H, *J* 7.5 Hz, $C\underline{H}_2CH_3$), 3.84 (s, 2H, $N\underline{H}_2$), 4.33 (q, 2H, *J* 7.5 HZ, $OC\underline{H}_2CH_3$), 6.77 (t, 1H, *J* 10.5 Hz, H-4′) [b], 6.80 (d, 1H, *J* 8 Hz, H-3′) [c], 7.06 (t, 1H, *J* 8.5 Hz, H-5′) [b], 7.25 (d, 1H, *J* 8.5 Hz, H-6′) [c], 8.82 (s, 1H, N<u>H</u>).

^{13}C NMR (125 MHz, $CDCl_3$) δ 14.4 (CH_3), 16.0 (CH_3), 21.6 (CH_2), 28.5 (CH_3), 61.1 (OCH_2), 81.1 (C), 105.2 (C), 116.5 (CH), 119.1 (CH), 125.3 (CH), 127.5 (CH), 127.6 (C), 128.1 (C), 129.0 (C), 141.7 (C), 161.3 (C), 164.7 (C=O), 166.2 (C=O).

HRMS (CI): *m/z* calcd for $C_{20}H_{27}N_2O_4S$ [MH^+], 391.1692; found,391.1282.

R_f: 0.4 (25% EtOAc in petroleum spirit)

4.5 Toward the synthesis of 145

2-Methyl-4-(4-methylpiperazin-1-yl)-10*H*-benzo[b]thieno[2,3-*e*][1,4]diazepine-10-carbaldehyde (145)

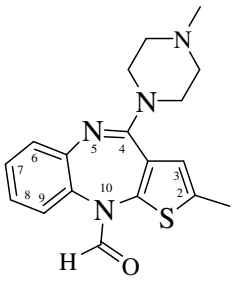

To a stirred solution of $POCl_3$ (0.15 mL, 1.64 mmol) in anhydrous DMF (0.11 mL, 1.42 mmol) under a nitrogen atmosphere was added dropwise at 0 °C a solution of olanzapine (100 mg, 0.32 mmol) in anhydrous DMF (0.5 mL). The reaction mixture was stirred at room temperature for 30 minutes and then heated at 80 °C for 3 hours. After cooling to 10 °C, the reaction mixture was treated with 2 N NaOH solution until pH 10. The obtained solution was extracted with dichloromethane the combined extractions were dried and concentrated under reduced pressure. The crude product was purified by column chromatography using 6% : 0.1% methanol : triethylamine in dichloromethane to afford **145** (70.7 mg, 65%) as a pink powder; m.p. 202-205 °C.

^{1}H-NMR (500 MHz, $CDCl_3$): δ 2.33 (s, 3H, N$\underline{C}H_3$), 2.43 (s, 4H, CH_2), 2.52 (s, 3H, CH_3), 3.60 (s, 4H, CH_2), 6.49 (s,1H, H-3), 7.00 (d, 1H, *J* 8 Hz, H-6) [a], 7.06 (t, 1H, *J* 7.5 Hz, H-7) [b], 7.18 (d, 1H, *J* 8.0 Hz, H-9)[a], 7.27 (d, 1H, *J* 8.0 Hz, H-8) [b] , 8.40 (s, 1H, C=O).

^{13}C NMR (125 MHz, $CDCl_3$) δ 15.9 (CH_3), 46.2 (CH_3), 46.9 (CH_2), 55.0 (CH_2), 128.8 (CH), 124.0 (CH), 124.8 (CH), 125.5 (C), 128.1 (CH), 128.8 (CH), 133.6 (C-3a), 138.9 (C-5a), 140.5 (C-9a), 144.4 (C-10a), 155.2 (C-4), 162.3 (C=O).

HRMS (EI): *m/z* calcd for $C_{18}H_{20}N_4SO$ [M^+], 340.1358; found, 340.1360.

R_f: 0.3 (6% : 0.1% / MeOH : NEt_3 in CH_2Cl_2)

CHAPTER 5: PHARMACOLOGICAL EVALUATION

5.1 Introduction

The competitive binding assay is a measurement of the binding at a single concentration of a labeled ligand in the presence of various concentrations of unlabeled ligand. Competitive binding assays are utilized for different purposes such as to confirm that radioligand has identified the correct receptor, to investigate the receptor number, to verify whether a drug binds to the receptor and also to explore the drug binding affinity with receptors.[64]

In most cases, a single concentration of a ligand is selected approximately equal in amount to that of the K_d value of the labeled ligand for binding to the receptor. The exact concentration of radioligand to be used in the displacement experiments can vary as lower concentrations of ligand decrease the nonspecific binding but result in fewer counts of specific binding and greater counting error. On the other hand, the higher concentrations lead to higher nonspecific binding but also result in lower counting error.[64]

In this project competitive binding assay was used to determine the affinity of the newly synthesized compounds **99**, **101**, **102** and **145** for the binding to the H-1 receptor. As previously discussed (Table 3.1, page 41), these new compounds with various modifications to the structure of olanzapine were expected to reduce the affinity of olanzapine for the H-1 receptor. The ability of each of these new compounds and also olanzapine to displace the binding of [^{3}H]pyrilamine to the H-1 receptor was investigated by the addition of 7 various concentrations (10^{-10} to 10^{-4} M) of each unlabeled compound. The single concentration of radioligand was chosen equal to the K_d value. The obtained data expressed as an IC_{50} value was then calculated and used to compare the affinity of the new compounds with olanzapine for binding to the H-1 receptor.

Therefore, this chapter aims to use a competitive binding assay to investigate the effect of the afore-mentioned modifications on the affinity of olanzapine derivatives for binding to the H-1 receptor.

5.2 Methods

5.2.1 Chemicals:

Synthesized compounds **99**, **101**, **102** and **145** were utilized as unlabeled displacers in a range concentration of 10^{-10}, 10^{-9}, 10^{-8}, 10^{-7}, 10^{-6}, 10^{-5} and 10^{-4} M. Each of these compounds was initially dissolved in DMSO and further diluted into 50 mM sodium potassium phosphate buffer (pH 7.4) for IC_{50} determination. Olanzapine (OChem, Inc. USA) was used as a control chemical at the same concentrations (10^{-10} to 10^{-4} M). [^{3}H]pyrilamine (specific activity 27.0 Ci/mmol) was obtained from Amersham Bioscience UK.

5.2.2 Histology

Brain tissues were obtained from the Centre for Translational Neuroscience Laboratory, UOW. These tissues corresponded to female Sprague Dawley rats weighing 220 - 250 grams which had been stored in a freezer (-80 °C). Brains were cut into coronal sections (14 µm thick) with a Cryostat (Clinicut 60 Cryostat, Bright Instrument Co Ltd, Cambridgeshire, UK) at –18 ºC and then thaw-mounted onto Polysine™ microscope slides (Menzel GmbH & Co KG, Braunschweig, Germany). The levels of brain sections used in this study contained the largest size of the VMH. The slides were stored at -20 ºC until they were used.

5.2.3 Receptor autoradiography

H-1 receptor binding was performed based on a described literature procedure.[21, 92] In brief, sections were incubated at room temperature for 1 hour in 50 mM sodium potassium phosphate buffer (pH 7.4) containing 4 nM [^{3}H]pyrilamine equal to the K_d value[34] plus olanzapine (2 sections for each concentration) whereas additional

sections were incubated in assay buffer, [^{3}H]pyrilamine (4 nM) and also DMSO with the same amount used in the olanzapine solutions. For each concentration of blank DMSO, 2 sections were incubated. These sections were used to prove that the presence of DMSO as a solvent did not affect the binding of unlabeled displacers. After the incubation, the sections were washed 4 x 2 minutes in iced cold buffer with a final dipping in ice-cold distilled water. The slides were then rapidly dried under a stream of cold air. The same procedure was followed for the H-1 receptor binding of compounds **99**, **101**, **102** and **145**.

Generating autoradiographic images was initially attempted by a β-image camera (BioSpace, Paris, France). The exposure time was 3.5 hours. A series of sections with a known amount of ligand was used as a standard in all scans. The beta imager measures the level of bound radioactivity in the brain sections by directly counting the number of β-particles emerging from the tissue sections. However, due to some technical problems with the scanner, the obtained images were not consistent and eventually the mother board of the computer driving this machine needed to be upgraded. Because of the time constrain, the receptor binding assays were performed using a Liquid scintillation analyzer (Tri-Crab 2800 TR).

The liquid scintillation counting technique measures radiation from β-emitting nuclides. Samples are dissolved or suspended in a liquid scintillation mixture (cocktail) comprising at least one scintillatable organic material in toluene or other aromatic solvent structurally related to toluene such as xylene or ditolylmethane in addition to small amount of fluors.[93] β-particles emitted from the sample transfer energy to the solvent molecules and subsequently to the fluors; the excited fluor molecules disperse the energy by emitting light.[94] Thus, each β-emission leads to a pulse of light. The number of light flashes or counts the LSC registered per minute are reported as Counts per minute (CPM).

Initially a standard table was produced based on the count of a number of samples with a known concentration of ligand ([^{3}H]pyrilamine) and also ligands along with one section of blank brain tissue which had not been incubated. The resultant data is summarized in Table 5.1. Measuring a series of samples with only one section of

blank tissue gave a range of 8 – 11 CPM as a background. Each sample was analyzed for 5 minutes in a normal count mode.

Table 5.1: Standard values of various [^{3}H]pyrilamine concentrations in scintillation counts

Number	Concentration of Radioligand (nM)	Radioligand (CPM)	Radioligand & 1 Section Brain Tissue (CPM)
1	700	506923	501232
2	350	299745	281807
3	175	12911	12451
4	87.5	6541	3241
5	43.7	3152	3038
6	21.9	1835	1747
7	10.9	431	427
8	5.5	141	138
9	2.7	97	86
10	1.4	68	69
11	0.7	31	35
12	0.3	21	24
13	0.2	13	17
14	0.1	10	13
15	0	8	7

Cutting out the VMH from sections for scintillation counting was first attempted; however, because the radioactivity was too low the scintillation machine was unable to give a reliable reading. Therefore, a whole section was used. According to the Table 5.1, it was decided to analyze the results of the receptor binding based on the count of two sections for each concentration of each compound. Thus, each count is a measurement of a binding of radioligand to the H-1 receptor of the whole two sections.

5.2.4 Protein Concentration Standardization

In order to compare the count of radioligand in each sample, the whole concentration of contained proteins was required. Therefore, the Bradford Protein Assay was attempted. This assay is compatible with a broad range of reagents including organic solvent, most buffers (PBS, TRIS, Hepes), sugars (sucrose, glucose), culture media (Eagles MEM), salt solution ($NaCl_2$, $MgCl_2$, KCl),

denaturating reagent (DTT, urea) and also some detergents (CHAPS, desoxycholate).[95, 96] However, it was not compatible with the scintillation liquid as the red form coomassie Bradford reagent was changed and stabilized to a blue precipitate by the addition of a blank scintillation cocktail. Dilution of the sample (x 20) also did not change the result of the assay. Thus, it was decided to measure the concentration of protein prior to the scintillation counting. To homogenize the brain sections various buffers (pH 7.5) such as Tris (50 mM), EDTA (1 mM), DTT (1 mM), NaCl (100 mM) and also Hepes (40 mM), $MgSO_4$ (2 mM), $CaCl_2$ (4 mM), KCl (3 mM), NaCl (288 mM) were attempted. However, none of these buffers could dissolve the sections.

Therefore, with the failure of measuring protein concentration, it was assumed that all sections contain the same amount of protein. Sections were scratched from slides and dissolved into 10 µL of ethanol (70 %) and then suspended in 4.5 mL of a scintillation cocktail. The same protocol as standard (5 min, normal mode) was applied to the count of all samples.

5.3 Results

The obtained data from the scintillation counter were statistically analyzed using the Graphpad 4.02 program. The ability of olanzapine and compounds **99**, **101**, **102** and **145** to displace the binding of [^{3}H]pyrilamine (4 nM) to the mounted tissue sections is displayed in Figure 5.1.

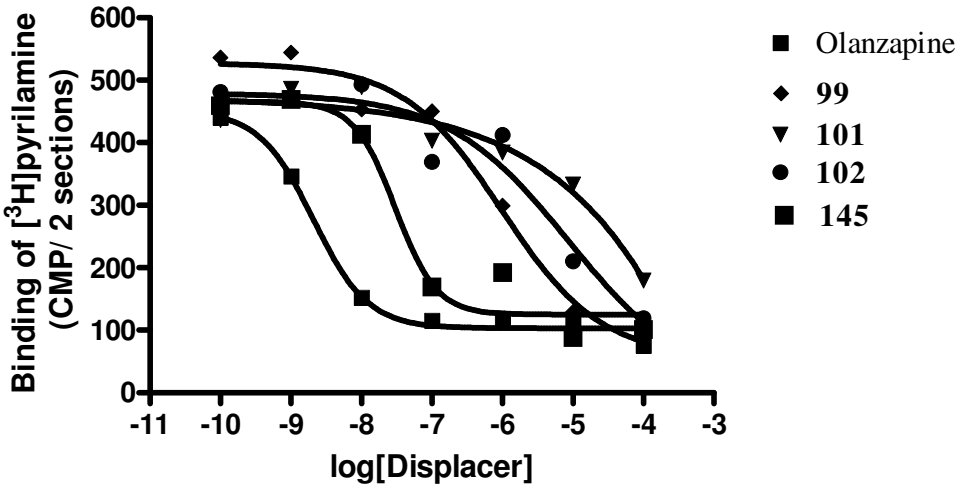

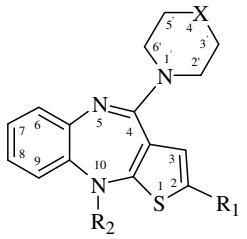

Olanzapine: X = NMe, R_1= Me, R_2 = H

99: X = NMe R_1= Et, R_2 = H

101: X = CH_2 R_1= Me, R_2 = H

102: X = CH_2 R_1= Et, R_2 = H

145: X = NMe, R_1= Me, R_2= CHO

Figure 5.1: Specificity of olanzapine, **99**, **101**, **102** and **145** to displace the H-1 receptor binding of the [^{3}H]pyrilamine.

The Y axis in this displacement curve is the radioligand binding expressed as CPM while the X axis is the log of the molarities of the displacers (olanzapine, **99**, **101**, **102** and **145**). The top of the each curve is a plateau representing total binding. Total binding shows the radioligand binding in the absence of the competing unlabeled compounds. The plateaus at the bottom of the curves represents nonspecific binding. The different values between the top and bottom plateaus show specific binding. Nonspecific binding is an additional binding of the radioligand to the nonspecific sites which are not the physiological target. As all the receptors are saturated by the unlabeled drug the radioligand can only bind nonspecifically. Therefore, to measure the specific binding both the amount of total and nonspecific binding should be taken into consideration.[64]

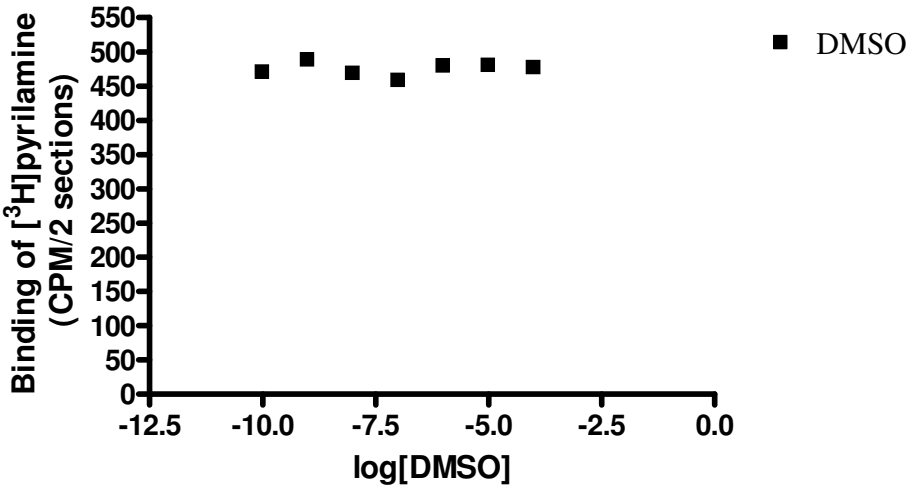

Figure 5.2: The effect of DMSO on the displacement of [^{3}H]pyrilamine.

Figure 5.2 confirms that the presence of DMSO as a solvent did not affect the binding. It can also show the maximal binding of the radioligand to the H-1 receptor.

The obtained displacement curves were used to compare the affinity of the new synthesized compounds with olanzapine. The IC_{50} values were calculated by the Graphpad program for each compound (Table 5.1). This value is the concentration of unlabeled ligands that results in the maximal halfway inhibitory of specific binding of radioligand. Thus a compound with a lower IC_{50} has a higher affinity for the H-1 receptor.

Table 5.2: Obtained IC_{50} values for unlabeled compounds in M.

Compound	Olanzapine	**99**	**101**	**102**	**145**
IC_{50}	2.08×10^{-9}	9.78×10^{-7}	0.50	8.63×10^{-6}	3.70×10^{-8}

.

5.4 Discussion

According to the Table 5.1, the obtained IC_{50} values for compounds **99**, **101**, **102** and **145** are higher than that value for olanzapine, indicating the lower affinity of the novel synthesized compounds for the H-1 receptor. As shown in Figures 5.1 while olanzapine reached to the bottom plateau at approximately 10^{-7} M, compound **99** and **102** showed a tendency to reach saturation around 10^{-4} M. This result is compatible with their IC_{50} values (**99**: 9.78 x 10^{-7} M; **102**: 8.63 x 10^{-6} M) which are remarkably greater than that obtained for olanzapine (2.08 x 10^{-9} M).

Compound **145** reached the plateau around 10^{-6} M resulting in an IC_{50} value of 3.70 x 10^{-8} M. This result indicated that compound **145** is a relatively potent binder to the H-1 receptor. However, the very high IC_{50} value (0.50 M) of compound **101** in the displacement curve (Figure 5.1) is out of line with the other compounds. Although at very high concentration, it replaced [^{3}H]pyrilamine from the H-1 receptor site, it had virtually no effects on receptor binding at all other concentrations. This result, however, needs further experiments for confirmation.

According to the discussion above, compound **99** had significantly reduced affinity compared to that of olanzapine for the H-1 receptor. This result may correspond to the effect of replacement of the methyl group with the ethyl group at position C-2 of olanzapine (Figure 5.1, page 95). The presence of the formamide in the structure of accidentally achieved **145** (Scheme 3.21, page 69), decreased the affinity of the olanzapine derivative approximately 10 times for binding to the H-1 receptor when compared to olanzapine. As shown in Figure 5.1 (page 95) compound **101** represents a single modification at position N-4` in the structure of olanzapine. However, due to the poor dose-response behavior of **101** in the displacement curve (Figure 5.5) the influence of this modification on the affinity of this olanzapine derivative is not clear. The high IC_{50} value of **102** (8.63 x 10^{-6} M) could be attributed to the modifications at position C-2 however, the effect of the modification at N-4′ can not be certain at this stage because of the uncertainty of the activity of **101** .

In order to double confirm these results, another set of brain sections, two sections for each concentration, were used to repeat the H-1 receptor binding assay. Instead of using the scintillation method, this time the tissue sections were exposed to Kodak Biomax MR film. This will take a 15 week exposure time in order to obtain an optimized image. At the next stage, BioRad Densitometer will be utilized to quantify the density of the H-1 receptor binding. In addition, to confirm our reported results using the scintillation method, specific areas of the brain, particularly the VMH will be selected for quantification. Obviously, this method takes a very long time and it is not possible to report the results in this thesis.

5.5 Conclusions

In conclusion, the ability of the olanzapine-modified compounds **99**, **101**, **102** and **145** to displace the binding of [^{3}H]pyrilamine at the H-1 receptor was investigated. Structural modification of olanzapine based on pharmacophore generation resulted in the formation of new compounds varying in their affinity to the H-1 receptor. Compound **99** had a significantly reduced binding affinity compared to that of olanzapine as a result of the replacement of the methyl group of olanzapine with an ethyl group at position C-3. Compound **145** displayed a reduced binding affinity to the H-1 receptor while the binding behavior was similar to olanzapine. It is a result of substitution of the formamide at position N-10 in the structure of olanzapine. Compound **101** showed no effect to H-1 receptor binding. The effect of removing the distal nitrogen (N-4′) from the structure of olanzapine (Table 3.1, page 41) is questionable and needs more exploration. This was attributed to the poor dose-response behavior of compound **101** in the displacement curve. The reduced affinity of **102** with two modifications at positions C-3 and N-4′ could possibly corresponding to the replacement of the methyl group with an ethyl group at position C-3; however, the effect of removing the distal nitrogen at position N-4′ is questionable.

CHAPTER 6: CONCLUSIONS AND FUTURE DIRECTIONS

6.1 Conclusions

Some structural modifications to olanzapine to develop a new antipsychotic drug with H-1 agonist propensity or to a drug with a lower affinity for the H-1 receptor were perused. Initially, computer-aided drug design techniques were applied to generate a pharmacophore model from published H-1 agonist compounds. The attempted hypothesis generation runs afforded a series of hypotheses represented as a three-dimensional set of structural elements. Qualitative and quantitative analysis of the obtained hypotheses suggested that hypothesis H-1 Agonist-1-1 with the feature composition of 3 HY, HBA and PI can be the optimized pharmacophoric pattern for modification of olanzapine. As a result of mapping olanzapine into the pharmacophore H-1 Agonist-1-1 three modifications sites were identified. It was proposed that replacement of the methyl group with an ethyl group at position C-2, substitution of a hydroxymethyl group at position C-3 and also removing the distal nitrogen from position N-4′ (Table 3.1, page 41) could decrease the affinity of olanzapine for the H-1 receptor.

In order to investigate the effect of these afore-mentioned modifications on the binding of olanzapine, the synthesis of compounds **99**, **100**, **101**, **102** and **87** was attempted. Compounds **99** and **101** representing a single modification to the structure of olanzapine with the alteration of R_1 to C_2H_5 (**99**) and the replacement of the *N*-methylpiperazine ring with a piperidine ring (**101**) were successfully obtained. the synthesis of compound **102** was also successfully achieved indicating two modifications at positions C-2 and N-4′. None of the attempted synthetic plans to the synthesis of **100** and the ultimate target, **87** were successful. For instance, instead of the production of **100** *via* Vilsmeier-Haack reaction of olanzapine, the novel formamide derivative **145** was obtained. The synthesized compounds **99**, **101**, **102** and accidentally achieved formamide **145** were used in pharmacological evaluation.

Exploring the H-1 agonist property of the newly synthesized compounds was out of the scope of this project. However, the binding affinities of these compounds for the H-1 receptor were evaluated. Competitive binding assay revealed that compound **99** which had a C-3 ethyl group rather than a C-3 methyl group had a significantly reduced binding affinity compare to olanzapine. Compound **145**, the *N*-formyl analogue of olanzapine, showed a reduced binding affinity to the H-1 receptor while the binding behavior was similar to olanzapine. Compound **101** showed very low H-1 receptor binding. Due to the poor dose-response behavior of compound **101** in the displacement curve the effect of the removing distal nitrogen (N-4′) from the structure of olanzapine is questionable and needs more exploration. The reduced affinity of **102** with two modifications at positions C-3 and N-4′ could possibly corresponding to the replacement of the methyl group with the ethyl group at position C-3, however, the effect of removing distal nitrogen at position N-4′ is not clear.

6.2 Future directions

Future directions for this project could involve a further investigation of the effect of substitution of a hydroxymethyl group at position C-3 of olanzapine on the binding affinity for the H-1 receptor. This would involve the development of the synthesis of compounds **100** and **87**.

Further pharmacological testing is required for compounds **99**, **145** and **101**. In particular, the H-1 receptor binding assay should be undertaken to establish whether these compounds have H-1 receptor agonist activity. In addition, neurochemical evidence for reduced binding affinity by these compounds for the H-1 receptor *in vivo* in rat is required. Furthermore, in order to explore the therapeutic properties of these new compounds more pharmacological testing is required. Particularly, to retain the therapeutic profile of olanzapine, these olanzapine-modified compounds would need to have antagonist activity at the other CNS receptors including D-2 and $5HT_2$.

CHAPTER 7: REFERENCES

1. Andreasen, C., Positive and Negative Symptoms: Historical and Conceptual Aspecta. In *Schizophrenia: Positive and Negative Symptoms and Syndromes*, Andreasen, C., Ed. Karger AG: Iowa city, **1990**; Vol. 24, pp 1-42.
2. Castle, D.; Wesseley, S.; Der, G.; Murray, R., The incidence of operationally defined schizophrenia in Camberwell, 1965-84 *Br. J. Psychiatry* **1991**, 159, 790-94.
3. Alison, D. B.; casey, D. E., Antipsychotic-Induced Weight Gain: A Review of the Literature. *J. Clin. Psychiatry.* **2001**, 62, 22-31.
4. Arguello, P. A.; Gogos, J. A., Schizophrenia: Modeling a Complex Psychiatric Disorder. *Drug Discovery Today: Disease Model* **2006**, 3, 319-25.
5. Kingdon, D. G.; Turkington, D., *Cognitive Theraphy of Schizophrenia*. The Guilford Press: New York, **2005**; Vol. 1, p 27.
6. Stahl, S. M., Psychosis and Schisophrenia. In *Essentional Psychopharmacology*, Cambridge University Press: Cambridge, **1998**; pp 249-62.
7. Conley, R. R.; Kelly, D. L., Second Generation Antipsychotics for Schizophrenia: A Review of Clinical Pharmacology and Medication -Associated Side Effects. *J. Psychiatr. Relat. Sci.* **2005**, 42, 51-60.
8. Boer, J. A. D.; westenberg, H. G. M., Atypical Antipsycotics in Schizophrenia: A Review of Recent Developement. In *Advances in the Neurobiology of Schizophrenia*, Boer, J. A. D.; westenberg, H. G. M.; Praag, H. M. V., Eds. John Wiley & Sons: Chichester, **1995**; Vol. 1, pp 266-73.
9. Leucht, S.; Wahlbeck, K.; Hamann, J.; Kissling, W., New Generation Antipsychotics Versus Low-Potency Conventional Antipsychotics: A Systematic Review And Meta-Analysis. *Lancet* **2003,** 361, 1581-9.
10. Marder, S., Pharmacological Treatment of Schizophrenia. In *Schizophrenia*, J., K. D., Ed. Chapman Hall: London, **1992**.
11. Tehan, B. G.; Lioyd, E. J.; Wong, M. G., Molecular Field Analysis of Clozapine Analogs in The Developement of A Pharmacophore Model of Antipsychotic Drug Action. *J. Mol. Graphics Model.* **2001**, 19, 418-26.
12. Minchin, S. A.; Csernansky, J. G., Classification schemes for antipsychotic drugs. In *Antipsychotics*, Csernansky, J. G. E., Ed. Springer: Berlin, **1996**; pp 1-21.
13. Kane, J. M., Psycopharmacologic Approaches to The Treatmant of Schizophrenia: Practical Aspect In *Advances in the Neurobiology of Schizophrenia*, Boer, J. A. D.; westenberg, H. G. M.; Praag, H. M. V., Eds. John Wiley & Sons: Chichester, **1995**; Vol. 1, pp 245-63.
14. Ashby, C. R.; wang, R. Y., Pharmacological Action of The Atypical Antipsychotic Drug Clozapine: A Review *Synapse* **1996**, 24, 349-94.
15. Bymaster, F. P.; Nelson, D. L.; Delapp, N. W.; Falcone, J. F.; Eckols, K.; Truex, L. L.; Foreman, M. M., Antagonist by Olanzapine of Dopamine D-1, Serotonin$_2$, Muscarinic, Histamine H-1 and α_1-Adrenergic Receptors In Vitro. *Schizophr. Res.* **1999**, 37, 107-22.
16. Calligaro, D. O.; Fairhurst, J.; Hotten, T. M., The synthesis and Bological Activities of Some Known and Putative Metabolites of The Atypical Antipsychotic Agent Olanzapine. *Bioorg & Med. Chem. Lett.* **1997**, 7, 25-30.
17. Roth, B. L.; Craigo, S. C.; Choudhary, M. S.; Uluer, A.; J., M.; Shen, Y.; Meltzer, H. Y.; Sibley, D. R., Binding of Typical And Atypical Antipsychotic

Agents to 5-Hydroxytryptamine-6 and 5-Hydroxytryptamine-7 Rceptors. *J. Pharmacol. Exp. Ther.* **1994**, 268, 1403-10.
18. Fuller, R. W.; Snoddy, H. D., Neuroendoctrine Evidence for Antagonist of Sertonin and Dopamine Receptors by Olanzapine, An Antipsychotic Drug Candidate. *Res. Commun. Chem. Pathol, Pharmacol.* **1992**, 77, 87-93.
19. Moore, N. A.; Tye, N. C.; Axton, M. S.; Risius, F. C., The Behavioral Pharmacology of Olanzapine A Novel ' Atypical ' Antipsychotic Agent *J. Pharmacol. Exp. Ther.* **1992**, 262, 545-51.
20. Bymaster, F. P.; Hemrick-Luecke, S. K.; Perry, K. W.; Fuller, R. W., Neurochemical Evidence for Antagonism by Olanzapine of Dopamine, Sertonine, α_1-Adrenegic and Muscarinic Receptors In Vivo in Rats. *PSCHO* **1996**, 124, 87-94.
21. Han, M.; Deng, C.; Burne, T. H. J.; Newell, K.; Huang, X., Short- and Long-Term Effects of Antipsychotic Drug Treatment on Weight Gain and H-1 Receptor Expression. *Psychoneuroendocrino* **2008**, 33, 569-80.
22. Allison, D. B.; Mentore, J. L.; Heo, M.; Chandler, L. P.; cappelleri, J. C., Antipsychotic-Induced Weight Gain: A Comprehensive Reserach Synthesis. *Am. J. Psychiatry.* **1999**, 156, 1686-96.
23. Jones, B.; Basson, B. R.; Walker, D. J.; Crawford, M. K.; Kinon, B. J., Weight Change and Atypical Antipsychotic Treatment in Patients With Schizophrenia. *J. Clin. Psychiatry.* **2001**, 62, 41-44.
24. Weiden, P. J.; mackell, J. A.; MacDonnell, D. D., Obesity As A Risk Factor for Antipsycotics Noncompliance *Schizophr. Res.* **2004**, 66, 51-7.
25. Fontaine, K. R.; Heo, M.; Harrigan, E. P.; Shear, C. L.; Lakshminarayanan, M.; Casey, D. E.; al., e., Estimating The Consequences of Antipsychotic Induced Weight Gain on Health And Mortality Rate. *Psychiatry. Res.* **2001**, 101, 277-88.
26. McIntyre, R. S.; McCann, S. M.; Kennedy, S. H., Antipsychotic Metabolic Effects: Weight Gain, Diabetes Mellitus, And Lipid Abnormalities. *Can. J. Psychiatry.* **2001**, 46, 273-81.
27. Taylor, D. M.; McAskill, R., Atypical Antipsychotics And Weight Gain A Systematic Review. *Acta. Psychiatry. Scand.* **2000**, 101, 416-32.
28. Wetterling, T., Body Weight Gain With Atypical Antipsychotics. A Comparative Review. *Drug Safety* **2001**, 24, 59-73.
29. Kinon, B. J.; Kaiser, C. J.; Saeed, A.; Rotelli, M. D.; Walker, S. K., Association Between Early and Rapid Weight Gain and Change in Weight Over one Year of Olanzapine Therapy in Patient with schizophrenia and Related Disorders *J. Clin. Psychopharmacol.* **2005**, 25, 255-8.
30. Nemeroff, C. B., Dosing The Antipsychotic Medication Olanzapine. *J. Clin. Psychiatry.* **1997**, 10, 45-9.
31. Kinon, B. J.; Basson, B. R.; Gilmore, J. A.; Tollefson, G. D., Long-Term Olanzapine Treatment: Weight Change and Weight-Related Health Factors in Schizophrenia. *J. Clin. Psychiatry.* **2001**, 2001, 92-100.
32. Kinon, B. J.; Basson, B. R.; Tollefson, G. D., Effect of Long-Term Olanzapine Treatment on Weight Change in Schizophrenia. *Schizophr. Res.* **2000**, 41, 195-6.
33. Basson, B. R.; Kinon, B. J.; Taylor, C. C.; Szymanski, K. A.; Gilmore, J. A.; Tollefson, G. D., Factors Influencing Acute Weight Change in Patients With Schizophrenia Treated With Olanzapine, Haloperidol, or Risperidone. *J. Clin. Psychiatry.* **2001**, 62, 231-238.
34. Kurt, R.; Benvenga, M. J.; Bymaster, F. P.; Calligaro, D. O.; Cohen, I. R.; Falcone, J. F.; *et al.*, Preclinical Pharmacology of FMDP [6-Fluoro-10-[3-(2-

methoxyethyl)-4-Methyl-piperazin-1-yl]-2-Methyl-4H-3-thia-4, 9-diaza-benzo[*f*]azulene]: A Potential Novel Antipsychotic with Lower Histamine H-1 Receptor Affinity Than Olanzapine. *J. Pharm. Exp. Ther.* **2005**, 315, 1265-77.
35. Mercer, L. P., Histamine and The Neuroregulation of Food Intake *Nutrition* **1997**, 13, 581-2.
36. Mercer, L. P.; Haq, A. U.; Kelley, D. S.; Bundrant, H. M.; Humphries, L. L.; Markesbery, W., Diet Composition And Sex Influence Bioperiodicity Rat`s Central Nervous System Histamine (H-1) receptors. *J. Nutr. Biochem.* **1998,** 9, 142-8.
37. Mercer, L. P.; Kelley, D. S.; Haq, A. U.; Humphries, L. L., Dietary Induced Anorexia: A Review of Involvement of The Histaminergic System. *J. Am. Coll. Nutr.* **1996**, 15, 223-30.
38. Mercer, L. P.; Kelley, D. S.; Humphries, L. L.; Dunn, J. D., Manipulation of Central Nervous System Histamine or Histaminergic Receptor (H1) Affect Food Intake in Rats. *J. Nutr.* **1994**, 124, 1029-36.
39. Kroeze, W. K.; Hufeisen, S. J.; Popadak, B. A.; Reock, S. M.; Steinberg, S.; Ernsberger, P.; Jayathilake, K.; Meltzer, H. Y.; Roth, B. L., H1-histamine Receptor Affinity Predicts Short-Term Weight Gain For Typical And Atypical Antipsychotic Drugs *Neuropsychopharmacol* **2003**, 28, 519-26.
40. Mercer, L. P.; Kelly, D. S.; Ul-Haq, A.; Humphries, L. L., Dietary Induced Anorexia: A Review of Involement of The Histaminergic System. *J. Am. Coll. Nutr.* **1996**, 15, 223.
41. Watanabe, T.; Taguchi, Y.; Maeyama, K., Histaminergic Neurons: Morphology and Function *Boca raton: CRC Press* **1991**, 11.
42. Bray, G. A., A Disorder of Nutrientpartitioning: The Mona Lisa Hypothesis. *Am. Inst. Nutr.* **1991**, 1, 1146.
43. Morley, J., Appetite regulation: the role of peptide and hormones. *J. Endocrinal. Invest.* **1989,** 12, 135.
44. Robinson, E. N.; Kelley, D. S.; Tiu, A.; Haq, A. U.; Mercer, L. P., The Efect of Sex on Centeral Histaminergic Responses and Corticosteron Bioperiodicity in Sprague-Dawley Rats. *J. Nutr. Biochem.* **2005**, 16, 38-43.
45. Wang, C. F.; Bomberg, E.; Levine, A.; Billington, C.; Kotz, C. M., Brain-Derived Neurotrophic Factor in The Ventromedial Nucleus of The Hypothalamus Reduces Energy Intake. *Am. Physiol. Regu. Integr. Comp. Physiol.* **2007**, 293, R1037-R1045.
46. Sakaguchi T, A. K., Bray GA., Sympathetic Activity And Food Intake of Rats With Ventromedial Hypothalamic Lesions. *Int. J. Obes.* **1988**, 12, 285–291.
47. Ruffin, M.; Nicolaidis, S., Electrical Stimulation of the Ventromedial Hypothalamus Enhances Both Fat Utilization and Metabolic Rate That Precede And Parallel The Inhibition of Feeding Behavior. *Brain. Res.* **1999**, 846, 23-9.
48. http://www.medscape.com/content/2004/00/46/73/467350/467350_fig, In. (**2008**)
49. www.nature.com/.../v10/n2/images/4001638f1.gif. (**2008**)
50. Satoh, N.; Ogawa, Y.; Katsuura, G.; Tsuji, T.; Masuzaki, H.; Hiraoka, J.; Okazaki, T.; Tamaki, M.; *et al*., Pathophysilogical Significance of The *Obese* Gene Product, Leptin, in Ventromedial Hypothalamus (VMH)-Lesioned Rats: Evidence for Loss of Its Satiety Effect in VMH-Lesioned Rats. *The Endocrine Soc.* **1997**.
51. Cox, J. E.; Sims, J. S., Ventromedial Hypothalamic And Paraventricular Lesions Damage A Common System to Produce Hyperphagia. *Behavioural brain Res.* **1988**, 28, 297-308.

52. Ookuma, K.; Yoshimatsu, H.; Sakata, T.; Fujimoto, K.; Fukagawa, K., Hypothalamic Sites of Neuronal Histamine Action on Food Intake by Rats. *Brain Res.* **1989**, 490, 268-75.
53. Gater, P. R. B.; Weber, S. E.; Gui, G. P. H.; Jordan, C. C.; Hayes, N. A.; *et al*., Some Studies of The Action of Betahistine at H-1 And H-2 Receptors for Histamine. *Agent. Actio.* **1986**, 18, 342-50.
54. Poyurovsky, M.; pashinian, A.; Levi, A.; Weizman, R.; Weizman, A., The Effect of Betahistine , A Histamine H-1 Receptor Agonist /H-3 Antagonist, on Olanzapine -Induced Weight Gain in First-Episode Schizophrania Patients. *Inter. Clini. Psychopharmacol.* **2005**, 20, 101-3.
55. Kristam, R.; Gillet, V. J.; Lewis, R. A.; Thorner, D., Comparison of Conformation Analysis Techniques To Generate Pharmacophore Hypotheses Using Catalyst. *J. Chem. Inf. Model.* **2005**, 45, 461-476.
56. Holtje, H., Pharmacophore Identification and Receptor Mapping. In *The practice of medicinal chemistry [electronic resource]* Wermuth, C. G., Ed. Academic Press: Amsterdam, Boston, **2003**; Vol. 24, pp 387-403.
57. Martin, Y., Distance Comparisons (DISCO): A New Strategy for 3DStructure-Activity Relationships. In *Classical and 3D QSAR in Agrochemistry*, Hansch, C.; Fujita, T., Eds. American Chemical Society: Washington DC, **1995**; pp 318-329.
58. Barnum, D.; Greene, J.; Smellei, A.; Sprague, P., Identification of Common Functional Configurations among Molecules. *J. Chem. Inf. Model.* **1996**, 36, 563-571.
59. Jones, G.; Willett, P.; Glen, R., A Genetic Algorithm for Flexible Molecular Overlay and Pharmacophore Elucidation. *J. Comput-Aided Mol. Des.* **1995**, 9, 532-549.
60. Dixon, S.; Smondyrev, A.; Knoll, E.; Rao, S.; Show, D.; Friesner, R., PHASE: A New Engine for Pharmacophore Perception, 3D QSAR Model Developement, and 3D Database Screening: 1. Methodology and Preliminary Results. *J. Comput-Aided Mol. Des.* **2006**, 20, 647-671.
61. Richmond, N.; Abrams, C.; Wolohan, P.; Abrahamian, E.; Willett, P.; Clark, R., GALAHAM: 1 Pharmacophore Identification by Hypermolecular Alignment of Ligands in 3D. *J. Comput-Aided Mol. Des.* **2006**, 20, 567-587.
62. *Catalyst 4.10 Tutorials.* Accelrys Inc. San Diego, CA, USA, **2005**.
63. Li, H.; Sutter, J.; Hoffman, R., HypoGen: An Automated System for Generation 3D Predivtive Pharmacophore Model. In *pharmacophore perception, development, and use in drug design*, Guner, O. F., Ed. International University Line: La Jolla, CA, **2000**; pp 171-181.
64. Motulsky, H., *The GraphPad Guide to Analazing Radioligand Binding Data*. Graphpad Software, Inc: **1996**; p 10-18.
65. Bakker, R. A.; Weiner, D. M.; Laak, T. t.; Beuming, T.; Zuiderveld, O. P.; Edelbroek, M.; Hacksell, U.; Timmerman, H.; Brann, M. R.; Leurs, R., 8-RLisuride Is A Potent Stereospecific Histamine H_1-Receptor Partial Agonist. *Mol. Pharmacol.* **2004**, 65, 538-549.
66. Bruysters, M.; Pertz, H. H.; Teunissen, A.; Bakker, R. A.; Gillard, M.; chatelain, P.; Schunack, W.; Timmerman, H.; Leurs, R., Mutational Analysis of The Histamine H_1-receptor Binding Pocket of Histaprodifens. *Eur. J. Pharmacol.* **2004**, 487, 55-63
67. Seifert, R.; Wenzel-Seifert, K.; Burckstummer, T.; Pertz, H. H.; Schunack, W.; Dove, S.; Buschauer, A.; Elz, S., Multiple Differences in Agonist and

Antagonist pharmacology between Human and Guinea Pig Histamine H_1-Receptor. *J. Pharmacol. Exp. Ther.* **2003**, 305, 1104-1115.
68. MacDougall, I. J. A.; Griffith, R., Selective Pharmacophore Design for α_1-Adrenoceptor Subtypes. *J. Mol. Graphics & Modell.* **2006**, 25, 146-157.
69. MacDougall, I. J. A. In Silico Investigations into the Alpha1 Adrenoceptors, The university of Newcastle, Callaghan, **2008.**
70. White, S. K., The Design and Pharmacophore Definition of Retinoid X Receptor Specific Ligands In *pharmacophore perception, development, and use in drug design*, Guner, O. F., Ed. International University Line: La Jolla, CA, **2000**; Vol. 17, pp 319-336.
71. Capmany , E. L. a.,Olanzapine Capsules, Granules , and Tables. In information, S.-E., Ed. Lilly Corporate Center, **2008**.
72. Chakrabarti, J. K.; Hicks, T. A.; Hotten, T. M.; Tupper, D. E., Heteroarene-fused Benzodiazepine. Part 1. Synthesis of Thieno-[2,3-*b*][1,5],-[3,2-*b*][1,5]-,and-[3,4-*b*][1,5]-benzodiazepinones. *J.Chem.Soc. Perkin Trans. I* **1978**, 937-941.
73. Chakrabarti, J. K.; Hotten, T. M.; Tupper, D. E. 2-methyl-thieno-benzodiazepine. **1997**, 11pp.; Ser . No. 44,844; US 5627178; *Chem. Abstract. No*, 127: 5106
74. Shastri, J. A.; Bhatnagar, A.; Thaper, R. K.; Dubey, S. K. A Process for Producing Pure Form of 2-Methyl-4-(4-Methyl-1-Piperazinyl)-10*H*-Thiono[2,3-*b*][1,5]Benzodiazepine **2006**, 20 pp; WO 2006006180; *Chem. Abstract. No*, 144: 150401
75. Sabnis, R. W.; Rangnekar, D. W.; Sonawane, N. D., 2-Aminothiophenes By The Gewald Reaction. *J. Heterocyclic Chem.* **1999**, 36, 333.
76. He, X.; Griesser, U. J.; Stowell, J. G.; Borchardt, T. B.; Byrn, S. R., Conformational Color Polymorphism and Control of Crystalization of 5-methyl-2-[(4-methyl-2-nitrophenyl)amino]-3-thiophenecarbonitrile. *J. Pharma.l Sci.* **2001**, 90, 371-388.
77. Bellamy, F. D.; Ou, K., Selective Reduction of Aromatic Nitro Compounds With Stannous Chloride in Non Acidic and Non Aqueous Medium. *Tetrahedron Lett.* **1955**, 25, 839–842.
78. Patel, H. V.; K., R. A.; Patel, P. B.; Patel, M. R. Process of Preparation of Olanzapine Form I. **2003**, 16pp; WO 2003101997; *Chem. Abstract. No*, 140: 16753
79. Abd-El. Aziz, A. S.; Afifi, T. H., Novel Azo Disperse Dyes Derived From Aminothiophens: Synthesis and UV-Visible Studies. *Dyes and Pigments* **2006**, 70, 8-17.
80. Chakrabarti, J. K.; Hotten, T. M.; A., P. I.; Tye, N. C., Synthesis Pharmacological Evaluation of a Series of 4-Piperazinylpyrazolo[3,4-*b*]- and -[4,3-*b*][1,5]benzodiazepine as Potential Anxiolytics. *J. Med. Chem.* **1989**, 32, 2573-2582.
81. Carey, F. A.; Sundberg, R. J., Functional Group Interconversion by Nucleophilic Substitution. In *Advance Organic Chemistry, Part B: Reaction and Synthesis*, Kluwer Academic / Plenum Publishers: New York, **2001**; Vol. 2, pp 141-189.
82. Pitt, G. R.; Batt, A. R.; Haigh, R. M.; Penson, A. M.; Robson, P. A.; P., R. D.; Tartar, A. L.; Trim, J. E.; Yea, C. M.; B., R. M., Non-Peptide Oxytocin Agonists. *Bioorg. & Med. Chem. Lett.* **2004**, 14, 4585-89.
83. Moore, K. P., Strategies Toward Improving the Brain Penetration of Macrocyclic Tertiary Carbinamine BACE-1 Inhibitors. *Bioorg. & Med. Chem. Lett.* **2007,** 17, 5831-35.

84. Chen, F.; Song, K.; Wu, Y.; Yang, D., Synthesis and Conformational Studies of -Aminoxy Peptides. *J. Am. Chem. Soc.* **2008,** 130, 743-55.
85. Mahony, G.; Sundgren, A.; Svensson, S.; Grotli, M., A Practical Synthesis of 2-Aminoacylamino-2-Deoxyadenosines. *Tetrahedron* **2007**, 63, 6901-08.
86. Carey, F. A.; Sundberg, R. J., Aromatic Substitution Reaction. In *Advance Organic Chemistry, Part B: Reaction and Synthesis*, Kluwer Academic / Plenum Publishers: New York, **2001**; Vol. 2, pp 693-745.
87. Dallemagne, P.; Khanh, L. P.; Alsaidi, A. A.; Renault, O.; Varlet, I.; Collot, V.; Bureau, R.; Rault, S., Synthesis and Biological Evaluaton of Cyclopenta[*c*]thiophene Related Compounds as New Antitumor Agents. *Bioorg & Med. Chem.* **2002,** 10, 2185-91.
88. Perrin, D. D.; Armarego, W. L. F., *Purification of Laboratory Chemicals.* **1988**; p 391.
89. Gross, J.; Gelev, V. M.; Wagner, G., A Sensitive and Robust Method for Obtaining Intermolecular NOEs Between Side Chains in Large Protein Complexes. *J. Biomolec. NMR,* **2003**, 25, 235-42.
90. Nakamura, K.; Inoue, K.; Ushino, K.; Oka, S.; Ohno, A., Stereochemical Control on Yeast Reduction of a-keto Esters. Reduction by Immobilized Bakers` yeast in Hexane. *J. Org. Chem.* **1987,** 53, 2589-93.
91. Singh, J.; kissick, T. P.; Mueller, R. H., Improved Procedure For The One Step Synthesis of a-ketoesters. *Org. Prep & proced. Inc.* **1989**, 501-4.
92. Palacios, J. M.; Young, W. S.; kuhar, M. J., Autoradiographic localization of H1-Histamine Receptors In Brain Using ^{3}H-Mepyramine: Preliminary Studies. *Euro. J. Pharmacol.* **1979,** 58, 295-304.
93. Krumbiegel, P. S., Heinz. Liquid Scintillation Mixtures Containing Perdeuterated Solvent - and/or Solubility- Increasing Agent. **1973**, 3pp; *Chem. Abstract. No*, 78: 91611
94. http://en.wikipedia.org/wiki/Liquid_scintillation_counting. (**2008**)
95. http://www.technomedica.com/publikazii/belur/Bio-Rad.pdf. (**2008**)
96. http://www.biocompare.com/review/926/Quick-Start(tm)-Bradford-Protein-Assay-Kits-From-Bio-Rad. (**2008**)